Technical University of Munich

Department of Mathematics

FEM error analysis of parabolic shape gradients

Master's Thesis

von

Leonardo Mutti

Supervisor: Prof. Dr. Michael Ulbrich
Advisor: Prof. Dr. Michael Ulbrich
Submission Date: [Day. Month. 2022]

I hereby declare that this thesis is my own work and that no other sources have been used except those clearly indicated and referenced.

Place, Date
original, hand-written signature

Acknowledgements

First and foremost, I would like to express my gratitude to my supervisor. Apart from suggesting this fascinating topic and providing his advice, he was encouraging and never pressuring, which helped me to get in the right mindset.

My path to the end this project was challenging, everybody who took me here must feel proud for this success. To my parents, family, friends, and to Anna: thank you.

Abstract

In the context of elliptic, PDE-constrained shape optimization, it has already been noted that a distributed expression for the shape gradient is more accurate than its boundary counterpart, when finite elements are employed to discretize the arising PDEs.

We further explore these observations in two directions: first, we work in a parabolic setting and second, we explicitly address the fact that finite element solutions live on polygons/polyhedra, but they approximate functions defined on smooth domains. We therefore prove, and numerically verify, semidiscrete estimates for the shape gradients in spatially semidiscrete, as well as in fully discrete cases. The implicit Euler or Crank-Nicolson methods are adopted for the time discretization.

Our analysis is based on a model shape optimization problem for the heat equation, where the goal is to determine the shape of a zero temperature inclusion given the temperature and heat flux at an external boundary. For such problem, the shape gradient is derived, a star-shaped ansatz is applied, and numerical results are discussed.

Contents

1. Introduction

To approximately solve PDE-constrained shape optimization problems, a discretization of several "continuous" quantities has to be performed. In particular, suitable numerical methods for the involved partial differential equations must be adopted, and then, an optimization routine has to be implemented, so as to obtain a hopefully reasonable estimate of the sought analytical solution.

The accuracy of the optimization procedure is influenced by many factors. In particular, when using gradient based optimization, one would like the discretized shape gradient to be the best possible approximation of the continuous counterpart. For the accuracy in this quantity there is a major design choice, which is whether a boundary or distributed/volumetric approach is taken: when sufficient smoothness is available, the boundary and distributed expressions of the shape gradient are equivalent, on the continous level, and this is the content of the so-called "structure theorem" (see theorem 1.4 of [58]). This equivalence, however, often breaks down on the discrete level, and one has to decide the form with which to work. There are of course advantages and disadvantages to both views (see e.g. [58]), but there seems to be numerical evidence for a superior accuracy of the distributed approach over the boundary one, at least when the finite element method is adopted to the arising PDEs (it is general, popular and flexible for different engineering applications, making it a natural choice). Theoretical analysis backing up this observation was presented in the work [39]. They analyzed a model elliptic problem, and showed that the discretized shape gradient can be expected to be a second order approximation to the continuous one in the volumetric case, and often only a first order one otherwise.

Such conclusions are however only drawn in an elliptic setting, but parabolic shape optimization has important applications too (see e.g. [11], [37] to mention a few), and deserves further analysis. With this in mind, we try to extend the observations of [39] in two ways:

- on one hand, we consider a time-dependent setting
- on the other one we try to account for the fact that continuous shape gradients are based on smooth domains, whereas discretized quantities naturally live on simplicial meshings

To this end, we borrow a model parabolic shape optimization problem from [37] and center our arguments around it. In [37], boundary expressions for the shape gradients are derived, and PDEs are approximated using the boundary element method. While this choice provides computational efficiency, it sacrifices generality (more complicated PDEs need not to be easily convertible to boundary integral equations). We take, in contrast, a distributed/volumetric approach and employ finite elements on the volume. As a byproduct, we obtain a very easy implementation that is amenable to pre-existing, high-performance software packages, such as FEniCS ([47]) and dolfin-adjoint ([31], [22], [50]).

This thesis is hence structured as follows:

- in chapter 2, we introduce the model parabolic shape optimization problem of interest, and proceed to compute the continuous shape gradient. We also discuss the star-shaped parametrization of domains that we adopted, for simplicity, in the implementation
- chapter 3 is then about the finite element discretization of the PDEs and of the geometry. When the implicit Euler method is adopted in time, we show that optimization and discretization commute, by employing a suitable scheme for the adjoints. We conjecture that such commutation is achievable also with the Crank-Nicolson method, and motivate this belief with theoretical and numerical arguments. Estimates for the errors between discrete and continuous shape gradients are then given, under the assumptions that the discrete domain interpolates the continuous one at the boundary nodes, in a commutative setting for the implicit Euler method, and in an optimize-then-discretize one for the Crank-Nicolson one
- in chapter 4 we discuss our discretize-then-optimize implementation and conduct two sets of experiments: on one hand we illustrate results for the shape optimization of the model problem, and on the other one we provide numerical evidence for the error estimates of chapter 3
- chapter 5 contains a brief summary of the thesis and lists some possible future research directions

For exposition purposes, we delegated many technicalities to appendices:

- some useful results from functional analysis are collected in appendix A
- many details about the parabolic equations that appear in the thesis can be found in appendix B
- several facts about domains deformations are found in appendix C
- in appendix D, the adopted finite element framework, in the context of smooth geometries, is explained

2. Infinite dimensional setting

This chapter is devoted to the analysis of the non-discretized shape optimization model problem:

- in section 2.1 we introduce it at first as a shape identification problem
- in section 2.2 we reformulate the latter as the shape optimization problem of interest, and compute the shape gradient of the cost functional to be minimized
- in section 2.3, we discuss the ansatz that the sought domains are star-shaped, to give some justification of our computer implementation, that is fully discussed in section 4.1
- in section 2.4 we further motivate our implementation, with respect to the scalar product in which optimization is performed, so as to explain the way in which descent directions are obtained from the knowledge of the shape gradient

2.1. Shape identification problem

Let $D \subseteq \mathbb{R}^n$ be a sufficiently smooth domain, and $\Omega \subset\subset D$. We call $\Gamma_f = \partial D$, $\Gamma_m = \partial\Omega$. We let $T > 0$ and introduce $I = (0, T)$, $\Sigma_f = I \times \Gamma_f$, $\Sigma_m = I \times \Gamma_m$.

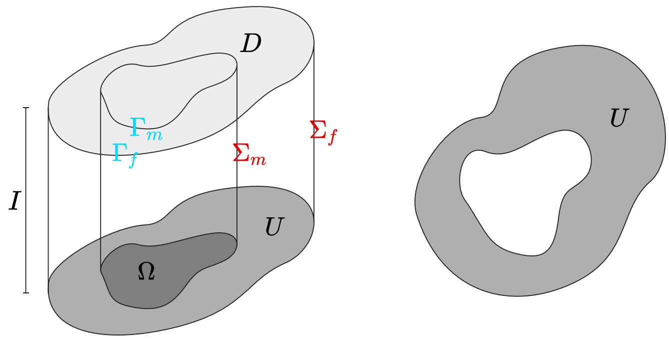

Figure 2.1.: Space-time cylinder and 2D domain

Let us interpret D as a uniform and isotropic body, inside of which an inclusion Ω of zero temperature is present (think of an ice cube submerged in water). The temperature u inside $D \setminus \overline{\Omega} = U$ evolves over time according to the heat equation, at least approximately, and we are interested in obtaining the shape of the inclusion, which we suppose to be inaccessible, so that we cannot directly measure it. We are however allowed to access the outer boundary ∂D and measure surface temperature and normal heat flux: we ask ourselves how to recover $\partial\Omega$ from the knowledge of this boundary data only. This is a non-linear and ill-posed inverse problem (according to e.g. [37]).

Summing up, our task is, given the outer temperature and heat flux, to reconstruct the shape of Ω that induced, through heat diffusion, those boundary quantities.

In more mathematical terms, let us consider a heat equation on the unknown cylinder $U \times I$, with zero initial condition and no volumetric forcing term, where on Σ_f are prescribed smooth enough Dirichlet and Neumann data simultaneously (call them f and g, they correspond to the outer temperature and heat flux), while on Σ_m, homogeneous Dirichlet conditions.

Problem 2.1.1 (Overdetermined heat equation)
Call $U := D \setminus \overline{\Omega}$. We look for $u : U \times I \to \mathbb{R}$ solving:

$$\begin{cases} u_t - \Delta u = 0 & \text{on } U \times I \\ u(0) = 0 & \\ u = f, \partial_\nu u = g & \text{on } \Sigma_f \\ u = 0 & \text{on } \Sigma_m \end{cases}$$

We introduce the splitting:

$$\begin{cases} v_t - \Delta v = 0 & \text{on } U \times I \\ v(0) = 0 & \\ v = f & \text{on } \Sigma_f \\ v = 0 & \text{on } \Sigma_m \end{cases}, \quad \begin{cases} w_t - \Delta w = 0 & \text{on } U \times I \\ w(0) = 0 & \\ \partial_\nu w = g & \text{on } \Sigma_f \\ w = 0 & \text{on } \Sigma_m \end{cases}$$

It can be shown that, for arbitrary f, g, there exists at most one Ω such that problem 2.1.1 is solvable (see [17], [16]) We can leverage this property to find a numerical approximation for such domain. In particular, the equations for v, w are always uniquely solvable, and $u = v$, $u = w$, in case u exists, i.e. when the shape identification problem admits a solution. One way to find $\partial\Omega$ is therefore, given data f, g and a guess $\hat{\Omega}$ of the sought domain, to simulate v, w on $\hat{\Omega}$, measure their discrepancy $\|v - w\|$ and use this knowledge to improve the iterate $\hat{\Omega}$ and get closer to the actual inclusion Ω, by trying to minimize $\|v - w\|$.

So, the thesis revolves around the following problem.

Problem 2.1.2 (Shape identification problem)
We aim at finding Ω such that u, defined in problem 2.1.1, exists, i.e. such that $v = w$.

This same problem was addressed in [37] using a slightly different approach than ours, involving boundary integral equations, boundary element methods and non-standard time stepping schemes. On the other hand our focus has a rather "volumetric" flavour, as we will make clear in the following chapters, and we make use of the well known implicit Euler or Crank-Nicolson algorithms.

As already mentioned, some uniqueness results for problem 2.1.2 are already available. We are not concerned with the issue of the existence of Ω, likewise this aspect is not addressed in the aforementioned work [37]. Some advances in this direction were made in the case where Ω is allowed to evolve with time, see [13].

In the following we will formalize assumptions, setting and notation, and we will tackle problem 2.1.2 by shape optimization techniques.

2.2. Treatment by shape optimization

Assumption 2.2.1 (Geometry assumptions for the shape optimization problem)
Let $D \subseteq \mathbb{R}^n$, $\Omega_r \subset\subset D$ be bounded Lipschitz domains, in the sense of [35], definition 1.2.1.1. Define $U_r := D \setminus \overline{\Omega_r}$, the so-called "reference domain", which is also bounded and Lipschitz.

Definition 2.2.2 (Admissible transformations)
Given D, we consider the set $\mathcal{T} := \{\tau : \mathbb{R}^n \to \mathbb{R}^n, \tau \text{ bi-Lipschitz}, \tau|_{D^c} = \mathrm{Id}\}$, endowed with the "perturbation space" $\Theta := \{\delta\theta \in W^{1,\infty}(\mathbb{R}^n; \mathbb{R}^n), \delta\theta|_{D^c} = 0\}$, see also definition C.1.3.
We will consider transformations of U_r that belong to $\mathcal{T}_a := \mathcal{T} \cap \{\tau \in W^{1,\infty}(\mathbb{R}^n, \mathbb{R}^n), \|\tau - \mathrm{Id}\|_{W^{1,\infty}(\mathbb{R}^n,\mathbb{R}^n)} < C(U_r)\}$, where the presence of the bound by $C(U_r)$ is to ensure that $\tau(U_r) \subset\subset D$ is also bounded Lipschitz, and the existence of such constant is guaranteed by theorem C.1.7.

We now recast problem 2.1.2 into a new form, suitable for shape optimization, as done in [37]. We mention that the equations for v, w of problem 2.1.1 are well posed, this is discussed in detail in the appendices. We remark that, given any extension $\bar{u}$ of f onto $U \times I$ (in the sense of proposition A.2.5), then v decomposes as $v = v_0 + \bar{u}$, where v_0 solves another heat equation with zero Dirichlet conditions. We therefore write $v^\tau = v_0^\tau + \bar{u}$ and w^τ to emphasize the dependence on τ, and refer the reader to problem B.2.2, eq. (B.2.7) and problem C.3.3 for additional details on the PDEs formulations.

Problem 2.2.3 (Shape optimization problem)
Suppose that assumption 2.2.1, assumption B.2.1 (applied to problem 2.1.1) hold. We want to solve:

$$\inf_{\tau \in \mathcal{T}_a} \frac{1}{2} \|v^\tau - w^\tau\|^2_{L^2(I, H_\tau)} =: J(\tau)$$

The notation for the spaces also comes from problem C.3.3: $\cdot_\tau$ means that the space is based on the moving domain $\tau(U_r)$, and $H = L^2, \mathtt{V} = H_0^1, \mathtt{W} = H^1_{0,m} = \{v \in H^1, v(\Gamma_m) = 0\}$ (see also appendix B.2 for the last space), so that e.g. $H_\tau = L^2(\tau(U))$.

Therefore, we are now concerned with finding a function τ, instead of a generic set Ω, and this way we can make use of functional analytic techniques and results from optimal control.

Observation 2.2.4 (Tracking type cost functional).
We have chosen the distributed $L^2(I, L^2)$ norm to measure the discrepancy $v^\tau \simeq w^\tau$ on the whole $\tau(U_r)$. Apart from having favourable functional analytic properties (Fréchet differentiability, to mention one), such cost functional will also allow us to obtain "better behaved" adjoint states. In fact, contrary to [37], the heat equations for the adjoint states (see proposition 2.2.10) will have better compatibility between initial condition and boundary conditions. This potentially simplifies the numerical analysis of such equations, as we will make clearer later on.

Now, let $U := \tau(U_r)$, for $\tau \in \mathcal{T}_a$ and let $\delta\theta \in \Theta$. To find a better (in the sense of the energy J) candidate τ for the solution of problem 2.2.3, we can use gradient information and perturb our current guess τ in the direction of steepest descent for J, a direction dictated by the shape gradient J' of J (for more details on how to extract such direction, see section 2.4). We are hence interested in finding $J'(\tau) \in \Theta^*$ such that, for all null sequences $\delta\theta_k \to 0$ in Θ, we have:

$$\lim_k \frac{|J(\tau + \delta\theta_k) - J(\tau) - J'(\tau)[\delta\theta_k]|}{\|\delta\theta_k\|_{W^{1,\infty}(\mathbb{R}^n;\mathbb{R}^n)}} = 0$$

Note, also thanks to proposition C.1.6, that a small $\delta\theta \in \Theta$ perturbation of $\tau \in \mathcal{T}_a$, small with respect to the $W^{1,\infty}(D; \mathbb{R}^n)$ topology, still yields and element of $\mathcal{T}_a$: it follows that, for k large enough, that $\tau + \delta\theta_k \in \mathcal{T}_a$.

Observation 2.2.5.
To carry out all the reasonings with such a general form of tranformation τ, an assumption of "smallness" (such as the one involving $C(U_r)$) was necessary, to keep $\tau(U_r)$ Lipschitz. A more transparent way of ensuring that $\tau(U_r) \subset\subset D$ is Lipschitz, can be found in section 2.3.
Also note, that τ has a Lipschitz inverse yields $\tau(U_r) \subset\subset D$: for $x \in D$, we have in fact $0 < \delta = \inf_{d\in\partial D} |x-d| \leq \|\tau^{-1}\|_{W^{1,\infty}(\mathbb{R}^n,\mathbb{R}^n)} \inf_{d\in\partial D} |\tau(x)-d|$.

Now, $\tau + \delta\theta_k = (\mathrm{Id} + \delta\theta_k \circ \tau^{-1}) \circ \tau$, and $\mathrm{Id} + \delta\theta_k \circ \tau^{-1}$ is in $\mathcal{T}_a$ (also by proposition C.1.6 and the reasoning above). We are then equivalently interested in:

$$\lim_k \frac{|J((\mathrm{Id} + \delta\theta_k \circ \tau^{-1}) \circ \tau) - J(\tau) - J'(\tau)[\delta\theta_k]|}{\|\delta\theta_k\|_{W^{1,\infty}(\mathbb{R}^n;\mathbb{R}^n)}}$$

We now introduce a "Lagrangian" functional in order to derive the expression of the shape gradient J' of J. There are several ways about this task in the literature (see e.g. [58], [15] or [44]), and we will adopt that contained in [58]. It requires the PDEs corresponding to $\tau+\delta\theta_k$ to be all reformulated on the domain $\tau(U_r)$, where τ is exactly the evaluation point of J'. To find a transported formulation of our PDEs to a different domain, we need to consider the variational formulations of $v^{\tau+\delta\theta_k}$ and $w^{\tau+\delta\theta_k}$ and then apply a change of variables to the appearing integrals. This is precisely addressed theorem C.3.2 (whose applicability is ensured by assumption B.2.1 and by assumption C.3.1, which holds by assumption 2.2.1).

For k large, i.e. $k \geq K(\tau)$, we have $\zeta_k := \mathrm{Id} + \delta\theta_k \circ \tau^{-1} \in \mathcal{T}_a$, as seen above, and having theorem C.3.2 in mind we can set:

$$\begin{aligned} &L_\tau(k, w, v_0, q, p) := \\ &\frac{1}{2}\int_I \int_{\tau(U_r)} |v_0 + \bar{u} \circ \zeta_k - w|^2 |\det(D\zeta_k)| + \\ &\int_I (w_t, q|\det(D\zeta_k)|)_{H_\tau} + (A_{\zeta_k}\nabla w, \nabla q)_{H_\tau} - \int_I (g, \mathrm{tr}_U q)_{L^2(\Gamma_f)} + \\ &\int_I (v_{0t}, p|\det(D\zeta_k)|)_{H_\tau} + (A_{\zeta_k}\nabla v_0, \nabla p)_{H_\tau} + \int_I ((\bar{u}\circ\zeta_k)', p|\det(D\zeta_k)|)_{H_\tau} + (A_{\zeta_k}\nabla(\bar{u}\circ\zeta_k), \nabla p)_{H_\tau} \end{aligned}$$

Here $w \in Q_0(I, \mathtt{W}_\tau), v_0 \in Q_0(I, \mathtt{V}_\tau), q \in Q^0(I, \mathtt{W}_\tau), p \in Q^0(I, \mathtt{V}_\tau)$, where the space Q is thoroughly described after its introduction in definition B.3.2, which we recall: $Q(I, V) = H^{1,1} = L^2(I, V) \cap H^1(I, H)$, and Q^0 means the imposition of a zero terminal condition (Q_0 stands for zero initial condition). We have set $A_\tau := (D\tau)^{-1}(D\tau)^{-t}|\det(D\tau)|$.

L_τ is composed of three parts: the cost functional and the two variational formulation of v_0^τ and w^τ, transported to the domain $\tau(U_r)$, which is fixed when computing the shape gradient.

Note that to be precise, $\bar{u}$ is any extension of the Dirichlet datum f to the domain $I \times \zeta_k(\tau(U_r))$ (see proposition A.2.5, eq. (B.2.7)). Because of this, let us fix $\bar{u}_\tau$, an extension of f on $\tau(U_r)$ and choose $\bar{u} := \bar{u}_\tau \circ \zeta_k^{-1}$, a legitimate extension of f.

Therefore, we can state the following definition.

Definition 2.2.6 (Lagrangian)
For a fixed $\tau \in \mathcal{T}_a$ and $k \geq K(\tau)$, for $\zeta_k := \mathrm{Id} + \delta\theta_k \circ \tau^{-1} \in \mathcal{T}_a$, we define:

$$\begin{aligned} &L_\tau(k, w, v_0, q, p) = \\ &\frac{1}{2}\int_I \int_{\tau(U_r)} |v_0 + \bar{u}_\tau - w|^2 |\det(D\zeta_k)| + \\ &\int_I (w_t, q|\det(D\zeta_k)|)_{H_\tau} + (A_{\zeta_k}\nabla w, \nabla q)_{H_\tau} - \int_I (g, \mathrm{tr}_U q)_{L^2(\Gamma_f)} + \\ &\int_I (v_{0t}, p|\det(D\zeta_k)|)_{H_\tau} + (A_{\zeta_k}\nabla v_0, \nabla p)_{H_\tau} + \int_I (\bar{u}_\tau', p|\det(D\zeta_k)|)_{H_\tau} + (A_{\zeta_k}\nabla\bar{u}_\tau, \nabla p)_{H_\tau} \end{aligned}$$

L_τ is defined as a map $\{k \geq K(\tau)\} \times Q_0(I, \mathtt{W}_\tau) \times Q_0(I, \mathtt{V}_\tau) \times Q^0(I, \mathtt{W}_\tau) \times Q^0(I, \mathtt{V}_\tau) \to \mathbb{R}$.
We call $u = (w, v_0)$, $\pi = (q, p)$ (states and adjoints), $G(k, u, \pi) = L_\tau(k, w, v_0, q, p)$ to ease the notation.
We also call $b(k, u) = \frac{1}{2}\int_I \int_{\tau(U_r)} |v_0 + \bar{u}_\tau - w|^2 |\det(D\zeta_k)|$ and $a(k, u, \pi) = G(k, u, \pi) - b(k, u)$, $E = Q_0(I, \mathtt{W}_\tau) \times Q_0(I, \mathtt{V}_\tau)$, $F = Q^0(I, \mathtt{W}_\tau) \times Q^0(I, \mathtt{V}_\tau)$, the spaces for states and adjoints.

The rest of this section is devoted to applying the averaged adjoint method [58] to our problem, so as to identify the volume expression of the shape gradient $J'(\tau)$. To this end we will have to state some properties of the Lagrangian L_τ, as required ni [58].

Proposition 2.2.7 (Properties of the Lagrangian)
L_τ satisfies the following properties:

1. $\psi \mapsto a(k, \phi, \psi)$ is linear, no matter what ϕ, k
2. G is Fréchet differentiable with respect to ψ at $(k, \phi, 0)$ for all k, ϕ

3. $d_\psi G(k,\phi,0)[\delta\psi]=0$ for all $\delta\psi\in F$, admits a unique solution $\phi=u^k$
4. $[0,1]\ni s\mapsto G(k,su^k+(1-s)u^0,\psi)$ is in $AC[0,1]$, no matter what k,ψ
5. G is Fréchet differentiable with respect to ϕ at (k,ψ,ϕ) for all k,ψ,ϕ
6. $[0,1]\ni s\mapsto d_\phi G(k,su^k+(1-s)u^0,\psi)[\delta\phi]$ is in $L^1(0,1)$, no matter what $k,\psi,\delta\phi$
7. there exists a unique solution $\psi=\pi^k$ to $\int_0^1 d_\phi G(k,su^k+(1-s)u^0,\psi)[\delta\phi]ds=0$ for all $\delta\psi$

In particular $\pi^k=(Q^k\circ\tau^k,P^k\circ\tau^k)$, where we introduced the averaged adjoint problems on $I\times(\zeta_k\circ\tau)(U_r)$:

Problem 2.2.8 (Averaged adjoint equations)

$$\begin{cases}-Q_t^k-\Delta Q^k=\frac{v_0^k-w^k+v_0^0-w^0}{2}\circ\zeta_k^{-1}+\bar u_\tau\circ\zeta_k^{-1}\\ Q^k(T)=0\\ \partial_\nu Q^k=0 \text{ on } \Sigma_f\\ Q^k=0\text{ on }\Sigma_{m,k}\end{cases},\quad \begin{cases}-P_t^k-\Delta P^k=-\frac{v_0^k-w^k+v_0^0-w^0}{2}\circ\zeta_k^{-1}-\bar u_\tau\circ\zeta_k^{-1}\\ P^k(T)=0\\ P^k=0 \text{ on } \Sigma_f\\ P^k=0\text{ on }\Sigma_{m,k}\end{cases}$$

Proof.

We give some comments for the non trivial points.

Proof of 3

Testing $d_\psi G(k,\phi,0)[\delta\psi]=$ separately with $\delta\psi=(\delta q,0)$ and $\delta\psi=(0,\delta p)$ we get back the state equations, so that a unique solution exists by theorem C.3.2 and theorem B.2.6.

Proof of 7

It is readily seen that:

$$\int_0^1 d_\phi G(k,su^k+(1-s)u^0,\psi)[\delta\phi]ds=$$
$$\int_I (((v_0^k+\bar u_\tau-w^k)+(v_0^0+\bar u_\tau-w^0))/2|\det(D\zeta_k)|,\delta v_0-\delta w)_{H_\tau}+$$
$$\int_I(\delta w_t,q|\det(D\zeta_k)|)_{H_\tau}+(A_{\zeta_k}\nabla\delta w,\nabla q)_{H_\tau}+\int_I(\delta v_{0t},p|\det(D\zeta_k)|)_{H_\tau}+(A_{\zeta_k}\nabla\delta v_0,\nabla p)_{H_\tau}=...$$

We get $\delta w_t=(\delta w\circ\zeta_k^{-1})_t\circ\zeta_k$, where $\delta w\circ\zeta_k^{-1}\in Q_0(I,\mathtt{W}_{\zeta_k\circ\tau})$ by proposition C.2.2, that can be applied thanks to the smallness of ζ_k. Applying a change of variables we are left with:

$$...=\int_I\left(\frac{v_0^k-w^k}{2}\circ\zeta_k^{-1}+\frac{v_0^0-w^0}{2}\circ\zeta_k^{-1}+\bar u_\tau\circ\zeta_k^{-1},\delta v_0\circ\zeta_k^{-1}-\delta w\circ\zeta_k^{-1}\right)_{H_{\zeta_k\circ\tau}}+$$
$$\int_I((\delta w\circ\zeta_k^{-1})_t,q\circ\zeta_k^{-1})_{H_{\zeta_k\circ\tau}}+(\nabla(\delta w\circ\zeta_k^{-1}),\nabla(q\circ\zeta_k^{-1}))_{H_{\zeta_k\circ\tau}}+\int_I((\delta v_0\circ\zeta_k^{-1})_t,p\circ\zeta_k^{-1})_{H_{\zeta_k\circ\tau}}+(\nabla\delta(v_0\circ\zeta_k^{-1}),\nabla(p\circ\zeta_k^{-1}))_{H_{\zeta_k\circ\tau}}$$

Here, as we saw in proposition C.2.2, we have $\delta w\circ\zeta_k^{-1},w\circ\zeta_k^{-1}\in Q_0(I,\mathtt{W}_{\zeta_k\circ\tau})$, $\delta v_0\circ\zeta_k^{-1},v_0\circ\zeta_k^{-1}\in Q_0(I,\mathtt{V}_{\zeta_k\circ\tau})$, $q\circ\zeta_k^{-1}\in Q^0(I,\mathtt{W}_{\zeta_k\circ\tau})$ and $p\circ\zeta_k^{-1}\in Q^0(I,\mathtt{V}_{\zeta_k\circ\tau})$.

Because $\circ\zeta_k^{-1}$ is a bijection of $Q_0(I,\mathtt{V}_{\zeta_k\circ\tau})$ and $Q_0(I,\mathtt{V}_{\zeta_k})$ by, again, proposition C.2.2 (and analogously for $\mathtt{W}$), we have that $\int_0^1 d_\phi G(k,su^k+(1-s)u^0,\psi)[\delta\phi]ds=0$ for all $\delta\phi\in E$ if and only if:

$$\int_I\left(\frac{v_0^k+w^k}{2}\circ\zeta_k^{-1}-\frac{v_0^0+w^0}{2}\circ\zeta_k^{-1}+\bar u_\tau\circ\zeta_k^{-1},\delta V_0-\delta W\right)_{H_{\zeta_k\circ\tau}}+$$
$$\int_I(\delta W_t,q\circ\zeta_k^{-1})_{H_{\zeta_k\circ\tau}}+(\nabla\delta W,\nabla(q\circ\zeta_k^{-1}))_{H_{\zeta_k\circ\tau}}+\int_I(\delta V_{0t},p\circ\zeta_k^{-1})_{H_{\zeta_k\circ\tau}}+(\nabla\delta V_0,\nabla(p\circ\zeta_k^{-1}))_{H_{\zeta_k\circ\tau}}=0$$

for all $\delta W\in Q_0(I,\mathtt{W}_{\zeta_k\circ\tau})$, $\delta V_0\in Q_0(I,\mathtt{V}_{\zeta_k\circ\tau})$.

We wish to find a (unique) solution $(q^k,p^k)\in Q^0(I,\mathtt{W}_\tau)\times Q^0(I,\mathtt{V}_\tau)$ of this problem. We can equivalently (by proposition C.2.2) find $(Q^k,P^k)\in Q^0(I,\mathtt{W}_{\zeta_k\circ\tau})\times Q^0(I,\mathtt{V}_{\zeta_k\circ\tau})$ satisfying:

$$\int_I\left(\frac{v_0^k-w^k}{2}\circ\zeta_k^{-1}+\frac{v_0^0-w^0}{2}\circ\zeta_k^{-1}+\bar u_\tau\circ\zeta_k^{-1},\delta V_0-\delta W\right)_{H_{\zeta_k\circ\tau}}+$$
$$\int_I(\delta W_t,Q^k)_{H_{\zeta_k\circ\tau}}+(\nabla\delta W,\nabla Q^k)_{H_{\zeta_k\circ\tau}}+\int_I(\delta V_{0t},P^k)_{H_{\zeta_k\circ\tau}}+(\nabla\delta V_0,\nabla P^k)_{H_{\zeta_k\circ\tau}}=0$$

for all $\delta W, \in Q_0(I, \mathtt{W}_{\zeta_k \circ \tau})$, $\delta V_0 \in Q_0(I, \mathtt{V}_{\zeta_k \circ \tau})$.

Upon testing first with $\delta W = 0$ and then with $\delta V_0 = 0$, an application of integration by parts in time (see proposition B.3.3) yields the problems which are the weak formulations (cfr. theorem C.3.2, problem B.2.2 and problem B.2.2) of the PDEs:

$$\begin{cases} -Q_t^k - \Delta Q^k = \frac{v_0^k - w^k + v_0^0 - w^0}{2} \circ \zeta_k^{-1} + \bar{u}_\tau \circ \zeta_k^{-1} \\ Q^k(T) = 0 \\ \partial_\nu Q^k = 0 \text{ on } \Sigma_f \\ Q^k = 0 \text{ on } \Sigma_{m,k} \end{cases}, \quad \begin{cases} -P_t^k - \Delta P^k = -\frac{v_0^k - w^k + v_0^0 - w^0}{2} \circ \zeta_k^{-1} - \bar{u}_\tau \circ \zeta_k^{-1} \\ P^k(T) = 0 \\ P^k = 0 \text{ on } \Sigma_f \\ P^k = 0 \text{ on } \Sigma_{m,k} \end{cases}$$

Applying the time reversal $t \mapsto T - t$ (where $I = (0, T)$), these are a couple of standard heat equations for which we have available existence, uniqueness and stability results (see appendix B, and theorem B.2.6).

By calling then $\pi^k = (Q^k \circ \tau^k, P^k \circ \tau^k)$ we conclude the proof. □

We now turn to the verification of Gateaux differentiability of J, applying the techniques proposed in [58].

Proposition 2.2.9 (Averaged adjoint method for Gateaux derivatives)
Let $\delta\theta \in \Theta$, $t_k \to 0$ and $\delta\theta_k = t_k \delta\theta$. If $J'(\tau) \in \Theta^*$ satisfies

$$\lim_k \frac{G(k, u^0, \pi^k) - G(0, u^0, \pi^k)}{t_k} = J'(\tau)[\delta\theta]$$

then $J'(\tau)$ is the Gateaux derivative of J at τ.

Proof.
See theorem 3.1, [58]. □

Proposition 2.2.10 (Gateaux differentiability of J)
Given $\tau \in \mathcal{T}_a$, J is Gateaux differentiable at τ with respect to the $W^{1,\infty}$ topology. The Gateaux differential is:

$$\begin{aligned} J'(\tau)[\delta\theta] = \\ \int_I (w_t^\tau \operatorname{div}(\delta\theta \circ \tau^{-1}), q^\tau)_{L^2(\tau(U_r))} + \int_I (A'(\delta\theta \circ \tau^{-1}) \nabla v^\tau, \nabla p^\tau)_{L^2(\tau(U_r))} + \\ \int_I (v_t^\tau \operatorname{div}(\delta\theta \circ \tau^{-1}), p^\tau)_{L^2(\tau(U_r))} + \int_I (A'(\delta\theta \circ \tau^{-1}) \nabla w^\tau, \nabla q^\tau)_{L^2(\tau(U_r))} + \\ \frac{1}{2} \int_I \int_{\tau(U_r)} |v^\tau - w^\tau|^2 \operatorname{div}(\delta\theta \circ \tau^{-1}) \end{aligned}$$

where p^τ, q^τ solve:

$$\begin{cases} -q_t^\tau - \Delta q^\tau = v^\tau - w^\tau \\ q^\tau(T) = 0 \\ \partial_\nu q^\tau = 0 \text{ on } \Sigma_f \\ q^\tau = 0 \text{ on } \Sigma_m \end{cases}, \quad \begin{cases} -p_t^\tau - \Delta p^\tau = -v^\tau + w^\tau \\ p^\tau(T) = 0 \\ p^\tau = 0 \text{ on } \Sigma_f \\ p^\tau = 0 \text{ on } \Sigma_m \end{cases}$$

and where $A'(\delta\theta) = -D\delta\theta - (D\delta\theta)^t + \operatorname{div}(\delta\theta) I$.

Proof.

<u>The shape derivative is linear and bounded</u>

Linearity is immediate. For the boundedness, with C independent of $\delta\theta$, τ:

$$|J'(\tau)[\delta\theta]| \le C \left(\left\| \operatorname{div}(\delta\theta \circ \tau^{-1}) \right\|_{L^\infty(\tau(U_r))} + \left(\sum_{ij} \left\| (A'(\delta\theta \circ \tau^{-1})_{ij} \right\|_{L^\infty(\tau(U_r))} \right) \right) \le C \left\| \delta\theta \right\|_{W^{1,\infty}(\mathbb{R}^n; \mathbb{R}^n)}$$

where in the last step we applied proposition C.1.5.

<u>Conclusion</u>

Assume at first that $p^k \rightharpoonup p^0$ in $Q(I, \mathtt{V}_\tau)$ and $q^k \rightharpoonup q^0$ in $Q(I, \mathtt{W}_\tau)$, something which will be later verified. Using that $u^0 = (w^\tau, v_0^\tau)$, and cancelling the boundary integrals:

$$G(k,u^0,\pi^k)-G(0,u^0,\pi^k)=$$
$$\frac{1}{2}\int_I\int_{\tau(U_r)}|v^\tau-w^\tau|^2(|\det(D\zeta_k)|-1)+$$
$$\int_I(w_t^\tau(|\det(D\zeta_k)|-1),q^k)_{H_\tau}+((A_{\zeta_k}-I)\nabla w^\tau,\nabla q^k)_{H_\tau}+\int_I(v_t^\tau(|\det(D\zeta_k)|-1),p^k)_{H_\tau}+((A_{\zeta_k}-I)\nabla v^\tau,\nabla p^k)_{H_\tau}$$

Now, the application $\delta\theta\mapsto \mathrm{Id}+\delta\theta\circ\tau^{-1}$ is Fréchet differentiable at $\delta\theta=0$, as a map of Θ into $\mathcal{V}^1$, with Fréchet derivative $\delta\theta\circ\tau^{-1}$, which is linear and bounded in $\delta\theta$ by proposition C.1.5.

Also, the maps $\delta\eta\mapsto|\det(D\eta)|$ and $\eta\mapsto(D\eta)^{-1}(D\eta)^{-t}|\det D\eta|$ are Fréchet differentiable at Id, from $\mathcal{V}^1$ into $L^\infty(\mathbb{R}^n;\mathbb{R})$ and $L^\infty(\mathbb{R}^n;\mathbb{R}^{n\times n})$, as stated in lemma 4.16, page 80 of [44]. Their Fréchet derivatives are $\mathrm{div}(\beta)$ and $I-D\beta-(D\beta)^t$, respectively.

Therefore, composition with $\delta\theta\mapsto\mathrm{Id}+\delta\theta\circ\tau^{-1}$ yields two Fréchet differentiable maps, $\delta\theta_k\mapsto|\det(D\zeta_k)|$ and $\delta\theta_k\mapsto A_{\zeta_k}$, whose derivatives at 0, in direction $\delta\theta\in\Theta$, are exactly $\mathrm{div}(\delta\theta\circ\tau^{-1})$ and $A'(\delta\theta\circ\tau^{-1})$, so that:

- $|\det(D\zeta_k)|-1=|\det(D\zeta_k)|-1-t_k\mathrm{div}(\delta\theta\circ\tau^{-1})+t_k\mathrm{div}(\delta\theta\circ\tau^{-1})=o_k^1+t_k\mathrm{div}(\delta\theta\circ\tau^{-1})$
- $A_{\zeta_k}-I=A_{\zeta_k}-I-t_kA'(\delta\theta\circ\tau^{-1})+t_kA'(\delta\theta\circ\tau^{-1})=o_k^2+t_kA'(\delta\theta\circ\tau^{-1})$

where $o_1^k\in L^\infty(\mathbb{R}^n;\mathbb{R})$ and $o_k^2\in L^\infty(\mathbb{R}^n;\mathbb{R}^{n\times n})$ are higher order terms, in L^∞ and with respect to t_k. We can then write $(G(k,u^0,\pi^k)-G(0,u^0,\pi^k))/t_k=a_k+o_k$.

Here:

$$a_k:=\frac{1}{2}\int_I\int_{\tau(U_r)}|v^\tau-w^\tau|^2\mathrm{div}(\delta\theta\circ\tau^{-1})+$$
$$\int_I(w_t^\tau\mathrm{div}(\delta\theta\circ\tau^{-1}),q^k)_{H_\tau}+(A'(\delta\theta\circ\tau^{-1})\nabla w^\tau,\nabla q^k)_{H_\tau}+\int_I(v_t^\tau\mathrm{div}(\delta\theta\circ\tau^{-1}),p^k)_{H_\tau}+(A'(\delta\theta\circ\tau^{-1})\nabla v^\tau,\nabla p^k)_{H_\tau}$$

Thanks to the assumed weak convergence, $a_k\to J'(\tau)[\delta\theta]$. So, we still have to show that:

$$o_k:=\frac{1}{2}\int_I\int_{\tau(U_r)}|v^\tau-w^\tau|^2o_k^1t_k^{-1}+\int_I(w_t^\tau o_k^1t_k^{-1},q^k)_{H_\tau}+(t_k^{-1}o_k^2\nabla w^\tau,\nabla q^k)_{H_\tau}+\int_I(v_t^\tau o_k^1t_k^{-1},p^k)_{H_\tau}+(t_k^{-1}o_k^2\nabla v^\tau,\nabla p^k)_{H_\tau}$$

goes to zero. This is true thanks to the boundedness of the averaged adjoint states, which stems from their weak convergence, and the properties of o_k^1,o_k^2.

Weak convergence of states

We assumed $p^k\rightharpoonup p^0$ in $Q(I,\mathtt{V}_\tau)$ and $q^k\rightharpoonup q^0$ in $Q(I,\mathtt{W}_\tau)$. We now prove these claims. We show at first $v_0^k\rightharpoonup v_0^0$ in $Q(I,\mathtt{V}_\tau)$ and $w^k\rightharpoonup w^0$ in $Q(I,\mathtt{W}_\tau)$. We do this by uniformly estimating these quantities on k. To do this, we use the equations of $V_0^k:=v_0^k\circ\zeta_k^{-1}$ and $W^k:=w^k\circ\zeta_k^{-1}$ (see theorem C.3.2) and theorem B.2.6, to obtain the stability estimates:

$$\left\|V^k\right\|^2_{C([0;T],H_{\zeta_k\circ\tau})}+\left\|V^k\right\|^2_{L^2(I,H_{\zeta_k\circ\tau})}+\left\|\nabla V^k\right\|^2_{L^2(I,H_{\zeta_k\circ\tau})}+\left\|(V^k)_t\right\|^2_{L^2(I,H_{\zeta_k\circ\tau})}\le C\left\|U^k\right\|^2_{H^1(I,\mathtt{W}_{\zeta_k\circ\tau})}$$
$$\left\|W^k\right\|^2_{C([0;T],H_{\zeta_k\circ\tau})}+\left\|W^k\right\|^2_{L^2(I,H_{\zeta_k\circ\tau})}+\left\|\nabla W^k\right\|^2_{L^2(I,H_{\zeta_k\circ\tau})}+\left\|W_t^k\right\|^2_{L^2(I,H_{\zeta_k\circ\tau})}\le C\left\|g\right\|^2_{H^1(I,L^2(\Gamma_f))}$$

where C is independent of k.

Now, consider theorem C.2.1. It says that for almost every time:

$$\left\|U^k\right\|_{\mathtt{W}_{\zeta_k\circ\tau}}\le\left(1+\|\det D\zeta_k\|_{L^\infty(\mathbb{R}^n)}\right)^{1/2}\left\|(D\zeta_k)^{-1}\right\|_{L^\infty(\mathbb{R}^n;\mathbb{R}^{n\times n})}\|\bar{u}\|_{H^1(\tau(U_r));\mathbb{R}^n)}$$

and a similar estimate we have for the first derivative. This bound is uniform on k by proposition C.1.5.

We conclude that $\left\|U^k\right\|^2_{H^1(I,\mathtt{W}_{\zeta_k\circ\tau})}$ is bounded and we thus have that $W^k\in Q_0(I,\mathtt{W}_{\zeta_k\circ\tau}),V_0^k\in Q_0(I,\mathtt{V}_{\zeta_k\circ\tau})$ are bounded.

Now, for almost all times, using theorem C.2.1, we obtain that, for instance:

$$\left\|v_0^k\right\|_{\mathtt{W}_\tau}\le\left(1+\left\|\det(D\zeta_k)^{-1}\right\|_{L^\infty(\mathbb{R}^n)}\right)^{1/2}\|D\zeta_k\|_{L^\infty(\mathbb{R}^n;\mathbb{R}^{n\times n})}\left\|V_0^k\right\|_{H^1(\zeta_k(\tau(U_r)))}$$

where we remember that H_0^1 was chosen to be normed with the full H^1 norm.

The same goes for w^k and the first derivatives in time, yielding that $w^k\in Q_0(I,\mathtt{W}_\tau),v_0^k\in Q_0(I,\mathtt{V}_\tau)$ are bounded.

We thus have $w^k\rightharpoonup w^?\in Q_0(I,\mathtt{W}_\tau)$, $v_0^k\rightharpoonup v_0^?\in Q_0(I,\mathtt{V}_\tau)$, in the weak topologies of, respectively, $Q(I,\mathtt{W}_\tau),Q(I,W_\tau)$, and modulo subsequences. The initial values are preserved because Q_0 is closed and convex in the Hilbert space Q (see also proposition B.3.3).

We now prove that $w^?=w^0$, $v^?=v^0$, and this will yield the weak convergence of the whole sequence. To prove e.g. that $v^?=v^0$, let us look at the weak formulations of v_0^k:

$$\int_I (v_{0t}^k, p|\det(D\zeta_k)|)_{H_\tau} + (A_{\zeta_k}\nabla v_0^k, \nabla p)_{H_\tau} + (\bar{u}', p|\det(D\zeta_k)|)_{H_\tau} + (A_{\zeta_k}\nabla \bar{u}, \nabla p)_{H_\tau} = 0$$

for all $p \in Q_0(I, \mathtt{V}_\tau)$. Let's analyze the first term, which is $\int_I (v_{0t}^k, p|\det(D\zeta_k)|)_{H_\tau}) = (v_{0t}^k, p|\det(D\zeta_k)|)_{L^2(I,H_\tau)}$. We can write:

$$(v_{0t}^k, p|\det(D\zeta_k)|)_{L^2(I,H_\tau)} = (v_{0t}^k, p)_{L^2(I,H_\tau)} + (v_{0t}^k, p(|\det(D\zeta_k)| - 1))_{L^2(I,H_\tau)}$$

Because $p \in Q(I, \mathtt{V}_\tau)$, the first term converges to $(v_{0t}^?, p)_{L^2(I,H_\tau)}$. The other term can be estimated as follows:

$$|(v_{0t}^k, p(|\det(D\zeta_k)| - 1))_{L^2(I,H_\tau)}| \leq \left\|v_{0t}^k\right\|_{L^2(I,H_\tau)} \|p\|_{L^2(I,H_\tau)} \||\det(D\zeta_k)| - 1\|_{L^\infty}$$

where the first term in the product is bounded by the weak convergence property, and the last one goes to 0 by continuity, see again proposition C.1.5. In a similar fashion for the other pieces, and by passing to the limit:

$$\int_I (v_{0t}^?, p)_{H_\tau} + (\nabla v_0^?, \nabla p)_{H_\tau} + (\bar{u}', p)_{H_\tau} + (\nabla \bar{u}, \nabla p)_{H_\tau} = 0$$

so that $v^? = v^0$.

Weak convergence of averages adjoint states

So, $v_0^k \rightharpoonup v_0^0, w^k \rightharpoonup w^0$ in $Q(I, \mathtt{V}_\tau)$ and $Q(I, \mathtt{W}_\tau)$. We now claim that $p^k \rightharpoonup p^0, q^k \rightharpoonup q^0$, and prove this similarly to before. We bound $P^k := p^k \circ \zeta_k^{-1}$ and $Q^k := q^k \circ \zeta_k^{-1}$. By proposition B.1.8, we will obtain a bound in Q as soon as we have a bound on $\dfrac{v_0^k - w^k + v_0^0 - w^0}{2} \circ \zeta_k^{-1}$ in the $L^2(I, H)$ norm, and of $U^k := \bar{u}_\tau \circ \zeta_k^{-1}$. The latter was proven above.

So, by theorem C.2.1 and proposition C.1.5, it suffices to have an $L^2(I, H)$ bound on $\dfrac{v_0^k + w^k + v_0^0 + w^0}{2} \circ \zeta_k^{-1} \circ \zeta_k = \dfrac{v_0^k + w^k + v_0^0 + w^0}{2}$ which we have, since we just proved that v_0^k, w^k are weakly convergent in e.g. $L^2(I, H)$. We conclude that Q^k, P^k are bounded in the $Q(I, \mathtt{W}_{\zeta_k \circ \tau})$ and $Q(I, \mathtt{V}_{\zeta_k \circ \tau})$ sense, so that, just as above, a bound on q^k, p^k in the $Q(I, \mathtt{W}_\tau)$ and $Q(I, \mathtt{V}_\tau)$ can be obtained.

We conclude that there exist $q^?, p^?$ in $Q^0(I, \mathtt{W}_\tau)$, $Q^0(I, \mathtt{V}_\tau)$, that are, modulo subsequences, the weak limits of q^k, p^k. To show e.g. $q^? = q^0$ and conclude the convergence of the full sequence, we analyze the weak formulation of q^k, which reads, after going to the moving domain and applying integration by parts in time (see proposition B.3.3):

$$-\int_I \left(\frac{((v_0^k + \bar{u}_\tau - w^k) + (v_0^0 + \bar{u}_\tau - w^0)}{2}\right) |\det(D\zeta_k)|, \delta w)_{H_\tau} = -\int_I (q_t^k, \delta w|\det(D\zeta_k)|)_{H_\tau} + (A_{\zeta_k}\nabla \delta w, \nabla q^k)_{H_\tau}$$

for all $\delta w \in Q_0(I, \mathtt{W}_\tau)$.

We show the convergence of e.g. the member: $\int_I (v_0^k|\det(D\zeta_k)|, \delta w)_{H_\tau}$. By splitting the scalar product as we saw above, we are left with checking that $\int_I (v_0^k, \delta w)_{H_\tau} \to \int_I (v_0^0, \delta w)_{H_\tau}$, which is true, since we proved that $v_0^k \rightharpoonup v_0^0$ in $Q(I, \mathtt{V}_\tau)$. We conclude, upon passing to the limit, that:

$$-\int_I \left(\frac{((v_0^0 + \bar{u}_\tau - w^0) + (v_0^0 + \bar{u}_\tau - w^0)}{2}), \delta w\right)_{H_\tau} = -\int_I (q_t^?, \delta w)_{H_\tau} + (\nabla \delta w, \nabla q^?)_{H_\tau}$$

which is satisfied also by q^0, therefore $q^? = q^0$ and we have weak convergence of the entire sequence. □

2.3. Domains parametrization

Here we reparametrize the shape optimization problem assuming the domains $D, \Omega = \tau(\Omega_r)$ to be star-shaped with respect to the origin. We do this to justify our computer implementation. In particular, we define and analyze certain maps that convert functions defined on spheres to "radial" deformation fields defined on $D \setminus \overline{\Omega}$ (see below for details), and based on those, detail the expression of the shape gradient of proposition 2.2.10. This will be the result of proposition 2.3.8. Essentially, this section is concerned with connecting the analysis previously done with general tranformations τ, to more special radial transformations, employing and adapting the framework of [21]. We start by recalling the definition of star-shaped domain.

Proposition 2.3.1 (Star-shaped domains)
Let $f \in C(\mathbb{S}^{n-1})$, $f > 0$. Define $\Omega_f := \{x, |x| < f(\hat{x})\} \cup \{0\}$, where $\hat{x} = x/|x|$. Then:

- Ω_f is open
- Ω_f has boundary $\{x, |x| = f(\hat{x})\}$
- Ω_f is a bounded Lipschitz domain if $f \in W^{1,\infty}(\mathbb{S}^{n-1})$

Proof.

For $x \in \partial\Omega_f$ (so, $x \neq 0$) we find $x_n, y_n \to x$ with $|x_n| < f(\widehat{x_n})$ and $|y_n| \geq f(\widehat{y_n})$. For large n and by continuity, $|x| = f(\hat{x})$ and we have shown one inclusion.

For the reverse, and $x, |x| = f(\hat{x})$ (so, $x \neq 0$), we define $x_n = \frac{n}{n+1}x$ which satisfies $|x_n| < |x| = f(\hat{x}) = f(\widehat{x_n})$, that is, $x_n \in \Omega_f$, and also $x_n \to x$. This shows that $x \in \partial\Omega_f$.

It is a bounded Lipschitz domain by lemma 2 at page 96 of [14], and lemma 5 at page 151 also of [14]. Note that the definition of Lipschitz domain of [14] is completely equivalent to that of [3] (and at least implies that of [48], [35], [43], [1], a fact which is needed in the sequel), by an application of the Lebesgue number lemma, whose statement can be found at e.g. page 179 of [51]. □

We now define maps relating a radial function to its correspondent a star-shaped domain. We choose $0 < \epsilon < f_D \in W^{1,\infty}(\mathbb{S}^{n-1})$, to parametrize the non moving part of the optimization domain. The reference domain U_r is taken to be $U_r := \Omega_{f_D} \setminus \overline{B}_\epsilon$, and we call $D := \Omega_{f_D}$

Proposition 2.3.2 (H_f, A_f)
Let $\epsilon < f_D \in W^{1,\infty}(\mathbb{S}^{n-1})$ and $0 < f \in W^{1,\infty}(\mathbb{S}^{n-1}), f < f_D$, and define:

- $H_f(x) := \begin{cases} \frac{x}{\epsilon} f(\hat{x}) & x \neq 0 \\ 0 & x = 0 \end{cases}$, as a function $\mathbb{R}^n \to \mathbb{R}^n$
- $A_f(x) := \left(f(\hat{x}) + \frac{f_D(\hat{x}) - f(\hat{x})}{f_D(\hat{x}) - \epsilon}(|x| - \epsilon) \right) \hat{x}$, as a function $\mathbb{R}^n \setminus \{0\} \to \mathbb{R}^n$

They enjoy the following properties:

1. $H_f(B_\epsilon) = \Omega_f$, $H_f(\epsilon\mathbb{S}^{n-1}) = \partial\Omega_f$
2. $A_f(D \setminus \overline{B_\epsilon}) = D \setminus \overline{\Omega_f}$, $A_f(\partial D) = \mathrm{Id}$, $A_f(\epsilon\mathbb{S}^{n-1}) = \partial\Omega_f$
3. $A_f = H_f$ on $\epsilon\mathbb{S}^{n-1}$
4. $H_f^{-1}(y) := \begin{cases} \epsilon \frac{y}{f(\hat{y})} & y \neq 0 \\ 0 & y = 0 \end{cases}$, as a function $\mathbb{R}^n \to \mathbb{R}^n$
5. $A_f^{-1}(y) := \left(\epsilon + \frac{f_D(\hat{y}) - \epsilon}{f_D(\hat{y}) - f(\hat{y})}(|y| - f(\hat{y})) \right) \hat{y}$, as a function $\overline{D} \setminus \Omega_f \to \overline{D} \setminus B_\epsilon$

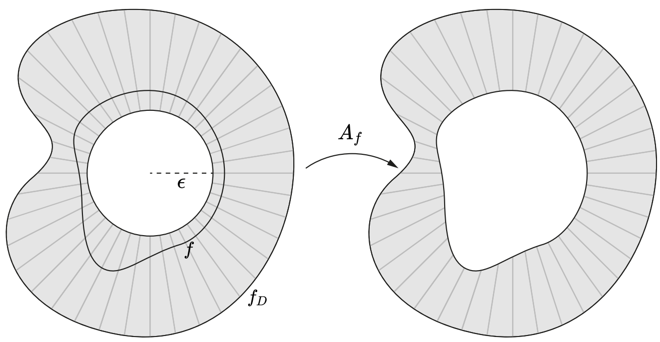

Figure 2.2.: Illustration of the action of A_f

Proof.

All the properties are straightforward from the definitions. It helps to recognize that A_f linearly maps the radial segment $[\epsilon, f_D(\hat{x})]$ to $[f(\hat{x}), f_D(\hat{x})]$. □

They also satisfy a bi-Lipschitz condition.

Proposition 2.3.3 (Bi-Lipschitz condition)
We have that $A_f : \overline{D} \setminus B_\epsilon \to \overline{D} \setminus \Omega_f$ is Lipschitz with Lipschitz inverse (bi-Lipschitz), and so is $H_f : \mathbb{R}^n \to \mathbb{R}^n$.

Proof.

$\underline{H_f}$

We can assume both $x, y \neq 0$. Then $|f(\hat{x})x - f(\hat{y})y| \leq |x||f(\hat{x}) - f(\hat{y})| + f(\hat{y})|x - y|$. Employing direct and reverse triangle inequalities we get $|\hat{x} - \hat{y}| \leq \frac{2}{|x|}|x - y|$. As f is Lipschitz, we obtain: $|f(\hat{x})x - f(\hat{y})y| \leq |x|C(f)\frac{2}{|x|}|x - y| + C(f)|x - y|$, see [21] for more details.

Now, $1/f$ is also Lipschitz and bounded, because $f > 0$ and is continuous on a compact set. Thus the same proof shows the Lipschitz property also for H_f^{-1}.

$\underline{A_f}$

Call $A_f(x) = \left(f(\hat{x}) + \frac{f_D(\hat{x})-f(\hat{x})}{f_D(\hat{x})-\epsilon}(|x|-\epsilon)\right)\hat{x} =: Q(x)\hat{x}$. Because $|x| \geq \epsilon$, as before, we obtain $|A_f(x) - A_f(y)| \leq 2/\epsilon Q(x)|x-y| + |Q(x) - Q(y)|$, so that we need to show that Q is bounded Lipschitz.

By continuity and compactness, $f_D(\hat{x}) - \epsilon \geq \delta > 0$ and boundedness follows. The Lipschitz property follows because Q is a sum of products of bounded Lipschitz functions.

Analogous reasonings let us prove also the Lipschitz property of A_f^{-1}. □

We now try to glue H_f, A_f together to still obtain a bi-Lipschitz function. Even the Lipschitz property doesn't hold after gluing, in general, see page 7 of [62] for a counterexample. We therefore proceed to the proof of this fact, starting with a lemma.

Lemma 2.3.4 (Gluing Lipschitz functions along $\epsilon\mathbb{S}^{n-1}$)
Let $\mathbb{R}^n \supseteq A \supseteq \epsilon\mathbb{S}^{n-1}$ be a set. Suppose that $g : A \to \mathbb{R}^n$ and $h : \overline{B_\epsilon} \to \mathbb{R}^n$ are Lipschitz and that they agree on $\epsilon\mathbb{S}^{n-1}$. The, their gluing $f : A \cup \overline{B_\epsilon} \to \mathbb{R}^n$ is Lipschitz.

Proof.
We can assume that $x \in B_\epsilon$, $y \in A \setminus \overline{B_\epsilon}$. Then, $|f(x) - f(y)| \leq |h(x) - h(\epsilon\hat{y})| + |g(\epsilon\hat{y}) - g(y)|$.

We claim at first that $|y - \epsilon\hat{y}| \leq |x - y|$. To see this, choose $n := \hat{y}$. Then $|y-x|^2 \geq |(y-x)\cdot nn|^2$ by Pythagoras' theorem, so that $|y-x| \geq |(y-x)\cdot n| = |(y-\epsilon\hat{y})\cdot n + (\epsilon\hat{y}-x)\cdot n|$. But $(y-\epsilon\hat{y})\cdot n = |y| - \epsilon \geq 0$, and $(\epsilon\hat{y}-x)\cdot n = \epsilon - x\cdot n \geq 0$ as $x \cdot n \leq |x| \leq \epsilon$.

Thus $|y-x| \geq |(y-\epsilon\hat{y})\cdot n| + |(\epsilon\hat{y}-x)\cdot n| \geq |(y-\epsilon\hat{y})\cdot n| = |y-\epsilon\hat{y}|$.

We also claim that $|x-\epsilon\hat{y}| \leq |x-y|$. To do so, pick $n := \frac{\epsilon\hat{y}-x}{|\epsilon\hat{y}-x|}$. By Pythagoras' theorem we obtain $|y-x| \geq |(y-x)\cdot n| = |(y-\epsilon\hat{y})\cdot n + (\epsilon\hat{y}-x)\cdot n|$. The second summand is non-negative and for the first one, it is directly proportional to $(y-\epsilon\hat{y})\cdot(\epsilon\hat{y}-x) = (|y|-\epsilon)(\epsilon-\hat{y}\cdot x) \geq 0$. So, $|x-y| \geq |(\epsilon\hat{y}-x)\cdot n| = |\epsilon\hat{y}-x|$.

Thus $|f(x) - f(y)| \leq C|x-y|$ as desired. □

Proposition 2.3.5 (Gluing H_f^{-1}, A_f^{-1})
H_f^{-1}, A_f^{-1}, or also A_f, H_f can be glued into a Lipschitz function $\overline{D} \to \overline{D}$.

Proof.
Call τ_f^{-1} the gluing. It is Lipschitz $\overline{D} \to \overline{D}$ if and only if $\tau_f^{-1} \circ H_f$ is Lipschitz $H_f^{-1}(\overline{D}) \to \mathbb{R}^n$, because we proved that H_f is bi-Lipschitz $\mathbb{R}^n \to \mathbb{R}^n$. We are therefore left to check that gluing Lipschitz functions along $\epsilon\mathbb{S}^{n-1}$ produces a Lipschitz function, which would also yield the claim for τ_f, that is the gluing of A_f, H_f. This is the content of lemma 2.3.4. □

Corollary 2.3.6 (Radial to volumetric transformation)
Let again $\epsilon < f_D \in W^{1,\infty}(\mathbb{S}^{n-1})$ and $0 < f \in W^{1,\infty}(\mathbb{S}^{n-1}), f < f_D$. Define:

- $$\tau_f(x) := \begin{cases} x & |x| \geq f_D(\hat{x}) \\ \left(f(\hat{x}) + \frac{f_D(\hat{x})-f(\hat{x})}{f_D(\hat{x})-\epsilon}(|x|-\epsilon)\right)\hat{x} & \epsilon \leq |x| \leq f_D(\hat{x}) \\ \frac{x}{\epsilon}f(\hat{x}) & 0 < |x| \leq \epsilon \\ 0 & |x| = 0 \end{cases}$$

- $$\tau_f^{-1}(y) := \begin{cases} x & |y| \geq f_D(\hat{y}) \\ \left(\epsilon + \frac{f_D(\hat{y})-\epsilon}{f_D(\hat{y})-f(\hat{y})}(|y| - f(\hat{y}))\right)\hat{y} & f(\hat{y}) \leq |y| \leq f_D(\hat{y}) \\ \epsilon\frac{y}{f(\hat{y})} & 0 < |y| \leq f(\hat{y}) \\ 0 & |y| = 0 \end{cases}$$

Then $\tau_f \in \mathcal{T}$, i.e. it is a bi-Lipschitz homeomorphism.

Proof.
The final gluing on the border of D yields a Lipschitz function: we can see this by taking $\mathrm{Id} - \tau_f^{\pm 1}$, which is Lipschitz and vanishing on ∂D, so that we are dealing with the zero extension outside D of a Lipschitz function, null on ∂D. Such extension is readily shown to be Lipschitz. □

Observation 2.3.7 (Obtaining Lipschitz domains).
Note that as long as $0 < f < f_D$ are Lipschitz, $\tau_f(U_r)$ will always be a bounded Lipschitz domain. This is a more transparent of securing this fact, than imposing $\|\tau - \mathrm{Id}\|_{W^{1,\infty}(\mathbb{R}^n;\mathbb{R}^n)} < C(U_r)$, as seen in definition 2.2.2.

We finally have a look at shape derivatives in this radial framework. The reparametrized cost functional is $j(\sigma) := J(\tau_{\epsilon+\sigma})$, where $0 < \sigma + \epsilon < f_D$. We are interested, for $h \in W^{1,\infty}(\mathbb{S}^{n-1})$, in the limit

$$\lim_{t\to 0} \frac{j(\sigma + th) - j(\sigma)}{t} = \lim_{t\to 0} \frac{J(\tau_{\epsilon+\sigma+th}) - J(\tau_{\sigma+\epsilon})}{t}$$

Now, we derive the expression of a displacement field V_h, to connect this difference quotient to the already computed shape derivative, see also [21]. The ansatz $\tau_{\sigma+th} = (\mathrm{Id} + tV_h \circ \tau_\sigma^{-1}) \circ \tau_\sigma$ brings us to $V_h = \dfrac{\tau_{\sigma+th} - \tau_\sigma}{t}$, and by some computations, we obtain:

$$V_h(x) := \begin{cases} 0 & |x| \geq f_D(\hat{x}) \\ h(\hat{x}) \frac{f_D(\hat{x}) - |x|}{f_D(\hat{x}) - \epsilon} \hat{x} & \epsilon \leq |x| \leq f_D(\hat{x}) \\ \frac{x}{\epsilon} h(\hat{x}) & 0 < |x| \leq \epsilon \\ 0 & |x| = 0 \end{cases}$$

This expression only depends on h and is the gluing of Lipschitz functions, that are either 0 at the gluing points, or such that the gluing points lie in $\epsilon\mathbb{S}^{n-1}$. Note, this vector field is just moving $\epsilon\mathbb{S}^{n-1}$ radially by h and radially damping this movement to 0 close to ∂D. Therefore:

Proposition 2.3.8 (Shape derivative, star shaped case)
We have the following facts, for $h \in W^{1,\infty}(\mathbb{S}^{n-1})$, $0 < \sigma < f_D$, $\sigma \in W^{1,\infty}(\mathbb{S}^{n-1})$:

- $\tau_{\sigma+th} = (\mathrm{Id} + tV_h \circ \tau_\sigma^{-1}) \circ \tau_\sigma$
- $V_h \in \Theta$
- j is Gateaux differentiable at every $0 < \sigma < f_D$, $\sigma \in W^{1,\infty}(\mathbb{S}^{n-1})$, with $j'(\sigma)[h] = J'(\tau_{\epsilon+\sigma})[V_h]$

Proof.
We only need to show that $h \mapsto V_h$ is linear bounded between $W^{1,\infty}(\mathbb{S}^{n-1}) \to \Theta$. Linearity is immediate and for the boundedness: $\sup_x |V_h(x)| = \|h\|_\infty$, so that there only remains to bound the Lipschitz constant of V_h.

To do so, we note that extending to zero a Lipschitz function doesn't increase its Lipschitz constant, so that we only need to look at the restriction to D.

The gluing lemma lemma 2.3.4 shows that it is sufficient to bound the Lipschitz constants of the two branches of V_h, separately. These bounds are, respectively: $C(\|h\|_\infty + 2\|D_T h\|_\infty)$ and $[2\epsilon^{-1}(\|D_T h\|_\infty + \|h\|_\infty)]C + C\|h\|_\infty$, where $C = (\epsilon, f_D) > 0$, which concludes the proof. □

2.3.1. Smooth star-shaped domains

To ensure that U has the smoothness required to perform numerical analysis, we want to increase the regularity of f and see an increase in the regularity of $\partial\Omega_f$.

Proposition 2.3.1.1 (Smooth radial function yields smooth star shaped domain)
Let $f > 0$ which is either $C^{1,1}(\mathbb{S}^{n-1})$ (that is, C^1 with all the components of $D_T f$ Lipschitz) or $C^2(\mathbb{S}^{n-1})$.
Then, Ω_f has boundary of class $C^{1,1}$ or C^2.

Proof.
In what follows we generically write C^o, $o = 1, 1$ or $o = 2$. The argument will go like this:

- we show that H_f preserves smooth boundaries, where smoothness here is in the sense of charts (see e.g. [56], pages II-39,40)
- using the implicit function theorem, we see that smoothness in the sense of charts implies smoothness in the sense of hypergraph, see e.g. [35], which is the notion we are working with, see definition 1.2.1.1

<u>Punctured diffeomorphisms</u>

We consider H_f, setting $\epsilon = 1$ for simplicity. It has gradient (see [21]) $DH_f(x) = f(\hat{x})I + \hat{x} \otimes D_T f(\hat{x})$, and $DH_f^{-1}(y) = 1/f(\hat{y})I - 1/f(\hat{y})^2 \hat{y} \otimes D_T f(\hat{y})$. We conclude that $H_f : \overline{B_\delta(0)}^c \to \overline{H_f(B_\delta(0))}^c$ is a C^o diffeomorphism, where the set on the right is open by H_f being a homeomorphism of $\mathbb{R}^n$, and $\delta < 1 = \epsilon$.

We have therefore obtained a homeomorphism $H_f^{-1} : \mathbb{R}^n \to \mathbb{R}^n$, which is $C^o(\overline{H_f(B_\delta(0))}^c; \overline{B_\delta(0)}^c)$, i.e. whose domain is a neighbourhood of $\partial\Omega_f$. For simplicity let's call such maps C^o punctured diffeomorphisms for Ω_f.

<u>Punctured diffeomorphism preserves C^o domains in the sense of charts</u>

Let Ω be of class C^o (always locally) and bounded. Assume we have F, a punctured diffeomorphism for Ω, so, $F : \mathbb{R}^n \to \mathbb{R}^n$ is a homeomorphism, and $F : U \to F(U)$ is C^o, $\partial\Omega \subset\subset U$. Then, by analyzing the composition of F with (small enough) charts of Ω we see that $F(\Omega)$ is another C^o domain.

<u>From charts to hypergraphs</u>

Let a radial function $f > 0$ be of class C^o. H_f is punctured diffeomorphism of class C^o, so that we have that $\partial\Omega_f$ is the image of $\epsilon\mathbb{S}^{n-1}$, a domain of class C^o in the sense of charts. So Ω_f is of class C^o too, in the sense of charts.

So, let $x \in \partial\Omega$. We obtain $A \ni x, B$ open, and $\eta : A \to B$ a C^o diffeomorphism, with $\eta^{-1}(B \cap \mathbb{R}^n_+) = A \cap \Omega$, and $\eta(x) = 0$.

Applying the implicit function theorem in a suitable way (e.g. through minor reworkings of the proofs at page 310, 311 of [33]), we obtain:

- a "square" and an interval V', I with $V' \times I \ni x$
- $\phi : V' \to I$, Lipschitz, of class C^o

- $\phi(V') \subset\subset J \subset\subset I$
- $z \in V' \times I, z_n < \phi(z) \iff z \in (V' \times I) \cap \Omega$
- (and consequently, $z \in V' \times I, z_n = \phi(z) \iff z \in (V' \times I) \cap \partial\Omega$)

By a compactness argument, finitely many $V_j = V_j' \times (a_n^j, b_n^j)$ are necessary to cover $\partial\Omega_f$.

So, we have $V_j \cap \Omega_f = V_j \cap \{x_n < \phi_j(x')\} = V \cap \{a_n^j < x_n < \phi_j(x'), x' \in V_j'\}$. Choose $d > 0$ to be the minimum gap between ϕ_j and I_j. $d > 0$ by the existence of $J_j \subset\subset I_j$. We call L the maximum Lipschitz constant of ϕ_j. We have therefore obtained a Lipschitz and C^o domain in the style of [14], which yields, modulo an application of the Lebesgue number lemma, a C^o and Lipschitz domain in the style of [35], whose definition we are working with. □

2.4. Descent directions

To approximate a solution of problem 2.2.3 one must apply a discretization strategy and solve an optimization problem in finite dimensions instead. We will adopt gradient based optimization algorithms, where we compute search directions from the knowledge of the discretized shape derivative. In general, the shape derivative on the continuous level is just a functional: one can try to extract a descent direction from its knowledge using the Riesz representation theorem.

In shape optimization, however, one works with spaces which are not Hilbert, e.g. $W^{1,\infty}$, so scalar products are not available. A way around this is illustrated in [21], where descent directions are directly searched in $W^{1,\infty}$ without relying on the Riesz theorem. Another possibility is to look for descent directions in a larger, Hilbert space $\mathcal{H} \supset W^{1,\infty}$, provided that j' extends to this space, where we can use the representation theorem. This "Hilbert space" approach was of easier implementation for us, and we decided to stick with it. Moreover, it is a standard trick in the shape optimization literature (see [2], section 5.2) and it can usually yield good results.

Nonetheless, this approach is not completely rigorous (because we want controls in $W^{1,\infty}$, at least, by perturbing them by $\mathcal{H}$ descent directions), and also, it is not immediate which $\mathcal{H}$, hence, which scalar product, one should use. Unfortunately, choosing the "wrong" one can yield descent directions that are too "squiggly" (see section 4.2 for an example, in particulare fig. 4.7), or mesh-dependence effects, where finer and finer meshes require more and more optimization iterations to converge (see [55]).

Through experimentations, see chapter 4 and specifically section 4.1 we observed decent results when using the H^1 scalar product, as opposed to when the L^2 product is used instead. On a continuous level, and in the star-shaped setting we described previously, this means finding descent directions $h \in H^1(\mathbb{S}^{n-1})$ from the equation:

$$(r(\sigma), h)_{H^1(\mathbb{S}^{n-1})} = j'(\sigma)[h]$$

where $r(\sigma)$ represents, via the Riesz representation theorem, the functional $j'(\sigma)$. $h := -r(\sigma)$ is e.g. a descent direction

For further details regarding this so-called "Hilbertian regularization" procedure, we again refer to [2]. We limit ourselves to sketching a proof of the fact that $j'(\sigma)$ can act on the larger space $H^1(\mathbb{S}^{n-1})$ and that it is continuous in the H^1 topology, thus making the operation of taking its Riesz representative well defined.

At first we remark that $h \mapsto V_h$ maps $H^1(\mathbb{S}^{n-1})$ functions into $H^1(\mathbb{R}^n; \mathbb{R}^n)$ functions. To see this, note that h can be approximated by smooth functions h_k, in the H^1 norm (see definition 2.3 of [4]). For the generic term of the approximating sequence we can employ integration in spherical coordinates and use the fact that h_k is Cauchy, to get that V_{h_k} is Cauchy in $H^1(\mathbb{R}^n; \mathbb{R}^n)$, and that it converges to V_h. This procedure also yields a bound on the norm of $H^1(\mathbb{S}^{n-1}) \to H^1(\mathbb{R}^n; \mathbb{R}^n) : h \mapsto V_h$.

Now, consider the expression of the shape derivative, given in proposition 2.2.10. We identify three different terms. We write u for a state v or w, and a for the corresponding adjoint, leaving out the dependence on τ for simplicity:

$$\int_I (u_t, \mathrm{div}(\delta\theta \circ \tau_\sigma^{-1})a)_{L^2(U)}, \quad \int_I (A'(\delta\theta \circ \tau_\sigma^{-1})\nabla u, \nabla a)_{L^2(U)}, \quad \frac{1}{2}\int_I \int_U |v - w|^2 \mathrm{div}(\delta\theta \circ \tau_\sigma^{-1})$$

Here, $U = \tau_\sigma(U_r)$, $\delta\theta = V_h$.

By the H^1 properties we have just shown and thanks to theorem C.2.1, we observe that $\mathrm{div}(\delta\theta \circ \tau_\sigma^{-1})$, $A'(\delta\theta \circ \tau_\sigma^{-1})$ are square integrable. Moreover, as we will discuss very soon, we can make hypothesis on the data and a suitable modification to the cost function so that $u, a \in H^1(I, H^2(U))$, see assumption 3.1.2, where we need the regularity of σ, to have ∂U smooth enough to guarantee H^2 regularity (we have discussed this in proposition 2.3.1.1). Now, the Sobolev embedding $H^1 \hookrightarrow L^4$ (for spatial dimensions $n = 2, 3$, see e.g. [1]) and the Hölder's inequality, allow us to deduce that $j(\sigma)$ can be indeed continuously extended to $H^1(\mathbb{S}^{n-1})$.

The same conclusions follow (more easily) when the star-shaped parametrization is not employed.

3. Discretization

In this chapter we describe the numerical approximation of the PDEs of problem 2.1.1 and analyze the error in doing so. While linear finite elements are used in space, the implicit Euler or the Crank-Nicolson methods are adopted for advancing in time.

We take into account the fact non-discretized domains are smooth, while the computational ones is polygonal/polyhedral.

We are not focusing here on optimization algorithms to solve the shape identification problem, nor on the specific boundary parametrization. This will be done in chapter 4.

As a summary of the discretization approach:

- the PDEs are numerically solved on a polygonal/polyhedral approximation of the smooth domain U
- such approximation involves only knowing a finite number of points of ∂U, and not its entire parametrization
- the boundary data is queried only on these boundary nodes (this is compatible, for instance, with the case where only finite number of measurements are available)
- implicit Euler or Crank-Nicolson time steppings are adopted

We chose the latter methods because of their simplicity, overall low regularity requirements (compared to more sofisticated e.g. Runge-Kutta methods), and the fact that they are unconditionally stable, i.e. no restriction on the time step size must be made, relative to the mesh width, to obtain convergence. We can reach the required smoothness in time for the state equations, by requiring smooth data, and certain compatibility relations between them (see e.g. chapter 2 of [45] and assumption B.2.3). Smoothness of the data alone is not enough: a regular solution can be obtained, but only away from the starting time, where a singularity can develop (see e.g. the discussion in [37]). For the state equations we can reach any compatibility order, provided we make suitable assumptions on the boundary data, but the adjoint equations are, in a certain sense, fixed by the particular cost functional we chose, and the state equations themselves: unfortunately, for our adjoints, we cannot tweak the problem data to obtain any level of compatibility.

In [37], the authors work in fact with adjoint equations that have "fully" incompatible boundary data, and devise a non-standard time stepping scheme to deal with this. On the other hand, our choice of cost functional makes it possible to obtain compatibility of "order zero". This would be enough for a low order space-time method without time quadrature (see e.g. [49]), but not for the chosen fully discrete schemes. To obtain more compatibility we need to modify the data that enters the adjoint equations, and since we cannot modify the structure of the PDEs solved by the states w, v, we can only modify the cost functional. This is what we will do, with the introduction of a suitable temporal weight in the cost functional of problem 2.2.3. Such operation will yield compatibility of arbitrary order for the adjoints, at the price of partially modifying the nature of the shape optimization problem. See section 3.1 for a more thorough discussion.

An in-depth presentation and analysis of the discretization algorithms for states and adjoints is discussed in appendix D. In what follows we will build on the results therein.

As a last note, let us mention the two canonical ways, in the literature on optimal control, of discretizing a problem posed on an infinite-dimensional level:

- optimize-then-discretize: the gradient of the cost functional is derived on the continuous level (see e.g. proposition 2.2.10 in our case), some adjoint states appear and first order conditions can be formulated. Then, one proceeds with discretizing states and adjoints and the continuous optimality system, and obtains one on the discrete level
- discretize-then-optimize: the states and cost function, i.e. the continuous problem (problem 2.1.1 and problem 2.2.3) are discretized, to obtain an optimization problem posed on the discrete level. Finite dimensional optimality conditions can now be derived

In any case, one starts from an infinite-dimensional problem and obtains discrete optimality conditions, that can be employed for a numerical implementation. When the obtained discrete optimality systems from the two strategies coincide, we say that optimization and discretization commute. That is, the following diagram is commutative:

$$\begin{tikzcd}
& \text{continuous optimality system} \arrow[dr, "\text{discretization}"] & \\
\text{continuous problem} \arrow[ur, "\text{optimization}"] \arrow[dr, "\text{discretization}"'] & & \text{discrete optimality system} \\
& \text{discrete problem} \arrow[ur, "\text{optimization}"'] &
\end{tikzcd}$$

Although in general not a trivial task, realizing a commutative scheme may produce several benefits, we refer to the introduction of [46] for a comparison between the two strategies, and a discussion of advantages and disadvantages of each. See also [29], in the context of parabolic optimal control.

We can show that optimization and discretization commute, when using the implicit Euler case for the states, and a suitable variant for the adjoints. We strongly suspect that commutation holds also when Crank-Nicolson is used, see the work of [29].

Now:

- in section 3.1, the continuous states and adjoints are discretized and the error in doing so, is quantified: we make heavy use here of the results from appendix D. In particular, optimal order estimates for the FEM solutions are recalled (optimal with respect to the approximation properties of the finite element spaces and time stepping schemes)

- in section 3.2, results about the convergence of the discrete shape gradient, to the continuous one, are presented in different settings: a spatially semidiscrete one, and two fully discrete ones, i.e. one with implicit Euler applied to the states and an overall discretize-then-optimize (and commutative) approach, the other with the Crank-Nicolson method applied to states and adjoints, in an optimize-then-discretize fashion

In what follows, $\lesssim$ stands for $\leq C$, with $C > 0$ independent of time and space discretization parameters δt and h, but possibly dependent on the current domain U.

3.1. Approximation of PDEs

Consider the state and adjoint equations as seen in problem 2.1.1 and proposition 2.2.10. Let us have for simplicity a unified notation (just like in problem B.2.2).

Problem 3.1.1 (Unified notation for state and adjoint equations)

$$\begin{cases} u_t - \Delta u = 0 & \text{in } U \times (0,T) \\ u = g_D & \text{on } \Gamma_D \times (0,T) =: \Sigma_D \\ \partial_\nu u = g_N & \text{on } \Gamma_N \times (0,T) =: \Sigma_N \\ u(0) = 0 & \end{cases}, \quad \begin{cases} -a_t - \Delta a = (-1)^{[a=v]}\eta(v-w) & \text{in } U \times (0,T) \\ a = 0 & \text{on } \Sigma_D \\ \partial_\nu a = 0 & \text{on } \Sigma_N \\ a(T) = 0 & \end{cases}$$

We mean that u stands either for v, in which case a is p, or u is w and then a is q. In particular, the following correspondences hold:

Variable	$u = v$	$u = w$	$a = p$	$a = q$
Dirichlet boundary	$\Gamma_D = \partial U$	$\Gamma_D = \Gamma_m$	$\Gamma_D = \partial U$	$\Gamma_D = \Gamma_m$
Neumann boundary	$\Gamma_N = \emptyset$	$\Gamma_N = \Gamma_f$	$\Gamma_N = \emptyset$	$\Gamma_N = \Gamma_f$
Dirichlet data	$g_D = \begin{cases} f & \text{on } \Gamma_f \\ 0 & \text{on } \Gamma_m \end{cases}$	$g_D = 0$ on Γ_m	$g_D = 0$ on ∂U	$g_D = 0$ on Γ_m
Neumann data	-	$g_N = g$ on Γ_f	-	$g_N = 0$ on Γ_f

We have dropped, for simplicity, all the references to the domain transformation τ. Let us discuss the appearance of the temporal weight η. This is a function $\eta : [0,T] \to \mathbb{R}$. Its presence in the right hand side of the adjoint equations can be justified by modifying the energy function in problem 2.2.3 to be:

$$J_\eta(\tau) = \frac{1}{2}\int_I \eta \left\|v^\tau - w^\tau\right\|_{H_\tau}^2$$

The proof of 2.2.10 works almost unchanged to derive the PDEs for the adjoints of problem 3.1.1, and the shape gradient, where we only have to make the change:

$$\frac{1}{2}\int_I\int_{\tau(U_r)} |v^\tau - w^\tau|^2 \operatorname{div}(\delta\theta \circ \tau^{-1}) \to \frac{1}{2}\int_I\int_{\tau(U_r)} \eta|v^\tau - w^\tau|^2 \operatorname{div}(\delta\theta \circ \tau^{-1})$$

The main purpose of this modification is to facilitate the analysis of the numerical discretization. In particular, we choose η to be a smooth cut-off function that is positive in $(0,T)$ and 0 in $[T,+\infty]$. Note that in case a solution to the "classical" problem exists, then it is also a solution to this new perturbed problem, and viceversa. In fact, $J_\eta(\tau) = 0 \implies \eta\left\|v_\tau - w_\tau\right\|_{H_\tau}^2 = 0 \implies v_\tau = w_\tau$. This equality holds on all $I = [0,T]$ by the time continuity of the states.

Modifying the final-time behaviour of the energy might of course have detrimental effects if the boundary data exhibits strong variations close to final time. However, for boundary conditions that e.g. stabilyze over time, then a heat equation will also produce a solution tending to a steady state, so that the presence of η shouldn't play a significant role. In any case, the shape of η can be adjusted according to the user's needs.

We now proceed to discretize states and adjoints using the scheme presented in problem D.3.2 (the adjoint equation can be cast into a standard heat equation by time reversal).

The spatial discretization is carried out on a polygonal approximation U_h of U, a smooth domain. We explicitly account for this discrepancy, see the introductory discussion in appendix D. We use a similar nomenclature for U and U_h, for instance, we write $\Gamma_{m,h} \simeq \Gamma_m, \Gamma_{f,h} \simeq \Gamma_f, \Gamma_{D,h} \simeq \Gamma_D$ and $\Gamma_{N,h} \simeq \Gamma_N$. We can also define $\Sigma_{D,h} := I \times \Gamma_{D,h}$ and so on.

Throughout, set $\theta = 1$ to obtain the implicit Euler method, $\theta = 1/2$ for the Crank-Nicolson method.

Assumption 3.1.2 (Hypothesis for the numerical discretization of problem 3.1.1)

1. $\partial U \in C^2$ (for instance, the star shaped functions must be of class C^2, see proposition 2.3.1.1), U_h is polygonal/polyhedral and ∂U_h interpolates ∂U. The mesh family of U_h must be (shape) regular and quasi-uniform (for such definitions, see [12])
2. $g_D \in H^{1/\theta+1}(I, H^{3/2}(\Gamma_D)) \cap H^1(I, H^2(\Gamma_D))$, $g_N \in H^{1/\theta+1}(I, H^{3/2}(\Gamma_N)) \cap L^2(I, H^2(\Gamma_N))$
3. $g_D(0) = 0$ and $g_N^{(k)}(0), g_D^{(k+1)}(0) = 0$ for $k = 0, ..., 1/\theta - 1$
4. $\eta^{(k)}(T) = 0$ for $k = 0, ..., 1/\theta - 1$, $\eta \geq 0$ and $\eta \in C^\infty([0,T]; \mathbb{R})$

Call now h the maximum element size of U_h, and δt the size of one of the K uniform length intervals $[t^k, t^{k+1}]$, $k = 0, ..., K-1$, into which we subdivide I. We indicate with S^1_h the space of linear finite element on U_h, and $S^1_{0,D,h} = \{v_h \in S^1_h, v_h|_{\Gamma_{D,h}} = 0\}$.

Here are the fully discrete problems we must solve if we apply the same schemes for adjoint and states, thus in an optimize-then-discretize fashion.

Problem 3.1.3 (Numerical solution of problem 3.1.1 in optimize-then-discretize fashion)
Consider $g^k_{N,h}, g^k_{D,h}$ to be the Lagrange interpolant of $g_N(t^k), g_D(t^k)$. We adopt a similar notation as in problem 3.1.1. So, we look for $u^k_h \in S^1_h$, $k = 0, ..., K$, with:

$$\left(\frac{u_h^{k+1}-u_h^k}{\delta t}, \phi_h\right)_{L^2(U_h)} + (\nabla(\theta u_h^{k+1} + (1-\theta)u_h^k), \nabla\phi_h)_{L^2(U_h)} = (\theta g_{N,h}^{k+1} + (1-\theta)g_{N,h}^k, \phi_h)_{L^2(\Gamma_{N,h})}, \quad 1 \le k \le K$$

$$u_h^{k+1}|_{\Gamma_{D,h}} = g_{D,h}^{k+1}, \quad 1 \le k \le K$$

$$u_h^0 = 0$$

and $\phi_h \in S^1_{0,D,h}$. The same scheme is applied to the adjoint equations, i.e. we look for $a^k_h \in S^1_{0,D,h}$, $k = 0, ..., K$, with:

$$\left(\frac{a_h^{k-1}-a_h^k}{\delta t}, \phi_h\right)_{L^2(U_h)} + (\nabla((1-\theta)a_h^k + \theta a_h^{k-1}), \nabla\phi_h)_{L^2(U_h)} =$$

$$(-1)^{[u=v]}((1-\theta)\eta(t^k)(v_h^k - w_h^k) + \theta\eta(t^{k-1})(v_h^{k-1} - w_h^{k-1}), \phi_h)_{L^2(\Gamma_{N,h})}, \quad 1 \le k \le K$$

$$a_h^K = 0$$

and $\phi_h \in S^1_{0,D,h}$. Further details can be found in the appendix after problem D.3.2, of which problem 3.1.3 is an instance.

Let us also briefly introduce the spatially semidiscretized shape optimization problem, and its shape gradient. This is an interesting quantity on its own, but it will also play a role in obtaining fully discrete estimates.

In the rest of the chapter, for simplicity but also for the sake of generality, we work again with general transformations, in place of radial fields. In particular, we write $U_h = \tau_h(U_{r,h})$ for $U_{r,h}$ interpolating U_r, and for τ_h a transformation that is a finite element vector field that fixes the external boundary $\Gamma_{f,h}$. τ_h thus preserves the finite element spaces and the polygonal/polyhedral nature of the discrete reference domain $U_{r,h}$.

Proposition 3.1.4 (Semidiscrete shape optimization problem)
We introduce the spatially semidiscrete state equation, with unified notation u_h, similarly to problem 3.1.3. Calling $g_{N,h}$ and $g_{D,h}$ the Lagrange interpolants (defined a.e. in time) of g_N, g_D, we look for $u_h : I \to S^1_h$ with:

$$(u_h', \phi_h)_{L^2(U_h)} + (\nabla u_h, \nabla\phi_h)_{L^2(U_h)} = (g_{N,h}, \phi_h)_{L^2(\Gamma_{N,h})}, \quad \text{for a.e. } t \in I$$

$$u_h|_{\Sigma_{D,h}} = g_{D,h}$$

$$u_h(0) = 0$$

and $\phi_h \in S^1_{0,D,h}$. This is an instance of problem D.2.5, to which we refer for further details. The shape optimization problem is to find τ_h, a vector valued finite element field that is the identity on $\Gamma_{m,h}$ (and with small enough $W^{1,\infty}$ norm, so as to keep $U_{r,h}$ bounded Lipschitz and preserve the mesh quality), minimizing:

$$J_h(\tau_h) = \int_I \int_{\tau_h(U_{r,h})} \eta |v_h - w_h|^2$$

The adjoint state $a_h : I \to S^1_{0,D,h}$ of u_h solves:

$$-(a_h', \phi_h)_{L^2(U_h)} + (\nabla a_h, \nabla\phi_h)_{L^2(U_h)} = (-1)^{[u_h = v_h]}\eta(v_h - w_h, \phi_h)_{L^2(U_h)}, \quad \text{for a.e. } t \in I$$

$$a_h(T) = 0$$

for $\phi_h \in S^1_{0,D,h}$, and the semidiscrete shape gradient in direction $\delta\theta_h$ (a vector valued finite element field that is zero on $\Gamma_{m,h}$) reads:

$$J_h'(\tau_h)[\delta\theta_h] =$$

$$\int_I (w_h' \operatorname{div}(\delta\theta_h \circ \tau_h^{-1}), q_h)_{L^2(\tau_h(U_{r,h}))} + \int_I (A'(\delta\theta_h \circ \tau_h^{-1})\nabla v_h, \nabla p_h)_{L^2(\tau_h(U_{r,h}))} +$$

$$\int_I (v_h' \operatorname{div}(\delta\theta_h \circ \tau_h^{-1}), p_h)_{L^2(\tau_h(U_{r,h}))} + \int_I (A'(\delta\theta_h \circ \tau_h^{-1})\nabla w_h, \nabla q_h)_{L^2(\tau_h(U_{r,h}))} +$$

$$\frac{1}{2}\int_I \int_{\tau_h(U_{r,h})} |v_h - w_h|^2 \operatorname{div}(\delta\theta_h \circ \tau_h^{-1})$$

Proof.
One can adopt the same techniques employed in the continuous case, or, use of the method proposed in and [11], section 4 (or more generally, [44]). Also note, it is important that τ_h is piecewise linear on the discretization, and continous, so that finite element functions remain finite element functions after an application of τ_h, and the geometry remains of polygonal/polyhedral nature. See again [11] for further details on this matter. □

We remark again that the continuous solution is defined on a smooth domain U, whereas the discretized solution on a polygonal/polyhedral approximation U_h. To compare e.g. u and u_h we must have a way of "lifting" u_h to u or viceversa. This procedure is possible and we denote its action by $(\cdot)^l$: we thus compare $u : U \times I \to \mathbb{R}$ and $u_h^l : U \times \{0, ..., K\} \to \mathbb{R}$. For details regarding the lifting action we refer to proposition D.1.3.

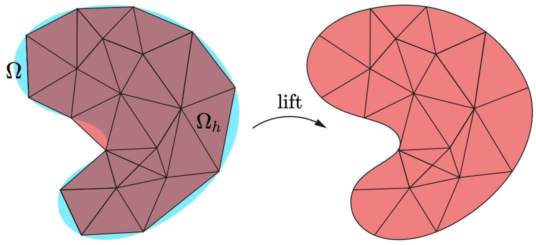

Figure 3.1.: Lifting action

Observation 3.1.5 (τ and τ_h).
Throughout the rest of the chapter, we will derive several error estimates, which depend also on ∂U, hence, on τ. We won't attempt to precisely track this dependency.

Remember that assumption 3.1.2 must hold, which implies a specific form of τ_h, i.e. that it must interpolate τ. Given therefore a reference discretization $U_{r,h}$ interpolating U_r, then τ_h, hence U_h, is completely determined by τ.
Choosing such $U_{r,h}$ is not restrictive, but confining τ_h to be the interpolant of τ, is: we refrain from generalizing our estimates to more arbitrary τ_h, and we note that our result may be a first step of a more general argument (just like in finite element error estimates, the error between exact and discretized solution is decomposed into two parts by the introduction of a suitable interpolant).

This is in any case a novelty with respect to e.g. [39], which contains similar estimates to the ones we are about to derive, but in which H^2 regularity is demanded on non-convex polygonal domains.

We now state the needed error estimates for states and adjoints of problem 3.1.1 when employing the optimize-then-discretize schemes of problem 3.1.3.

Proposition 3.1.6 (Optimize-then-discretize approximation of state and adjoint equations)
Let assumption 3.1.2 be fulfilled. Then:

$$\sup_{t\in I} \left\| u(t) - u_h^l(t) \right\|_{L^2(U)} + h\sqrt{\int_0^T \left\| u - u_h^l \right\|_{H^1(U)}^2} \lesssim h^2$$

$$\sup_{t\in I} \left\| a(t) - a_h^l(t) \right\|_{L^2(U)} + h\sqrt{\int_0^T \left\| a - a_h^l \right\|_{H^1(U)}^2} \lesssim h^2$$

$$\sup_{k=0,\dots,K} \left\| u_h(t^k) - u_h^k \right\|_{L^2(U)} + \sqrt{\delta t \sum_{k=0}^{K-1} \left\| \theta(u_h(t^{k+1}) - u_h^{k+1}) + (1-\theta)(u_h(t^k) - u_h^k) \right\|_{H^1(U)}^2} \lesssim (\delta t)^{1/\theta}$$

$$\sup_{k=0,\dots,K} \left\| a_h(t^k) - a_h^k \right\|_{L^2(U)} + \sqrt{\delta t \sum_{k=1}^{K} \left\| \theta(a_h(t^k) - a_h^k) + (1-\theta)(a(t^{k-1}) - a_h^{k-1}) \right\|_{H^1(U)}^2} \lesssim (\delta t)^{1/\theta}$$

For the states, we will also need:

$$\sqrt{\int_0^T \left\| \partial_t u - (\partial_t u_h)^l \right\|_{L^2(U)}^2} \lesssim h$$

$$\sqrt{\delta t \sum_{k=0}^{K-1} \left\| \frac{u_h(t^{k+1}) - u_h(t^k)}{\delta t} - \frac{u_h^{k+1} - u_h^k}{\delta t} \right\|_{L^2(U_h)}^2} \lesssim (\delta t)^{1/\theta}$$

Proof.

The proposition is just a recollection of the results from appendix D (namely proposition D.3.3, theorem D.2.10, corollary D.2.17, proposition D.3.8): we need to show that assumption 3.1.2 guarantees the validity of the hypothesis under which those results hold, and then to bound the constants A, B, C, D, E that appear therein, uniformly on δt and h. Since these tasks are not be particularly enlightening, we only report the main steps to be performed. We do not track the dependency on the domain U as already remarked.

The hypothesis which need to be verified are assumption D.2.6, assumption D.2.4, assumption B.2.1 and assumption D.3.1.

We note at first that in the star-shaped setting, $\partial U \in C^2$ can be ensured by proposition 2.3.1.1.

States

Hypothesis 1 to 3 guarantee that $u \in H^1(I, H^2(U))$ (by theorem B.2.6, which we apply with $k = 1$). This is assumption D.2.4. The other hypothesis follow directly from $1-3$.

The constants A, B, C, D, E for u are also easily bounded employing $1-3$: in particular, no volumetric source terms are present, and all the compatibility "residuals" $\delta_h^{(k)}(0)$ are 0, $k = 1, ..., 1/\theta$ (see proposition D.3.3 for the notation).

Adjoints

We can re-use the reasonings done for the states. There are of course some peculiarities for the adjoints.

Indeed, we also need the conditions on $\eta(T), \eta'(T)$ (point 4) when applying theorem B.2.6 to obtain $a \in H^1(I, H^2(U))$, and also when ensuring that the compatibility "residuals" $\delta_h^{(k)}(0)$ for the adjoints, $k = 1, ..., 1/\theta$, are bounded uniformly with respect to h.

Moreover, the adjoint equations have non trivial source terms like $\eta(v-w)$, $\eta(v_h - w_h)$ and $\eta(t^k)(v_h^k - w_h^k)$. By the results that we now know hold for the states (again, proposition D.3.3, theorem D.2.10, corollary D.2.17, proposition D.3.8), we know that $\eta(v-w) \simeq \eta(v_h - w_h) \simeq \eta(t^k)(v_h^k - w_h^k)$, so that we can satisfy all the requirements on these right hand sides of the adjoint equations. □

Only for $\theta = 1$, we now define a fully discrete shape optimization problem. This is necessary to justify that optimization and discretization commute, for $\theta = 1$.

Problem 3.1.7 (Discrete shape optimization problem)
As before, given a polygonal/polyhedral reference domain $U_{r,h}$ and transformations τ_h (vector valued finite element fields that preserve the discrete fixed boundary $\Gamma_{f,h}$), we solve:

$$\inf_{\tau_h} \frac{\delta t}{2} \sum_{k=1}^{K} \left\| v_h^k - w_h^k \right\|^2_{L^2(\tau_h(U_{r,h}))} =: J_{h,\delta t}(\tau_h)$$

where v_h^k, w_h^k are defined in problem 3.1.3, and their dependence on τ_h is not highlited in the notation. We also ask τ_h to have small enough $W^{1,\infty}$ norm, so as to keep $U_h = \tau_h(U_{r,h})$ bounded Lipschitz and preserve the mesh quality.

Proposition 3.1.8 (Discrete shape gradient)
The discrete shape gradient of problem 3.1.7 is:

$$\begin{aligned} J'_{h,\delta t}(\tau_h)[\delta\theta_h] = {} & \\ \delta t \sum_{k=1}^{K} \left(\frac{w_h^k - w_h^{k-1}}{\delta t}, \operatorname{div}(\delta\theta_h \circ \tau_h^{-1}) q_h^{k-1} \right)_{L^2(\tau_h(U_{r,h}))} & + \delta t \sum_{k=1}^{K} (A'(\delta\theta_h \circ \tau_h^{-1}) \nabla w_h^k, \nabla q_h^{k-1})_{L^2(\tau_h(U_{r,h}))} + \\ \delta t \sum_{k=1}^{K} \left(\frac{v_h^k - v_h^{k-1}}{\delta t}, \operatorname{div}(\delta\theta_h \circ \tau_h^{-1}) p_h^{k-1} \right)_{L^2(\tau_h(U_{r,h}))} & + \delta t \sum_{k=1}^{K} (A'(\delta\theta_h \circ \tau_h^{-1}) \nabla v_h^k, \nabla p_h^{k-1})_{L^2(\tau_h(U_{r,h}))} + \\ & \frac{\delta t}{2} \sum_{k=1}^{K} \int_{\tau_h(U_{r,h})} \eta(t^k) |v_h^k - w_h^k|^2 \operatorname{div}(\delta\theta_h \circ \tau_h^{-1}) \end{aligned}$$

Again, we dropped the dependence of v, w on τ_h, for simplicity. With unified notation as in problem 3.1.1, the adjoint state $a_h^k \in S^1_{0,D,h}$ to u_h^k, $k = 0, ..., K$, satisfies:

Problem 3.1.9

$$\left(\frac{a_h^{k-1} - a_h^k}{\delta t}, \phi_h \right)_{L^2(\tau_h(U_{r,h}))} + (\nabla a_h^{k-1}, \nabla a_h)_{L^2(\tau_h(U_{r,h}))} = (-1)^{[u_h^k = v_h^k]} \eta(t^k)(v_h^k - w_h^k, \phi_h)_{L^2(\tau_h(U_{r,h}))}, \quad 1 \le k \le K$$

$$p_h^K = 0$$

for $v_h \in S^1_{0,D,h}$.

Proof.

It can be done similarly to proposition 3.1.4. □

We now give a quantitative estimate on the approximation power of the discrete adjoints we just obtained, for $\theta = 1$. This is needed, because the scheme they satisfy is not exactly the implicit Euler treated in problem 3.1.3.

Proposition 3.1.10 (Error estimates for adjoint states in a discretize-then-optimize fashion)
The discretize-then-optimize adjoints with implicit Euler from proposition 3.1.8 satisfy the same asymptotic, optimal order error estimates of proposition 3.1.6, under the same assumptions.

Proof.
The proof is exactly that of proposition 3.1.6. The only difference comes from the fact that the right hand sides of the fully discrete adjoint equations are not "correct", i.e. they are shifted by δt. But this is not an issue, as we shall now show.

We see that we only need to show a bound of $\delta t \sum_{k=1}^{K} \left\|\eta(t^{k-1})u_h(t^{k-1}) - \eta(t^k)u_h^k\right\|^2_{L^2(U_h)}$, where u denotes the generic state corresponding state to the generic adjoint a (this is the same notation as in the proof of proposition 3.1.6), and where $U_h = \tau_h(U_{r,h})$.

Applying the triangle inequality and using again the proof of proposition 3.1.6, we see that we actually only need to bound the term:

$$\delta t \sum_{k=1}^{K} \left\|\eta(t^{k-1})u_h(t^{k-1}) - \eta(t^k)u_h^k\right\|^2_{L^2(U_h)} \lesssim$$
$$\underbrace{\delta t \sum_{k=1}^{K} \left\|\eta(t^{k-1})(u_h(t^{k-1}) - u_h(t^k))\right\|^2_{L^2(U_h)}}_{1} + \underbrace{\delta t \sum_{k=1}^{K} \left\|(\eta(t^{k-1}) - \eta(t^k))u_h(t^k)\right\|^2_{L^2(U_h)}}_{2} + \underbrace{\delta t \sum_{k=1}^{K} \left\|\eta(t^k)(u_h^k - u_h(t^k)))\right\|^2_{L^2(U_h)}}_{3}$$

There holds $2 \leq \|\eta'\|^2_\infty \delta t^3 \sum_{k=1}^{K} \left\|u_h(t^k)\right\|^2_{L^2(U_h)}$. Call $\pi u_h := u_h(t^k)$ for $t \in (t^k, t^{k+1})$. By lemma A.2.6 we see that, for δt small enough, one has $\|\pi u_h\|_{L^2(I,L^2(U_h))} \lesssim \|u_h\|_{H^1(I,L^2(U_h))}$. This yields:

$$2 \leq \|\eta'\|^2_\infty \delta t^3 \sum_{k=1}^{K} \left\|u_h(t^k)\right\|^2_{L^2(U_h)} = \|\eta'\|^2_\infty \delta t^2 \int_I \|\pi_h u_h\|^2_{L^2(U_h)} \lesssim \delta t^2 \|u_h\|^2_{H^1(I,L^2(U_h))} \|\eta'\|^2_\infty$$

On the other hand, $1 \leq \|\eta\|^2_\infty \delta t \sum_{k=1}^{K} \left\|u_h(t^{k-1}) - u_h(t^k)\right\|^2_{L^2(U_h)}$, and upon using teh fundamental theorem of calculus, we conclude $1 \leq \|\eta\|^2_\infty \delta t \sum_{k=1}^{K} \delta t \int_{I_k} \|u_h'\|^2_{L^2(I_k,L^2(U_h))}$.

In both 1, 2, $\|u_h\|^2_{H^1(I,L^2(U_h))}$ can be bounded, uniformly with respect to h (and δt), by suitable stability estimates which can be proved using the techniques of appendix B.2.

It is clear from this estimate that a very steep η may yield higher discretization errors.

Finally, by proposition 3.1.6, we obtain $3 \lesssim (h^2 + \delta t) \|\eta\|^2_\infty$. □

Observation 3.1.11 (Optimization and discretization commute).
So, optimization and discretization commute, for $\theta = 1$: the perturbed implicit Euler method of proposition 3.1.8, applied to the adjoints, is a "legitimate" scheme, as we have just shown in proposition 3.1.10). With a diagram:

$$\begin{tikzcd}
 & \text{proposition 2.2.10} \arrow[dr, "\text{discretization}"] & \\
\text{problem 2.2.3} \arrow[ur, "\text{optimization}"] \arrow[dr, "\text{discretization}"'] & & \text{proposition 3.1.8} \\
 & \text{problem 3.1.7} \arrow[ur, "\text{optimization}"'] &
\end{tikzcd}$$

3.2. Approximation of shape gradients

In our numerical experiments (see chapter 4) we adopt a discretize-then-optimize approach. When employing the implicit Euler method in time, we can see that optimization and discretization commute, as we have explained just above. We are moreover able to quantify the error generated when substituting the continuous shape gradient with the fully discretized one.

A future line of research could be to extend such conclusions to the case of the Crank-Nicolson method, in a discretize-then-optimize setting, so as to fully justify the adopted algorithms in some of the numerical experiments we conducted. A promising direction would be to find a way to adapt the arguments of [29] in our context of smooth geometries, at least to show commutativity of optimization and discretization. We will prove, as a partial replacement, optimize-then-discretize error estimates for the shape gradient.

These estimates are similar to those in [39], although formulated in a slightly different context: in a time-dependent setting, and with a more precise handling of the geometry mismatch. In [39], order 2 estimates (in space) are obtained: this is because the deformation field $\delta\theta$ in which the shape gradient is tested, is assumed to have two orders of differentiability, so that certain duality techniques may be employed. Such a result doesn't fully explain why superconvergence happens in the context of just $W^{1,\infty}$ displacements, a fact which is indeed observable in our experiments.

For smoother displacement fields $\delta\theta \in W^{2,\infty}$, a similar superconvergence result for the shape gradient is available also in our context. This is shown initially for the spatial semidiscretization, and from here we speculate that such a result may be available also in the fully discrete case. This is also confirmed by the experiments in section 4.2. With regards to fully discrete estimates: in a commutative setting for the implicit Euler scheme, we are able to give full theoretical justification . In the Crank-Nicolson case, we could only arrive at non-commutative optimize-then-discretize estimates.

In case displacement fields are not smooth enough, $O(h^2)$ orders, as noted in [39], don't seem to be so easily obtainable: we are also are able to only prove $O(h)$ estimates (but numerically observe an $O(h^2)$ order, see section 4.2).

Theorem 3.2.1 (Semidiscrete error estimates for shape gradient)
Let assumption 3.1.2 hold. There exists a constant γ that depends on U, the shape regularity and quasi-uniformity of the meshes, but independent of h, such that, for h small enough and for all $\delta\theta \in W^{1+s,\infty}(U;\mathbb{R}^n)$, $s = 0, 1$, we have:

$$\left| J'(U)[\delta\theta] - J'_h(U_h)[\delta\theta^{-l}] \right| \le \gamma h^{1+s} \|\delta\theta\|_{W^{1+s,\infty}(U;\mathbb{R}^n)}$$

The notation $J'(U)[\delta\theta] := J'(\tau)[\delta\theta \circ \tau]$, if $U = \tau(U_r)$, is to emphasize that the dependence on τ is not tracked. Analogously $J'_h(U_h)[\delta\theta] := J'_{h,\delta t}(\tau_h)[\delta\theta_h \circ \tau]$, with $U_h = \tau_h(U_{r,h})$ and a suitable τ_h that (linearly) interpolates τ on the spatial discretization nodes. Note that no assumptions on the boundary values of $\delta\theta$ are made here.

Observation 3.2.2. In the remaining proofs of this chapter, we apply stability estimates to bound the norms of discretized quantities independently of h, without explicitly writing this out in detail. Such estimates can be easily derived with the techniques of appendix B.2 and appendix D. We refer to e.g. proposition D.2.7 and to the proof of proposition D.3.8 for some hints in this direction. We also don't write the norms of the continuos quantities, because they don't depend on h (or δt). Moreover, proposition D.1.3 is used liberally to relate the norms of lifted and unlifted functions, and we will not mention every time it is invoked.

Proof for $\delta\theta \in W^{1,\infty}$.
We compare "time derivative" terms, "gradient" terms and "cost function" terms in the difference $J'(U)[\delta\theta] - J'_h(U_h)[\delta\theta^{-l}]$, terms that come from proposition 3.1.4 and proposition 2.2.10, and use the estimates in proposition 3.1.6 and proposition D.1.5 to bound every term like $\lesssim h \|\delta\theta\|_{W^{1,\infty}(U;\mathbb{R}^n)}$.

<u>Time derivatives</u>

We recover the notation $u \to$ generic state (v or w), $a \to$ adjoint state of u. We have:

$$\int_I (u', a\mathrm{div}(\delta\theta))_{L^2(U)} - \int_I (u'_h, a_h \mathrm{div}(\delta\theta_h))_{L^2(U_h)} =$$
$$\underbrace{\int_I ((u - u_h^l)', a\mathrm{div}(\delta\theta))_{L^2(U)}}_{1} + \underbrace{\int_I ((u'_h)^l, (a - a_h^l)\mathrm{div}(\delta\theta))_{L^2(U)}}_{2} + \underbrace{\int_I ((u'_h)^l, a_h^l \mathrm{div}(\delta\theta))_{L^2(U)} - \int_I (u'_h, a_h \mathrm{div}(\delta\theta^{-l}))_{L^2(U_h)}}_{3}$$

We apply proposition 3.1.6 to 1, 2 to obtain $\left|1\right|, \left|2\right| \lesssim h \|\mathrm{div}\delta\theta\|_{L^\infty(U)}$. Moreover, employing proposition D.1.5, we find:

$$\left|3\right| \lesssim h \|u'_h\|_{L^2(I,L^2(U_h))} \|a_h\|_{L^2(I,L^2(U_h))} \|\delta\theta\|_{W^{1,\infty}(U)} \lesssim h \|\delta\theta\|_{W^{1,\infty}(U)}$$

<u>Gradients</u>

We perform the splitting:

$$\int_I (A'(\delta\theta)\nabla u, \nabla a)_{L^2(U)} - \int_I (A'(\delta\theta^{-l})\nabla u_h, \nabla a_h)_{L^2(U_h)} =$$
$$\underbrace{\int_I (A'(\delta\theta)\nabla(u - u_h^l), \nabla a)_{L^2(U)}}_{4} + \underbrace{\int_I (A'(\delta\theta)\nabla u_h^l, \nabla(a - a_h^l))_{L^2(U)}}_{5} + \underbrace{\int_I (A'(\delta\theta)\nabla u_h^l, \nabla a_h^l)_{L^2(U)} - \int_I (A'(\delta\theta^{-l})\nabla u_h, \nabla a_h)_{L^2(U_h)}}_{6}$$

With proposition 3.1.6, we get $\left|4\right|, \left|5\right| \lesssim h \|\delta\theta\|_{W^{1,\infty}(U)}$. With proposition D.1.5, we obtain, as above, that the same estimate holds for $\left|6\right|$.

<u>Cost function</u>

There holds:

$$\underbrace{\int_I\int_U \eta((v-v_h^l)-(w-w_h^l))((v+v_h^l)-(w+w_h^l))\mathrm{div}(\delta\theta)}_{7} + \underbrace{\int_I\int_U \eta(v_h^l-w_h^l)^2\mathrm{div}(\delta\theta_h^l) - \int_I\int_{U_h} \eta(v_h-w_h)^2\mathrm{div}(\delta\theta^{-1})}_{8} + $$

where the left-hand side reads

$$\int_I\int_U \eta|v-w|^2\mathrm{div}(\delta\theta) - \int_I\int_{U_h} \eta|v_h-w_h|^2\mathrm{div}(\delta\theta^{-1}) =$$

There holds $7 \lesssim h^2 \|\delta\theta\|_{W^{1,\infty}(U)}$ thanks to the Cauchy-Schwarz inequality and theorem D.2.10, the same holds for 8 but because of proposition D.1.5. $\square$

Proof for $\delta\theta \in W^{2,\infty}$.
We note that for the difference in the "cost function" terms, the previous proof works fine. We thus concentrate on the remaining ones. We will partly reason analogously to [39], although we have to take some additional steps to circumvent the unavailability of Galerkin orthogonality, due to the mismatch in geometry.

<u>Duality argument and splitting</u>

Let us call:

$$\mathcal{G}(\phi,a,\delta\theta) := \int_I(\phi', a\mathrm{div}(\delta\theta))_{L^2(U)} + \int_I (A'(\delta\theta)\nabla\phi,\nabla a)_{L^2(U)}$$
$$\mathcal{G}_h(\phi_h,a_h,\delta\theta^{-l}) := \int_I(\phi_h', a_h\mathrm{div}(\delta\theta^{-l}))_{L^2(U_h)} + \int_I (A'(\delta\theta^{-l})\nabla\phi_h,\nabla a_h)_{L^2(U_h)}$$

Then:

$$\mathcal{G}(u,a,\delta\theta) - \mathcal{G}_h(u_h,a_h,\delta\theta^{-l}) = \underbrace{\mathcal{G}(u_h^l-u,a-a_h^l,\delta\theta)}_{1} + \underbrace{\mathcal{G}(u_h^l-u,a_h^l,\delta\theta) - \mathcal{G}_h(u_h-u^{-l},a_h,\delta\theta^{-l})}_{2} +$$
$$\underbrace{\mathcal{G}(u,a_h^l-a,\delta\theta) - \mathcal{G}_h(u^{-l},a_h-a^{-l},\delta\theta^{-l})}_{3} + \underbrace{\mathcal{G}(u,a,\delta\theta) - \mathcal{G}_h(u^{-l},a^{-l},\delta\theta^{-l})}_{4} + \mathcal{G}(u-u_h^l,a,\delta\theta) + \mathcal{G}(u,a-a_h^l,\delta\theta)$$

We now focus on $\mathcal{G}(u-u_h^l,a,\delta\theta)$. We consider the following dual problem, where we take inspiration from a technique used in [39]:

$$\mathcal{E}^*(z,\phi) = \tilde{\mathcal{G}}(\phi,a,\delta\theta), \quad \forall\phi\in L^2(I,V) \tag{3.2.3}$$
$$z(T) = 0 \tag{3.2.4}$$
$$z \in L^2(I,V)\cap H^1(I,V^*) \tag{3.2.5}$$

where $V = H^1_{0,D}(U)$, $\mathcal{E}^*(z,\phi) := -\int_I(z',\phi)_{L^2(U)} + \int_I(\nabla z,\nabla\phi)_{L^2(U)}$, $\tilde{\mathcal{G}}(\phi,a,\delta\theta) = -\int_I(F,\phi)_{L^2(U)} + \int_I((A'(\delta\theta)\nabla a)\nu,\phi)_{L^2(\partial U)}$, and $F := a'\mathrm{div}(\delta\theta) + \mathrm{div}(A'(\delta\theta)\nabla a) \in L^2(I,L^2(U))$. Note that $(A'(\delta\theta)\nabla a)\nu \in H^1(I,H^{1/2}(\partial U))$, because $a \in H^1(I,H^2(U))$ (see the proof of proposition 3.1.6), $A'(\delta\theta)\in W^{1,\infty}$ (by our hypothesis) and $\nu \in C^1(\partial U)$ (as $\partial U \in C^2$). By theorem B.2.6 we therefore obtain that $z \in L^2(I,H^2(U))\cap H^1(I,L^2(U))$, where the assumed smoothness of $\delta\theta$ is crucial.

Now, call $e := u - u_h^l$. Then, using integration by parts in time, but also in space (see proposition B.3.3 and theorem A.1.1):

$$\mathcal{G}(e,a,\delta\theta) = \underbrace{(e(T),a(T)\mathrm{div}(\delta\theta))_{L^2(U)} - (e(0),a(0)\mathrm{div}(\delta\theta))_{L^2(U)}}_{5} + \tilde{\mathcal{G}}(e,a,\delta\theta)$$

We note that e is a legitimate test function $e=\phi$ in the case $u=w$, as $w=0$ on $\Gamma_m=\Gamma_D$. In the case $u=v$, we don't have $e=0$ on the whole Dirichlet boundary ∂U. However, eq. (3.2.3) yields that for a.e. $t\in I$, there holds $-z'-\Delta z = F$ in $L^2(U)$, so that in general we can say that:

$$\tilde{\mathcal{G}}(e,a,\delta\theta) = \mathcal{E}^*(z,e) + \underbrace{[u=v]\int_I(\partial_\nu z,e)_{L^2(\Gamma_f)}}_{6} = 6 - \underbrace{(e(T),z(T))_{L^2(U)} + (e(0),z(0))_{L^2(U)}}_{7} + \mathcal{E}(e,z)$$

where we used at last integration by parts in time and $\mathcal{E}(e,z) := \int_I (e', z)_{L^2(U)} + \int_I (\nabla e, \nabla z)_{L^2(U)}$, which is the "left hand side" in the variational formulation of u. We further split $\mathcal{E}(e,z)$, introducing at first the additionl notation $\mathcal{E}_h(\phi_h, z_h) := \int_I (\phi', z_h)_{L^2(U_h)} + \int_I (\nabla\phi, \nabla z_h)_{L^2(U_h)}$:

$$\mathcal{E}(e,z) = \underbrace{\mathcal{E}(e, z - I_c z)}_{8} + \underbrace{\mathcal{E}(u, I_c z) - \mathcal{E}_h(u_h, I_h z)}_{9} + \underbrace{\mathcal{E}_h(u_h, I_h z - z^{-l}) - \mathcal{E}(u_h^l, I_c z - z)}_{10} + \underbrace{\mathcal{E}_h(u_h - u^{-l}, z^{-l}) - \mathcal{E}(u_h^l - u, z)}_{11} + \underbrace{\mathcal{E}_h(u^{-l}, z^{-l}) - \mathcal{E}(u,z)}_{12}$$

Here, $I_h z$ is the Lagrange interpolant of z on U_h and $I_c z = (I_h z)^l$, see proposition D.1.4. With analogous reasonings for $\mathcal{G}(u, a - a_h^l, \delta\theta)$, calling $e_a = a - a_h^l$ and $y \in L^2(I, H^2(U))$ the counterpart to z:

$$\tilde{\mathcal{G}}(u, a - a_h^l, \delta\theta) = \mathcal{E}(y, e_a) = \underbrace{(e_a(T), y(T))_{L^2(U)} - (e_a(0), y(0))_{L^2(U)}}_{13} + \underbrace{\mathcal{E}^*(e_a, y - I_c y)}_{14} + \underbrace{\mathcal{E}^*(a, I_c y) - \mathcal{E}_h^*(a_h, I_h y)}_{15} +$$
$$\underbrace{\mathcal{E}_h^*(a_h, I_h y - y^{-l}) - \mathcal{E}^*(a_h^l, I_c y - y)}_{16} + \underbrace{\mathcal{E}_h^*(a_h - a^{-l}, y^{-l}) - \mathcal{E}^*(a_h^l - a, y)}_{17} + \underbrace{\mathcal{E}_h^*(a^{-l}, y^{-l}) - \mathcal{E}^*(a, y)}_{18}$$

Estimations

We are now going to show that every circled quantity can be bound as $\lesssim h^2 \|\delta\theta\|_{W^{2,\infty}(U)}$.

For 5, 7, 13, it suffices to apply proposition 3.1.6, with our problem these terms are even 0. With proposition 3.1.6 in addition, we are able to bound 1 too. Combining proposition 3.1.6 and proposition D.1.5 we are able to handle 2, 11, 17. 4, 12, 18 can be handled by proposition D.1.5 alone. To bound 10 and 16 we need to use proposition D.1.5 and proposition D.1.4. For 8, 14 we use proposition 3.1.6 and proposition D.1.4.

Now, 6 $= 0$ if $u = w$, whereas if $u = v$ we can say $\left|6\right| \lesssim \int_I \|z\|_{H^2(U)} \left\|u - u_h^l\right\|_{L^2(\Gamma_f)} \lesssim \|z\|_{L^2(I,H^2(U))} \|g_D - g_{D,h}\|_{L^2(I,L^2(\Gamma_D))}$. We recall that $g_{D,h} = I_h g_D$ and thus we can apply proposition D.1.4.

Finally, 9 $= [u = w]\left(\int_I (g_N, I_c z)_{L^2(\Gamma_N)} - \int_I (g_{N,h}, I_h z)_{L^2(\Gamma_{N,h})}\right)$, because of the definition of u, u_h. This term we can then bound by proposition D.1.5 and proposition D.1.4. We also have $\pm$15 $= \int_I \eta(v - w, I_c y)_{L^2(U)} - \int_I \eta(v_h - w_h, I_h y)_{L^2(U_h)}$. We need to make the additional step:

$$\pm 15 = \int_I \eta((v-w) - (v_h^l - w_h^l), I_c y)_{L^2(U)} + \int_I \eta(v_h^l - w_h^l, I_c z)_{L^2(U)} - \int_I \eta(v_h - w_h, I_h y)_{L^2(U_h)}$$

before applying proposition 3.1.6, proposition D.1.5 and proposition D.1.4.

For the sake of completeness, we mention that, thanks to H^2 regularity estimates that can be found in e.g. [35], and to theorem B.2.6, we obtain $\|z\|^2_{L^2(I,H^2(U))} \lesssim \|F\|^2_{L^2(I,L^2(U))} + \|(A'(\delta\theta)\nabla a)\nu\|_{H^1(I,H^{1/2}(\partial U))}$. Using the definition of F and trace theorems, $\|z\|^2_{L^2(I,H^2(U))} \lesssim (\|a'\|^2_{L^2(I,L^2(U))} + \|a\|^2_{L^2(I,H^2(U))}) \|\delta\theta\|^2_{W^{2,\infty}(U;\mathbb{R}^n)}$. An equal estimate holds for $\|y\|^2_{L^2(I,H^2(U))}$. □

Corollary 3.2.6 (Fully discrete error estimates for discretize-then-optimize shape gradient, implicit Euler case)
With the same assumptions and notation of theorem 3.2.1 and in the discretize-then-optimize framework of proposition 3.1.8, we can conclude, for $s = 0, 1$:

$$\left|J'(U)[\delta\theta] - J'_{h,\delta t}(U_h)[\delta\theta^{-l}]\right| \leq \gamma(h^{s+1} + \delta t) \|\delta\theta\|_{W^{s+1,\infty}(U)}$$

Proof.

The overall argument amounts to "inserting J'_h between J' and $J'_{h,\delta t}$". Two pieces must then be estimated, and the first is exactly addressed in theorem 3.2.1. The second one is $J'_h(U)[\delta\theta^{-l}] - J'_{h,\delta t}(U_h)[\delta\theta^{-l}]$. Of this member, we give an appropriate splitting, where every piece is $\lesssim \delta t \|\delta\theta\|_{W^{1,\infty}(U;\mathbb{R}^n)}$. This splitting is:

$$\int_I\int_{U_h} u_h' a_h \mathrm{div}(\delta\theta^{-l}) - \delta t\sum_{k=1}^K\int_{U_h}\frac{u_h^k-u_h^{k-1}}{\delta t}a_h^k\mathrm{div}(\delta\theta^{-l}) =$$

$$\underbrace{\int_I\int_{U_h} u_h'(a_h-\pi a_h)\mathrm{div}(\delta\theta^{-l})}_{1} + \underbrace{\delta t\sum_{k=1}^K\int_{U_h}\frac{u_h(t^k)-u_h(t^{k-1})}{\delta t}(a_h(t^k)-a_h^k)\mathrm{div}(\delta\theta^{-l})}_{2} +$$

$$\underbrace{\delta t\sum_{k=1}^K\int_{U_h}\left(\frac{u_h(t^k)-u_h(t^{k-1})}{\delta t}-\frac{u_h^k-u_h^{k-1}}{\delta t}\right)a_h^k\mathrm{div}(\delta\theta^{-l})}_{3}$$

$$\int_I\int_{U_h}(A'(\delta\theta^{-l})\nabla u_h,\nabla a_h) - \delta t\sum_{k=1}^K\int_{U_h}(A'(\delta\theta^{-l})\nabla u_h^k,\nabla a_h^{k-1}) =$$

$$\underbrace{\int_I\int_{U_h}(A'(\delta\theta^{-l})\nabla(u_h-\tilde{\pi}u_h),\nabla a_h)}_{4} + \underbrace{\int_I\int_{U_h}(A'(\delta\theta^{-l})\nabla\tilde{\pi}u_h),\nabla(a_h-\pi a_h))}_{5} +$$

$$\underbrace{\delta t\sum_{k=1}^K\int_{U_h}(A'(\delta\theta^{-l})\nabla u_h(t^k),\nabla(a_h(t^{k-1})-a_h^{k-1}))}_{6} + \underbrace{\delta t\sum_{k=1}^K\int_{U_h}(A'(\delta\theta^{-l})\nabla(u_h(t^k)-u_h^k),\nabla a_h^{k-1})}_{7}$$

$$\frac{1}{2}\int_I\int_{U_h}\eta|v_h-w_h|^2\mathrm{div}(\delta\theta^{-l}) - \frac{\delta t}{2}\sum_{k=1}^K\int_{U_h}\eta(t^k)(v_h^k-w_h^k)^2\mathrm{div}(\delta\theta^{-l}) =$$

$$\underbrace{\frac{1}{2}\int_I\int_{U_h}(\eta-\tilde{\pi}\eta)|v_h-w_h|^2\mathrm{div}(\delta\theta^{-l})}_{8} + \underbrace{\frac{1}{2}\int_I\int_{U_h}\tilde{\pi}\eta(|v_h-w_h|^2-|\tilde{\pi}v_h-\tilde{\pi}w_h|^2)\mathrm{div}(\delta\theta^{-l})}_{9} +$$

$$\underbrace{\frac{1}{2}\sum_{k=1}^K\int_{U_h}\eta(t^k)((v_h(t^k)-w_h(t^k))^2-(v_h^k-w_h^k)^2)\mathrm{div}(\delta\theta^{-l})}_{10}$$

with $\tilde{\pi}$ being defined in lemma A.2.6. We can treat 1, 4, 5, 8, 9 with lemma A.2.6, 2, 6 necessitate proposition 3.1.10 and stability estimates. For the remaining pieces 3, 7, 10 we make use of proposition 3.1.6. □

As previously mentioned, we couldn't prove convergence for the adjoint states obtained after discretization, with $\theta = 1/2$. As a partial replacement for this, we derive a fully discrete estimate similar to the above ones, but in an optimize-them-discretize setting.

Corollary 3.2.7 (Fully discrete error estimates for optimize-then-discretize shape gradient, Crank-Nicolson case)
With the same assumptions and notation of theorem 3.2.1, and defining the optimize-then-discretize shape gradient as:

$$\tilde{d}J_{h,\delta t}(U_h)[\delta\theta^{-l}] :=$$
$$\delta t\sum_{k=0}^{K-1}\int_{U_h}\frac{w_h^{k+1}-w_h^k}{\delta t}\frac{q_h^k+q_h^{k+1}}{2}\mathrm{div}(\delta\theta^{-l}) + \delta t\sum_{k=1}^K\int_{U_h}\left(A'(\delta\theta^{-l})\nabla\frac{w_h^k+w_h^{k+1}}{2}\right)\nabla\frac{q_h^k+q_h^{k+1}}{2}$$
$$\delta t\sum_{k=0}^{K-1}\int_{U_h}\frac{v_h^{k+1}-v_h^k}{\delta t}\frac{p_h^k+p_h^{k+1}}{2}\mathrm{div}(\delta\theta^{-l}) + \delta t\sum_{k=1}^K\int_{U_h}\left(A'(\delta\theta^{-l})\nabla\frac{v_h^k+v_h^{k+1}}{2}\right)\nabla\frac{p_h^k+p_h^{k+1}}{2}$$
$$\frac{\delta t}{2}\sum_{k=0}^{K-1}\int_{U_h}\frac{\eta(t^k)(v_h^k-w_h^k)^2+\eta(t^{k+1})(v_h^{k+1}-w_h^{k+1})^2}{2}\mathrm{div}(\delta\theta^{-l})$$

we have, for $s = 0, 1$:

$$\left|J'(U)[\delta\theta] - \tilde{d}J_{h,\delta t}(U_h)[\delta\theta^{-l}]\right| \le \gamma(h^{s+1}+\delta t^2)\,\|\delta\theta\|_{W^{s+1,\infty}(U)}$$

Proof.
Also here we only need to compare the semidiscrete and the fully discrete shape gradients, and to proceed to a suitable splitting of such discrepancy. We begin by the time derivatives terms:

$$\int_I \int_{U_h} u_h' a_h \mathrm{div}(\delta\theta^{-l}) - \delta t \sum_{k=0}^{K-1} \int_{U_h} \frac{u_h^{k+1}-u_h^k}{\delta t}\frac{a_h^k+a_h^{k+1}}{2}\mathrm{div}(\delta\theta^{-l}) =$$

$$\underbrace{\int_I \int_{U_h} (u_h-\pi_1 u_h)' a_h \mathrm{div}(\delta\theta^{-l})}_{12} + \underbrace{\int_I \int_{U_h} \frac{u_h(t^{k+1})-u_h(t^k)}{\delta t}(a_h-\pi_1 a_h)\mathrm{div}(\delta\theta^{-l})}_{13} +$$

$$\underbrace{\delta t \sum_{k=0}^{K-1} \int_{U_h} \left(\frac{u_h(t^{k+1})-u_h(t^k)}{\delta t} - \frac{u_h^{k+1}-u_h^k}{\delta t}\right) T_k a_h \mathrm{div}(\delta\theta^{-l})}_{14} + \underbrace{\delta t \sum_{k=0}^{K-1} \int_{U_h} \frac{u_h^{k+1}-u_h^k}{\delta t}\left(T_k a_h - \frac{a_h^k+a_h^{k+1}}{2}\right)\mathrm{div}(\delta\theta^{-l})}_{15}$$

For the gradients:

$$\int_I \int_{U_h} (A'(\delta\theta^{-l})\nabla u_h)\nabla a_h - \delta t \sum_{k=1}^{K} \int_{U_h} \left(A'(\delta\theta^{-l})\nabla \frac{u_h^k+u_h^{k+1}}{2}\right)\nabla \frac{a_h^k+a_h^{k+1}}{2} =$$

$$\underbrace{\int_I \int_{U_h} (A'(\delta\theta^{-l})\nabla(u_h-\pi_1 u_h))\nabla a_h + (A'(\delta\theta^{-l})\nabla \pi_1 u_h)\nabla(a_h-\pi_1 a_h)}_{16} + \underbrace{\int_I \int_{U_h} (A'(\delta\theta^{-l})\nabla \pi_1 u_h)\nabla \pi_1 a_h - \delta t \sum_{k=0}^{K-1} (A'(\delta\theta^{-l})T_k \nabla u_h)\nabla T_k a_h}_{17}$$

$$+\underbrace{\delta t \sum_{k=0}^{K-1} \left(A'(\delta\theta^{-l})\left(T_k\nabla u_h - \nabla\frac{u_h(t^k)+u_h(t^{k+1})}{2}\right)\right)\nabla T_k a_h}_{18} + \underbrace{\delta t \sum_{k=0}^{K-1} \left(A'(\delta\theta^{-l})\nabla \frac{u_h(t^k)+u_h(t^{k+1})}{2}\right)\nabla\left(T_k a_h - \frac{a_h(t^k)+a_h(t^{k+1})}{2}\right)}_{19}$$

For the cost functions:

$$\frac{1}{2}\int_I \int_{U_h} \eta |v_h-w_h|^2 \mathrm{div}(\delta\theta^{-l}) - \frac{\delta t}{2}\sum_{k=0}^{K-1}\int_{U_h} \frac{\eta(t^k)(v_h^k-w_h^k)^2+\eta(t^{k+1})(v_h^{k+1}-w_h^{k+1})^2}{2}\mathrm{div}(\delta\theta^{-l}) =$$

$$\underbrace{\int_I \int_{U_h} \eta(v_h-w_h)^2 \mathrm{div}(\delta\theta^{-l}) - \delta t \sum_{k=0}^{K-1}\int_{U_h} T_k\left[\eta(v_h-w_h)^2\right]\mathrm{div}(\delta\theta^{-l})}_{20} +$$

$$\underbrace{\frac{\delta t}{2}\sum_{k=0}^{K-1}\int_{U_h} \frac{\eta(t^k)((v_h(t^k)-w_h(t^k))^2-(v_h^k-w_h^k)^2)+\eta(t^{k+1})((v_h(t^{k+1})-w_h(t^{k+1}))^2-(v_h^{k+1}-w_h^{k+1})^2)}{2}\mathrm{div}(\delta\theta^{-l})}_{21}$$

Now, 12, 13, 16 can be treated with lemma A.2.6, remembering that $\|u_h''\|_{L^2(I,L^2)}$ is bounded as in the proof of proposition D.3.8 for 12, and that the difference quotient of 13 can be handled as in the proof of proposition D.3.8. We obtain bounds by $\|\delta\theta_h\|_{W^{1,\infty}(U_h;\mathbb{R}^n)}\,\delta t^2$.

For 14, 15, 18, 19, 21 we must use the finite element estimates 3.1.6, or proposition D.3.8, in the case of 14: we obtain bounds by $\|\delta\theta\|_{W^{1,\infty}(U;\mathbb{R}^n)}\,\delta t^2$.

Consider now the function $I \ni t \mapsto i(t) := \eta(t)\int_{U_h}(v_h(t)-w_h(t))^2\mathrm{div}(\delta\theta^{-l})$, where $T_k f = (f(t^k)+f(t^{k+1}))/2$. Using basic properties of Sobolev and Bochner spaces (see at the end of the proof), it can be shown that $i \in W^{2,1}(I;\mathbb{R})$, and the same arguments as in [20] ensure that 20 $\le \delta t^2 \int_I |i''|$. The latter term can be bounded as $\lesssim \|\delta\theta_h\|_{W^{1,\infty}(U_h;\mathbb{R}^n)}\,\delta t^2$, where we have to use the boundedness of v_h'', w_h'' in $L^2(I,L^2)$ as we saw it in the proof of proposition D.3.8.

Let us now come to 17. In this case some algebraic computations show that:

$$\textcircled{17} = \frac{\delta t^2}{12}\delta t \sum_{k=0}^{K-1}\left(A'(\delta\theta^{-l})\nabla\frac{u_h(t^{k+1})-u_h(t^k)}{\delta t}, \nabla\frac{a_h(t^{k+1})-a_h(t^k)}{\delta t}\right)_{L^2(U_h)}$$

Let us call $\overline{u'}_h$ the function that on each I_k is $\delta t^{-1}\int_{I_k} u_h' = \frac{u_h(t^{k+1})-u_h(t^k)}{\delta t}$. We immediately get:

$$\left|\textcircled{17}\right| \lesssim \delta t^2 \left\|\delta\theta\right\|_{W^{1,\infty}(U;\mathbb{R}^n)} \sqrt{\delta t \sum_{k=0}^{K-1}\left\|\overline{u'}_h|_{I_k}\right\|^2_{H^1(U_h)}} \sqrt{\delta t \sum_{k=0}^{K-1}\left\|\overline{a'}_h|_{I_k}\right\|^2_{H^1(U_h)}}$$

A minor reworking of lemma 3.2 of [40] gives $\left|\textcircled{17}\right| \lesssim \delta t^2 \left\|\delta\theta\right\|_{W^{1,\infty}(U;\mathbb{R}^n)} \left\|u_h'\right\|_{L^2(I,H^1(U_h))} \left\|a_h'\right\|_{L^2(I,H^1(U_h))}$. Now we only need to apply stability estimates to conclude $\left|\textcircled{17}\right| \lesssim \delta t^2 \left\|\delta\theta\right\|_{W^{1,\infty}(U;\mathbb{R}^n)}$.

A technicality

Here is why i'' is $W^{2,1}(I;\mathbb{R})$. η is smooth in time, so that we want $j(t) := \int_{U_h}(v_h(t)-w_h(t))^2\mathrm{div}(\delta\theta^{-l})$ to be $W^{2,1}(I;\mathbb{R})$. But by proposition A.2.1 it suffices $t \mapsto (v_h(t)-w_h(t))^2\mathrm{div}(\delta\theta^{-l})$ to be in $W^{2,1}(I;L^1)$. First of all, the constant factor $\mathrm{div}(\delta\theta^{-l})$ doesn't play a role in time smoothness, so that we now only need to check that $(v_h - w_h)^2 \in W^{2,1}(I;L^1)$. This will follow from repeated application of the following lemma: $uv \in W^{1,1}(I,L^1)$ if $u,v \in H^1(I,L^2)$, with $(uv)' = uv' + u'v$.

The latter claim follows by density of smooth functions $C^\infty(\overline{I},L^2)$ in $H^k(I,L^2)$, see [42], corollary 3.12.

□

4. Implementation

We now discuss our implementation and numerically verify some of the results that were previously shown:

- section 4.1 is devoted to the illustration of the computer implementation of the shape optimization problem, problem 2.2.3
- in section 4.2 some numerical experiments are reported and commented: we focus on shape optimization results and on the error estimates for shape gradients of section 3.2

4.1. Algorithmic set-up

We anticipate that all the experiments and the code are hosted at the following GitHub page:

`https://github.com/leom97/Master-s-thesis.git`.

We wrote our code in Python, making substantial use of the FEniCS package ([47]). This is the main tool to simulate the partial differential equations. One of the reasons for choosing FEniCS is the compatibility with dolfin-adjoint, an automatic differentiation toolbox that "derives the discrete adjoint and tangent linear models from a forward model written in the Python interface to FEniCS" (see [31], [22] and [50]). That is, we only needed to implement the "forward model" (cost functional and partial differential equations), whereas the shape gradients, that are exact on the discrete level, were automatically derived for us by dolfin-adjoint. Their correctness was nonetheless checked through comparisons based on proposition 3.1.8 and through Taylor tests. In addition, for the shape optimization part, we made use of Moola, "a set of optimisation algorithms specifically designed for PDE-constrained optimisation problems" (see here). GMSH ([32]) was used for the meshing.

The shape identification problem, problem 2.1.2, lends itself very well to debugging and numerical experimentation, as one can build "exact" solutions (on the discrete level) and then analyze whether that is recovered by the optimization process. One can for instance artificially create the "optimal" inclusion $\Omega_{e,h}$, invent Neumann measurements g, simulate the heat equation for w (see problem 2.1.1) and then obtain the correct Dirichlet data f. Starting then from an initial guess for the inclusion and making use of g, f, optimization can be started: Ω_e should be recovered.

Before delving into more details, here is an overview of the different components of the shape optimization code:

1. meshing the reference domain
2. transforming the reference domain to $\Omega_{e,h}$
3. simulating the heat equation on $\Omega_{e,h}$ with artificial Neumann data g, to obtain the synthetic Dirichlet data f
4. running the optimization routines with f, g as data form a guess of $\Omega_{e,h}$

Let us now discuss more thoroughly some of the above components.

Meshing

We want to remark that in the meshing procedure, we started from a smooth shape modeled in GMSH, and then we triangulated it into a mesh, whose boundary nodes lie on the boundary of the smooth shape, as is required in e.g. assumption 3.1.2 and appendix D. Instead of choosing a base mesh and then performing (uniform) refinements on it, we loaded a sequence of meshes with increasingly finer mesh widths. In fact, after a uniform refinement, not all discrete boundary nodes need to be again on the smooth boundary. One would need to correct for this effect, and to do so, have knowledge of a parametrization of the entire boundary: as we tried to use the least possible knowledge of the smooth boundary, we opted for generating a mesh sequence, instead of performing refinements.

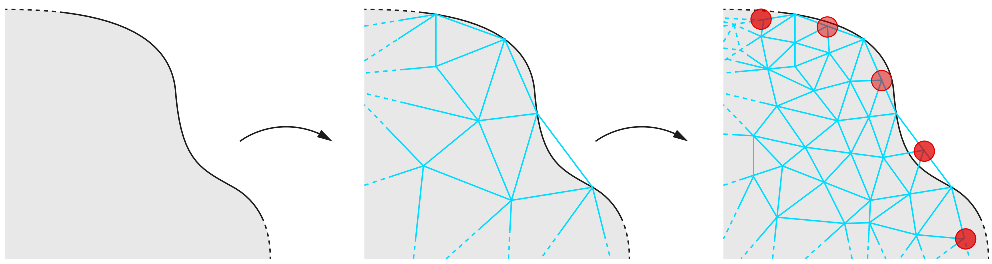

Figure 4.1.: Problems with uniform refinements

Star-shaped parametrization

For simplicity, we assume that the computational domain can only undergo radial displacements of the form given in corollary 2.3.6. This is realized as follows. The reference domain is fixed to be a meshing of $D \setminus \overline{B_\epsilon(0)} =: U_r$, meshing which induces the space of linear finite elements S_h^1, as we have denoted it in e.g. appendix D. Consider also a meshing of the unit sphere $\mathbb{S}^{n-1}$, potentially independent of the previous one to allow some flexibility, inducing the space of (surface) linear finite elements $B^1_{\tilde{h}}$. Our control, i.e. our optimization variable, will be a function $\sigma_{\tilde{h}} \in B^1_{\tilde{h}}$, and we should be solving:

$$\min_{\sigma_{\tilde{h}} \in B^1_{\tilde{h}}} J_{h,\delta t}(\tau_{\epsilon+\sigma_{\tilde{h}}}) = J_{h,\delta t}(\mathrm{Id} + V_{\sigma_{\tilde{h}}})$$

with $V_{\sigma_{\tilde{h}}}$ being the vector field described in corollary 2.3.6. The issue with this formulation is that $V_{\sigma_{\tilde{h}}}$ doesn't preserve the polygonal/polyhedral nature of the volume meshes. Therefore, we actually implement:

$$\min_{\sigma_{\tilde{h}} \in B^1_{\tilde{h}}} J_{h,\delta t}(\mathrm{Id} + I_h V_{\sigma_{\tilde{h}}})$$

where I_h means Lagrange interpolation onto piecewise linears.

We chose finite element functions on the sphere for simplicity. A downside that is more of theoretical nature, is that it is not clear to which smooth domain a deformed mesh corresponds to. One could then opt for smoother radial functions, like spherical harmonics, as it is done in [37].

Synthetic data

As previously mentioned, to obtain the needed boundary data to perform shape optimization, we simulate the heat equation for w on the exact computational domain $\Omega_{e,h}$. Because we are in a "volumetric" setting, we give the Neumann data and obtain the Dirichlet nodal values, unlike in [37], where the opposite is done. In fact, in our setting, the finite element Neumann trace need not to have a boundary representation.

Using the same discretization parameters to generate the synthetic data, and then perform shape optimization, will result in committing an "inverse crime" (see [64]). To avoid this, there are at least two possibilities: either some noise is added to the synthetic data, or different computational models must be employed in synthesis and inversion/optimization. We experiment with both options, and in particular, for the second, we synthethize the data with a finer discretization than during the optimization process. We mention that in [37], synthesis and inversion are performed by solving integral equations of different kinds, but on the same discretization. The authors also add noise to the synthetic data.

Finite elements

We are adopting, as already mentioned, linear (instead of e.g. quadratic) finite elements, for simplicity, but also computational efficiency. This is in constrast with [37], where the authors employ order 2 isoparametric elements (in the context of the boundary element method). The framework of appendix D could nonetheless potentially accommodate higher order isoparametric elements, see the works of e.g. [24], [26], [25]. Isoparametric elements are necessary, when adopting higher order basis functions, in order to preserve optimal accuracy (see section 4.4 of [57] for a discussion on this). The version of FEniCS we are using (2019.1) doesn't provide support for curved geometries, and the latest release FEniCSx is not yet interfaced with dolfin-adjoint. Alternatively, Firedrake (see [54]) could be employed, which has compatibility with dolfin-adjoint, although we encountered several difficulties in the transfering of functions between non conforming meshes, something we needed at several places throughout our code.

Also, we recall that the motivation for using the FEM method is that the analysis of [39], which we partially repeated in our setting, suggests that the volume form of the shape gradient is more accurate a boundary form, when PDEs are discretized with the finite element method. Finite elements are also appreciated and widespread in the engineering community. The main drawback of adopting a distributed setting is the added computational cost: the entire domain must be meshed, and the solution computed on interior nodes too.

Optimization

As previously mentioned, we make use of the package Moola. This is because of its capabilities to natively handle optimization with respect to custom scalar products, and we found this to be especially important in our case, see section 2.4 for a theoretical justification and section 4.2 for a further discussion.

We mostly experimented with an L-BFGS algorithm, but also with a modified Newton's method. We implemented the latter following the observations contained in [27], a work centered around a similar shape optimization problem as ours, in an attempt to alleviate some spurious oscillations we observed, most likely coming from the ill-posedness of the shape identification problem. We will soon discuss these aspects in section 4.2.

With regards to the temporal weight (see section 3.1 for details), we chose $\eta(t) = \exp\{-a/(t-T)^2\}$, with a suitable $a > 0$ ($a = 0.005$ in our runs). η roughly looks like this:

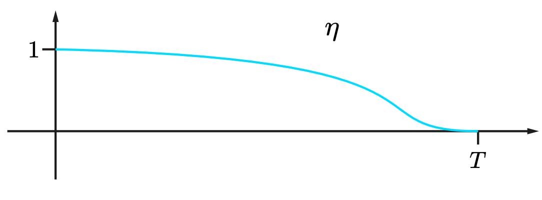

Figure 4.2.: The temporal weight η

4.2. Experiments

All the experiments were conducted on a laptop with an Intel® i7-6700HQ, 2.60GHz CPU, and 16 GB of RAM.

For simplicity we work in two dimensions and with $D := B_2(0)$, $\Omega_r := B_1(0)$, so that U_r is an annulus centered at the origin.

4.2.1. Shape optimization results

We set $T = 2$ throughout. Note that in the following plots, the "exact" control (yielding the exact domain $\Omega_{e,h}$ is always interpolated into the finite element space of the control $\tilde{\sigma}_h$, to emphasize what is the best possible result that can be attained by the optimization routine.

Some exploratory runs

Let us illustrate a few runs, performed with different Neumann data g and with an hourglass-shaped inclusion. The challenge of this example is to correctly resolve the "corners" in the middle of the hourglass, which have a strong derivative (in the sense of radial functions), are far away from the external boundary (so that the influence on the boundary data of the heat equations may be weak), and where the mesh becomes very distorted, which worsens the quality of the mesh and thus, possibly, of the finite element solution.

To avoid the inverse crime, the Dirichlet data is generated on a mesh that is twice as fine as the to-be-optimized one, and with 120 steps of the Crank-Nicolson method, whereas 60 are used in the simulation. The parameter $\tilde{h}$ is set to 0.03 during synthesis, and to 0.15 during inversion. Such configuration will be referred to as "standard configuration".

We show the results of six runs performed with six different Neumann sources, having a common behaviour in time: $g_1 = t^2$, $g_2 = x_1 g_1$, $g_3 = x_2 g_2$, $g_4 = t^2 \sin(4t)$, $g_5 = t$, $g_6 = 1$. The examples took $25, 20, 20, 25, 25, 25$ L-BFGS iterations to converge, amounting to around 4 minutes for each run.

g_2, g_3, g_4 represent various complications of the base example g_1, and we experiment with them to point out that there doesn't seem to exist a recurring "error shape" when varying the boundary data.

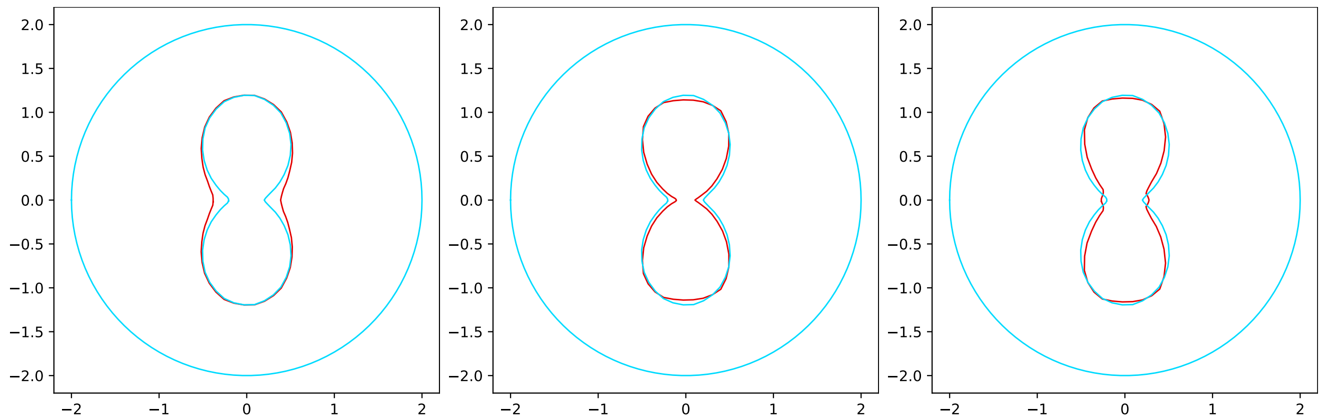

Figure 4.3.: Exact and simulated inclusion (in red) for the runs with g_2, g_3 adn g_4, in order from left to right

On the other hand, the heat equations with g_5, g_6 lack, respectively, one and two orders of compatibility, that are required in assumption 3.1.2. We can see a better result in g_1, then in g_5 and lastly in g_6:

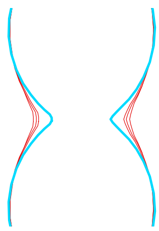

Figure 4.4.: From the outside to the inside: run with g_6, g_5, g_1 and exact solution in blue

For completeness, with g_1, we also report the history of the cost function and the gradient l^∞ norm:

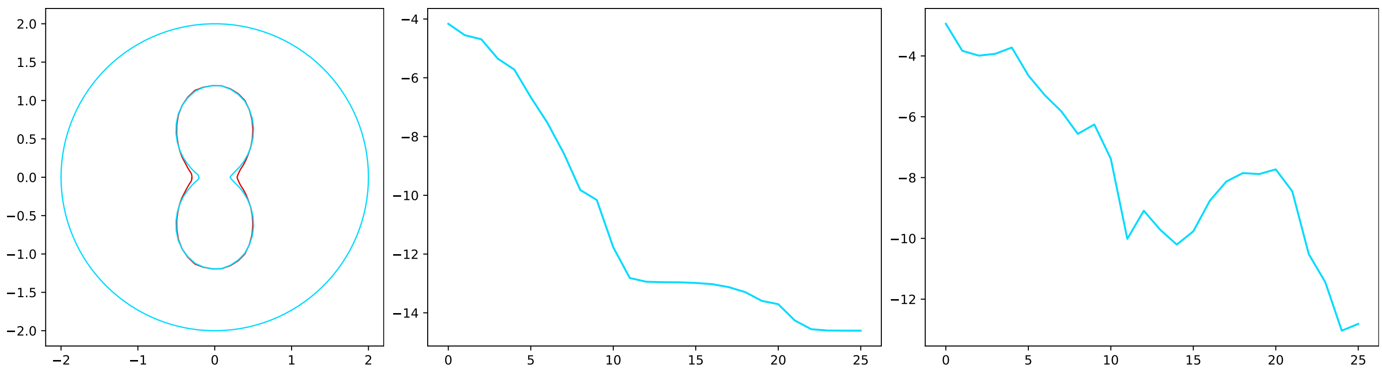

Figure 4.5.: Reconstruction, cost function (logarithm) and gradient history (logarithm) for the g_1 run and 25 iterations

The effect of η

We now show a visual comparison of the same example g_1, run with three different values a for $\eta(t) = \exp\{-a/(t-T)^2\}$, which are $a = 0.005, a = 0.05$ and $a = 0$.

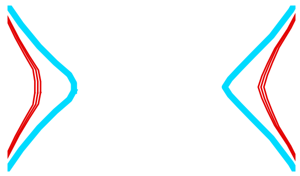

Figure 4.6.: From outside to inside: run with g_1 and $a = 0$, $a = 0.05$, $a = 0.005$ and exact solution in blue

Some very small differences can be noticed: it seems that small values of a yield an improvement over a 0 value of a. Our hypothesis for this is in accordance with the behaviour of fig. 4.4: $a = 0$ means losing some compatibility. A too large value of a, on the other hand, perturbs the problem too much (so that the plot corresponding to $a = 0.005$ is yields the best result here). From here, we conjecture that a should be chosen small enough, but positive.

Inner product

We found it beneficial to work with smooth descent directions by making use of the H^1 inner product during optimization, instead of the L^2 one. This is natively handled by Moola. In doing so we obtained less squiggly boundaries, and more admissible ones: note in fact that we are working in an unconstrained setting for simplicity, whereas the optimization variable $\tilde{\sigma}_h$ should be positive and small enough for the computational domain to be contained in $B_2(0)$. With the L^2 scalar product we found that iterates were sometimes assuming negative values.

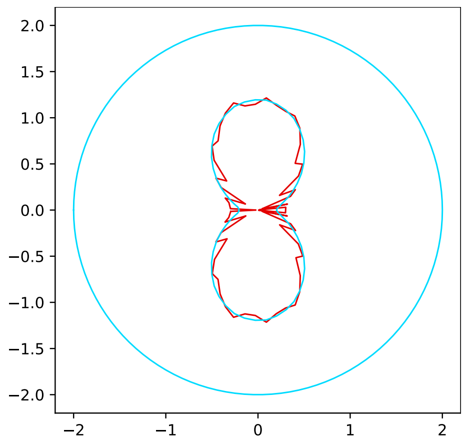

Figure 4.7.: Reconstruction for the run g_1 and the L^2 inner product

Ill-posedness

Degeneration of the boundary

It has already been noted in [37] that problem 2.1.2 is "severely ill-posed". The ill-posedness of the inverse problem is mirrored in the ill-posedness of the shape optimization problem, problem 2.2.3, where the responsible for such ill-posedness is the compactness of the continuous shape Hessian at the optimal domain: this phenomenon has been exhaustively analyzed in [27] in an "elliptic" version of problem 2.1.2, but we expect their conclusions to apply also to our case.

We computed the shape Hessian at the optimal domain with the help of dolfin-adjoint and observed indeed large condition numbers, as expected (with values $\simeq 10^5$).

This means that small changes in the problem data might yield large changes in the reconstruction, and instabilities in the reconstruction process. In fact, as is commonplace in solving ill-posed inverse problems, proceeding further with the iterations of the solution algorithm will only at first improve the reconstruction, but later result in a degradation of the result (see e.g. [41], section 2.1). As a remedy, one should impose prior knowledge on the reconstruction through regularization, and/or adopt some form of early stopping.

We did experience these phenomena: up to a certain number of L-BFGS iterations, we obtained acceptable results, the ones we showed above. Proceeding further led to a degradation of the inner boundary. The run with g_1 and stopping at 75 iterations instead 25, produced:

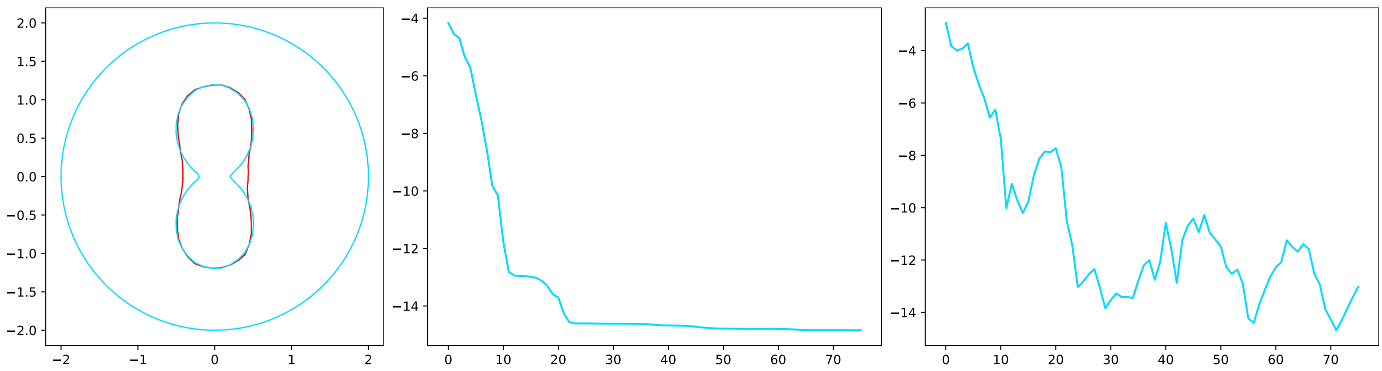

Figure 4.8.: Reconstruction, cost function (logarithm) and gradient history (logarithm) for the g_1 run and 75 iterations

The solution obtained at around 25 iterations remains unchanged and stable until about iteration 35, then the cost function is further reduced, along some spurious descent direction.

This degeneration is even more evident and quicker, in case the implicit Euler method is used during optimization, in place of the Crank-Nicolson one, all the other parameters being unchanged (so that the exact data is still generated with the Crank-Nicolson method). This is because the implicit Euler's method converges more slowly in time, so that the discrepancy in the computed PDEs and the synthetic PDEs, is $O(\delta t)$ and not $O(\delta t^2)$. This is one of the reasons for adopting the Crank-Nicolson method: the implicit Euler method yields a faster, worse degeneration of the boundary, and a less accurate one, when early stopping is applied. We have nonetheless analyzed the implicit Euler case in chapter 3 because this method has already been successfully employed in less ill-posed parabolic shape optimization (see [11]). We show reconstruction, cost function and gradient history for a run with implicit Euler.

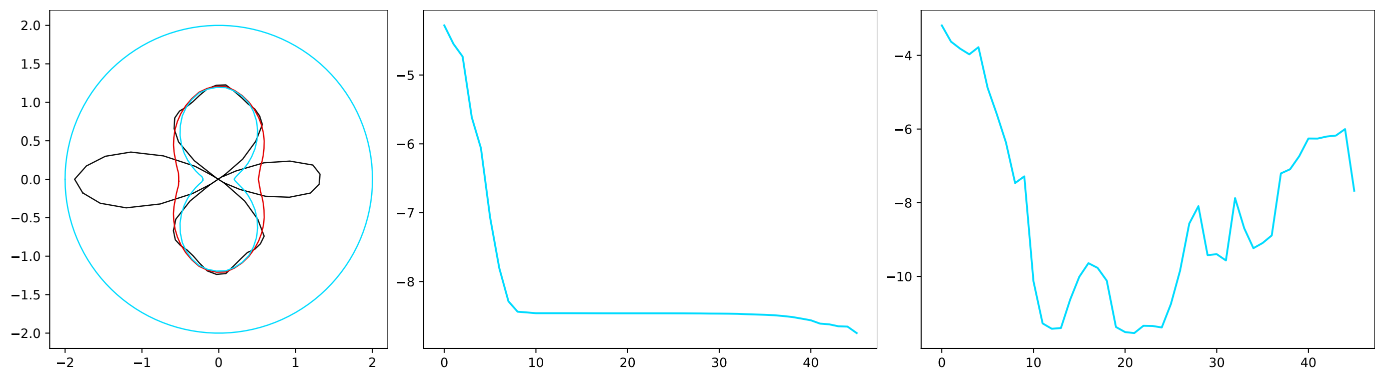

Figure 4.9.: Reconstruction, cost function (logarithm) and gradient history (logarithm) for the g_1 run. The black boundary corresponds to 45 iterations, the blue one to 25. The presence of the lateral lobes in the black reconstruction indicates a negative radial function.

About the inverse crime

Let us avoid the inverse crime in a different way, through application of noise to the problem data f, g. We therefore set the discretization parameters for the synthetization, equal to those used for the inversion. The noise level is 1%, with respect to the $L^\infty(I, L^\infty)$ norm of the data, and the perturbation is random uniform.

We noticed that the optimization process is much more stable with the number of iterations, than when different discretizations are adopted, for inversion and synthesis. The reconstructed boundary is very similar to those of the above runs, and it starts to present spurious oscillations very late (only after iteration 80, in the case of the g_1 run). In the present case, the discrepancy between exact data, and data available during optimization, is randomly distributed and of zero mean, whereas we noted that it presents a "trend" given by the chosen PDEs discretization algorithm, when different discretizations are employed. This seems to be a key ingredient to the degeneration behaviour that we observed.

We did most of the experiments with different discretizations between inversion and synthesis, because this approach better highlited the ill-posedness of the problem. Moreover, in a real-world situation, the data can be interpreted to be sampled from a solution with discretization parameters tending to zero, this is another reason to proceed as we did.

Second order information

As previously mentioned, there is evidence for saying that the shape optimization problem is ill-posed: this is reflected in an ill-conditioned Hessian, at the optimal domain. This can cause undesired oscillations when employing only first order optimization methods, a possible way out being the usage of additional second order information, like the shape Hessian.

We thus experimented with a regularized Newton method, following the observations of [27] (to which we refer the reader for further details about the method), and found out that, indeed, spurious oscillations don't seem to happen: using g_1 as Neumann data, we find that it takes about 20 iterations for the shape to stabilize. However, the runtime increases to about 2.75 minutes per iteration, the shape Hessian being automatically computed by dolfin-adjoint. On top of this, the reconstruction seems to be less precise than when employing the L-BFGS method, with early stopping. This convinced us to stick with the L-BFGS method.

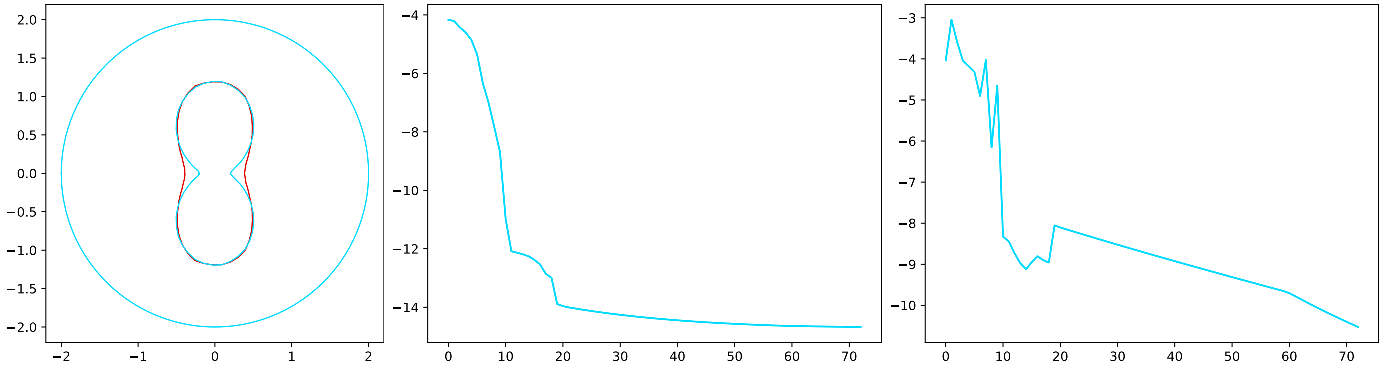

Figure 4.10.: Reconstruction, cost function (logarithm) and gradient history (logarithm) for the g_1 run, and the regularized Newton method from [27]. The reconstructions after 20 and 70 shape are visually indistinguishable.

Sea urchin

Lastly, we show the reconstruction of a 2D version of the more complicated "sea urchin" inclusion of [37]. The discretization configuration is the standard one. The reconstruction ran for 30 iterations. This time, for completeness, we applied also 1% noise to the data, apart from employing different discretizations in inversion and synthesis.

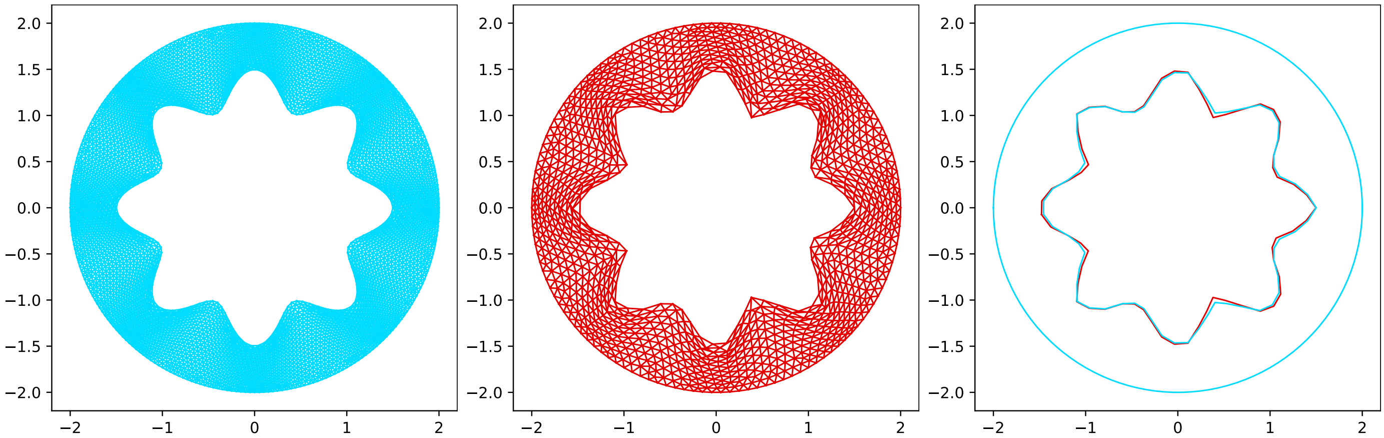

Figure 4.11.: "Exact" domain, reconstruction, and comparison between reconstruction and the exact domain, interpolated to the optimization finite element space.

4.2.2. Estimates for the shape gradients

We now present some numerical evidence of the estimates shown in section 3.2. Throughout, U_h will be approximating $U = B_2(0) \setminus \overline{B_1(0)}$.

For $\theta = 1$ (implicit Euler) or $\theta = 1/2$ (Crank-Nicolson), we set $\delta t = Ch^{2\theta}$, $C > 0$. We choose a number of spikes s from 0 to 9, an amplitude among 0.1 and 0.2 and we consider the resulting sinusoidal radial function $\sigma(t) = A\cos(st)$, interpolated on a spherical mesh of size $\tilde{h} = 0.5$. This mesh parameter stays fixed across all the runs, when h varies. Note, this yields a very coarse spherical mesh: the rationale is to have the resulting displacement fields (finite element vector fields on the mesh of size h) approximating a vector field that is in $W^{1,\infty}$ but not $W^{2,\infty}$, as h is refined. We thus obtain 20 different displacement fields $\delta\theta^i_{h,\tilde{h}}$, $i = 1, ..., 20$, with which we test the shape gradients.

Not being able to represent non-discretized shape gradients, we content ourselves with analyzing the asymptotic behaviour of the quantity:

$$Q_h := \max_{i=1,\ldots,20} \frac{|J'_{h_f,\delta t_f}(U_{h_f})[\delta\theta^i_{h_f,\tilde{h}}] - J'_{h,\delta t}(U_h)[\delta\theta^i_{h,\tilde{h}}]|}{\left\|\delta\theta^i_{h,\tilde{h}}\right\|_{W^{1,\infty}(U_{h_f})}}$$

where $h_f \ll h$, $\delta t_f \ll \delta t$.

In particular, we set $h_f = 0.03125$, and $h = 2^l h_f$, for l integer, where we refer to 2^l as "multiplier". We report the orders of convergence $\dfrac{\log Q_h - \log Q_{2h}}{\log h - \log 2h}$ in four cases, corresponding to $\theta = 1, 1/2$ and $a = 0.05, 0$, where $\eta = \exp\{-a/(t-T)^2\}$. We set $C = 1$ (for $\delta t = Ch^{2\theta}$) for Crank-Nicolson, and $C = 5$ for implicit Euler, to have a number of timesteps that is always greater than 1. For reasons of computational resources, we made one less refinement in the implicit Euler case.

Of course we register an infinite order of convergence when the refinement brings us from $2h_f$ to h_f. Moreover, the order of convergence value in the refinement before this is larger than expected, most probably because of a "saturation" effect. We nonetheless think that, at least in the case $a > 0$, these results confirm the theoretical considerations in section 3.2. In particular, we note the following facts:

Run with Crank-Nicolson, $a = 0.05$ and $C = 1$						
Multiplier	32	16	8	4	2	1
Q_h	0.0557	0.0139	0.0047	0.0013	0.0003	0.0
OOC	2.356	1.8261	2.0785	2.4573	∞	$-$
Run with Crank-Nicolson, $a = 0$ and $C = 1$						
Multiplier	32	16	8	4	2	1
Q_h	0.0697	0.0078	0.0021	0.0006	0.0001	0.0
OOC	3.7204	2.1859	2.1446	2.3489	∞	$-$

Table 4.1.: Order of convergence study with Crank-Nicolson

Run with implicit Euler, $a = 0.05$ and $C = 5$					
Multiplier	16	8	4	2	1
Q_h	0.0549	0.0154	0.0047	0.001	0.0
OOC	2.1202	1.9637	2.3004	∞	$-$
Run with implicit Euler, $a = 0$ and $C = 5$					
Multiplier	16	8	4	2	1
Q_h	0.0594	0.0126	0.005	0.0011	0.0
OOC	2.5864	1.5225	2.2349	∞	$-$

Table 4.2.: Order of convergence study with implicit Euler

- the above tables suggest a superconvergence effect, for the implicit Euler's method, even with "rough" displacement vector fields, cfr. corollary 3.2.6
- although we haven't given a proof of the convergence behaviour in the case of the Crank-Nicolson method and a discretize-then-optimize approach, the above results suggest that the quantity Q_h is $O(h^2 + \delta t^2)$, as we suspected. Note, also here it suffices to test with $W^{1,\infty}$ displacements, to obtain the spatial superconvergence effect
- the value of 1.5225 in table 4.1 might be due to a lack of regularity of the adjoint states, since $a = 0$. This does not contradict our predictions, which were done in conditions of $a > 0$

5. Conclusion

We considered a model parabolic shape optimization problem and treated it in a volumetric fashion: the expression of the distributed shape gradient was derived, also in connection to a star-shaped parametrization of the domains.

The finite element method was employed to perform the spatial discretization of the arising PDEs, whereas a Crank-Nicolson or implicit Euler scheme was adopted for the temporal one. In the latter case, optimization and discretization are seen to commute.

We derived a semidiscrete (in space) error estimate relating the continuous shape gradient at a smooth enough domain U, and the discrete shape gradient at a polygonal/polyhedral interpolation U_h of U. In the case of the implicit Euler method, we were able to derive fully discrete estimates in a discretize-then-optimize commutative setting, for the Crank-Nicolson one only in an optimize-then-discretize framework.

Numerical experiments support such conclusions, and even suggest that what was only proved for the implicit Euler method, might be obtainable with the Crank-Nicolson method. We also show the results from the shape optimization process itself.

There are some interesting directions in which our work can be expanded:

- one could at first prove that discretization and optimization commute also for Crank-Nicolson, as [29] suggests
- from here, fully discrete estimates analogous to those for implicit Euler, should be derivable
- the error estimates for the shape gradients were derived assuming a specific form of U_h: it could be worth to try to eliminate the requirement that ∂U_h must interpolate ∂U. Moreover, one could try to explicitly account for the fact that $U = \tau(U_r), U_h = \tau(U_{r,h})$, in these estimates

Appendix A. Functional spaces

Let us collect, for the convenience of the reader, some technical results that will be used throughout our work. Where appropriate, we give a short proof or a reference for one.

A.1. Sobolev spaces

Theorem A.1.1 (Integration by parts)
Let Ω be a bounded Lipschitz domain. Let $1 < p < \infty$ and $f, g \in W^{1,p}(\Omega), W^{1,q}(\Omega)$, $q = p'$, the dual Hölder exponent. Then:

$$\int_\Omega f \partial_i g = -\int_\Omega g \partial_i f + \int_{\partial\Omega} \mathrm{tr} u \nu_i d\mathcal{H}^{n-1}$$

Proof.
This follows from [43], theorem 18.1 at page 592, where g needs to be $C^1_c(\mathbb{R}^n)$. But [1], theorem 3.18 at page 54, says that (thanks to the smoothness of the boundary) the set of the restrictions to Ω of such functions is dense in $W^{1,q}(\Omega)$, so that we can conclude by a density argument. □

Proposition A.1.2 (Characterization of $W^{1,\infty}$)
Let Ω be a bounded Lipschitz domain, or $\mathbb{R}^n$. Then $W^{1,\infty}(\Omega) = C^{0,1}(\overline{\Omega}) \cap L^\infty(\Omega)$.
This means that $u \in W^{1,\infty}(\Omega)$ if and only if u has a (unique) representative that is bounded, Lipschitz continuous. Weak and classical derivatives coincide a.e.

Proof.
In any case, Ω is an extension domain for $W^{1,\infty}(\Omega)$ (see [43], theorem 13.17 at page 425, 13.13 at page 424, and definition 9.57 at page 273).
Let $u \in W^{1,\infty}(\Omega)$. By [43], 11.50 at page 339, because Ω is an extension domain, we obtain that u has a representative $\bar{u}$ that is bounded Lipschitz. Let $\phi \in C^\infty_c(\Omega)$. By The Kirszbraun theorem (see e.g. [5]), we can extend $\bar{u}$ to a Lipschitz on $\mathbb{R}^n$. Then, by Fubini's theorem and integration by parts for AC functions, we conclude $\int_\Omega \bar{u}\partial_i\phi = -\int_\Omega \partial_i\bar{u}\phi$, so that $\nabla\bar{u} = \nabla u$ almost everywhere.
Conversely, let u be bounded Lipschitz. The above reasoning shows that u has (bounded) weak derivatives equal to the a.e. classical derivatives. Their measurability follows by approximation by difference quotients. □

A.2. Bochner spaces

Proposition A.2.1 (Bochner integral and bounded operators)
Let X, Y be separable Banach, let $T \in L(X, Y)$ be a linear bounded operator. For $f \in L^1(I, X)$ define $Tf(t) := T(f(t))$. Then $Tf \in L^1(I, Y)$ with $T \int_I f = \int_I Tf$.
More generally, for $k \geq 0$, $1 \leq p < \infty$, $f \in W^{k,p}(I, X) \implies Tf \in W^{k,p}(I, Y)$, with weak derivatives $\partial_{t^i} Tf = T\partial_{t^i} f$, $0 \leq i \leq k$.
The map $f \mapsto Tf$, $W^{k,p}(I, X) \to W^{k,p}(I, Y)$ is linear, and bounded by $\|T\|$.

Proof.
Let f_n be simple, $f_n \to f$ a.e., with $\lim_n \int_I f_n = \int_I f$ in X and $\|f_n\|_X \leq C \|f\|_X$ (see page 6, and corollary 2.7 at page 8 of [42]).
For almost all t, $T(f_n(t)) \to T(f(t)) = Tf(t)$ in Y, so that Tf is measurable (strongly).
By dominated convergence (corollary 2.6 of [42]), Tf is integrable. Thus $\int_T Tf = \lim_n \int_I Tf_n = \lim_n T \int_I f_n$, because f_n is simple. And now, by the choice of f_n, $\int_T Tf = \lim_n T \int_I f_n = T \lim_n \int_I f_n = T \int_I f$.
The rest of the claim is an easy consequence of this first part. □

Proposition A.2.2 (Continuous representatives)
Let X be separable Banach. $f \in L^1(I, X)$ has at most a continuous representative on $[0, T]$.

We now check that a vector valued test function has weak derivatives of all orders.

Proposition A.2.3 (Weak derivatives of test functions)
Let $\phi \in C^1([0,T],X)$, for X separable Banach. It means that the limit of the difference quotients exists for all points of I, that $t \mapsto \phi(t), \phi'(t)$ are continuous, and that they can be continuously extended to $[0,T]$.
Then these classical derivatives coincide a.e. with the weak derivatives of u.

Proof.
Apply proposition 3.8 of [42] at page 26, thanks to theorem 6 at page 146 of [30], a mean value theorem for vector valued function. □

We also need a time dependent trace lemma, which we provide in a space-time "tensor product" form, but under non-optimal regularity assumptions, for the sake of making some arguments more transparent.

Definition A.2.4 (Time dependent trace)
Let Ω be a bounded Lipschitz domain (in the sense of [35], definition 1.2.1.1). For $k \geq 0$ we define $\mathrm{tr}_k : H^k(I, H^1(\Omega)) \to H^k(I, H^{1/2}(\partial\Omega))$ by $\mathrm{tr}_K(u)(t) := \mathrm{tr}(u(t))$, so that we can drop the subscript k

Below are some properties of this operator.

Proposition A.2.5 (Properties of trace operator)
The trace operator just defined:

1. is well posed, linear and bounded
2. admits a linear bounded right inverse, for instance, $E_k(g)(t) := E(g(t))$ (for E a right inverse of the "static" trace)
3. $\mathrm{tr}_k u = \mathrm{tr}_0 u$, for $u \in L^2(I, H^1(\Omega))$ and $E_k g = E_0 g$ gor $g \in L^2(I, H^{1/2}(\partial\Omega))$

Proof.
Proof of the proposition

We recall that the trace operator is bounded surjective onto $H^{1/2}(\partial\Omega)$, with a right inverse E (see theorem 3.37 at page 102 of [48]). The first two points are consequences of this fact and of proposition A.2.1.
The third property follows from the definition of tr, E and the fact that $H^l(I, H^1(\Omega)) \subseteq H^k(I, H^1(\Omega))$, for $k \leq l$.

□

Lemma A.2.6 (Some interpolants)
Let X be a separable Banach space, and $u \in H^1(I,X)$. Discretize I into uniform subintervals $I_k := [t^k, t^{k+1}]$ of width $\delta t > 0$. Call πu the function $\pi u(t) = u(t^k)$, for $t \in (t^k, t^{k+1})$, $\tilde{\pi} u(t) = u(t^{k+1})$ for $t \in (t^k, t^{k+1})$ and $\pi_1 u(t) = u(t^k)(t^{k+1} - t)/\delta t + u(t^{k+1})(t - t^k)/\delta t$ for $t \in (t^k, t^{k+1})$. Then:

- $\|u - \pi u\|_{L^2(I,X)}, \|u - \tilde{\pi} u\|_{L^2(I,X)} \leq C \delta t \|u'\|_{L^2(I,X)}$, for $C = 1/\sqrt{2}$
- for $v \in H^2(I,X)$, if X is Hilbert with $(\cdot,\cdot)_X$, there holds $\displaystyle\int_I ((u - \pi_1 u)', v)_X \leq \delta t^2 \|u\|_{H^2(I,X)} \|v\|_{H^1(I,X)}$
- if $u \in H^2(I,X)$, then $\|u - \pi_1 u\|_{L^2(I,X)} \leq C \delta t^2 \|u''\|_{L^2(I,X)}$, $C = 1/4\sqrt{3}$.

Proof.
There holds $\displaystyle\int_{I_k} \|\pi u - u(t)\|_X^2 \, dt = \int_{I_k} \left\| \int_{t^k}^t u'(s) ds \right\|_X^2 dt \leq \int_{I_k} \left(\int_{t^k}^t \|u'(s)\|_X \, ds \right)^2 dt.$
By Hölder's inequality we then see that $\displaystyle\int_{I_k} \|\pi u - u(t)\|_X^2 \, dt \leq \int_{I_k} \|u'(s)\|_X^2 \, ds \int_{I_k} (t - t^k) dt = \frac{\delta t^2}{2} \|u'\|_{L^2(I_k,X)}^2$. The result follows after summation. For $\tilde{\pi}$ the same reasonings work.
Now, on I_k there holds $(u - \pi_1 u)' = u' - \delta t^{-1} \displaystyle\int_{I_k} u'$, so that by a straightforward adaptation of lemma 3.2 of [40] one gets $\left\| u' - \delta t^{-1} \displaystyle\int_{I_k} u' \right\|_{L^2(I,X)}^2 \leq \delta t^2 \|u'\|_{H^1(I_k,X)}^2$. To conclude, note that $\displaystyle\int_{I_k} \left(u' - \delta t^{-1} \int_{I_k} u', v \right)_X = \int_{I_k} \left(u' - \delta t^{-1} \int_{I_k} u', v - \delta t^{-1} \int_{I_k} v \right)_X$ and apply the just derived $L^2(I,X)$ estimate to both arguments ot $(\cdot,\cdot)_X$.
For the last result, it suffices to note that $\pi_1 u(t) - u(t) = \displaystyle\int_{I_k} \frac{(t^{k+1} - \max(t,s))(\min(t,s) - t^k)}{\delta t} u''$ on I_k and suitably estimate the latter integral using the Cauchy-Schwarz inequality and some algebraic computations. □

Appendix B. Parabolic equations

Let us discuss the functional analytic setting for the various (parabolic) PDEs we are concerned with. We start with an abstract approach, which we then apply to a general boundary value problem.

B.1. Abstract theory

Assumption B.1.1 (Basic assumption for parabolic problems)
Let $V \subseteq H$ be real separable Hilbert spaces, V dense in H. Then $H \hookrightarrow V^*$ is also dense, as stated in [61] at page 147. This embedding is $H \ni f \mapsto (f, \cdot)_H$. We thus obtain a Gelfand triple, and we have $W(I,V) \subseteq C(I,H)$ (this is stated in [61], page 148).
Let $A : V \to V^*$ be linear bounded, $u \in W(I;V)$, $f \in L^2(I,V^*)$ and $u_0 \in H$.
We also assume that $\langle Av, v\rangle_{V^*,V} + \lambda \|v\|_H^2 \geq \alpha \|v\|_V^2$ for $\lambda \geq 0, \alpha > 0$.

We are interested in the following problem:

Problem B.1.2 (Abstract parabolic equation)

$$u_t + Au = f \text{ in } V^* \text{ and for a.e. } t \in (0,T) \tag{B.1.3}$$
$$u(0) = u_0 \tag{B.1.4}$$

Theorem B.1.5 (Basic well-posedness of problem B.1.2)
Under assumption B.1.1, problem B.1.2 has a unique solution u. Moreover u satisfies the stability estimate:

$$\|u\|_{W(I,V)} + \|u\|_{C([0,T],H)} \leq C(\lambda, \alpha, \|A\|_{V^*}, T)(\|u_0\|_H + \|f\|_{L^2(I,V^*)}) \tag{B.1.6}$$

Proof.
See [34] at page 19, theorem 26. □

We can also obtain additional regularity. Here are further assumptions to make this possible.

Assumption B.1.7 (Assumptions for additional regularity in time)
We assume $u_0 \in V$, $f = f_1 + f_2 \in L^2(I,H) + H^1(I,V^*)$. We also need A to be symmetric (i.e. $\langle Au, v\rangle_{V^*,V} = \langle Av, u\rangle_{V^*,V}$).

Proposition B.1.8 (Time regularity)
With assumption B.1.1 and additionally assumption B.1.7 we obtain $u \in H^1(I,H)$ with:

$$\|u'\|_{L^2(I,H)}^2 \leq C(\lambda, \alpha, \|A\|_{V^*}, T)(\|f_2\|_{H^1(I,V^*)}^2 + \|u_0\|_V^2 + \|f_1\|_{L^2(I,H)}^2)$$

Proof.
We do it in detail, following [34], to precisely track the dependence of the appearing constants. This wil be important in the proof of proposition 2.2.10.
We tie to page 25 of [34]. In particular:

$$\int_0^t \|u_n'\|_H^2 + \int_0^t \langle Au_n, u_n'\rangle_{V^*,V} = \int_0^t (f_1, u_n')_H + \int_0^t \langle f_2, u_n'\rangle_{V^*,V}$$

Then:

$$\int_0^t \langle Au_n, u_n'\rangle_{V^*,V} \geq \frac{\alpha}{2}\|u_n(t)\|_V^2 - \frac{\lambda}{2}\|u_n(t)\|_H^2 - \frac{\|A\|}{2}\|u_{n0}\|_V$$

whereas, with integration by parts:

$$\left|\int_0^t \langle f_2, u_n'\rangle_{V^*,V}\right| \leq \frac{1}{2}\|f_2'\|_{L^2(I,V^*)}^2 + \frac{1}{2}\|u_n\|_{L^2(I,V)}^2 + \frac{\alpha}{4}\|u_n(t)\|_V^2 + \frac{4}{\alpha}\|f_2\|_{L^\infty(I,V^*)}^2 + \frac{1}{2}\|f_2\|_{L^\infty(I,V^*)}^2 + \frac{1}{2}\|u_{n0}\|_V^2$$

Also:

$$\int_0^t (f_1, u_n')_H \leq \frac{1}{2}\|f_1\|^2_{L^2(I,H)} + \frac{1}{2}\int_0^t \|u_n'\|^2_H$$

This brings us to:

$$\frac{1}{2}\int_0^t \|u_n'\|^2_H + \frac{\alpha}{4}\|u_n(t)\|^2_V - \frac{\lambda}{2}\|u_n(t)\|^2_H \leq \frac{1}{2}\|f_2'\|^2_{L^2(I,V^*)} + \frac{1}{2}\|u_n\|^2_{L^2(I,V)} + \frac{8+\alpha}{2\alpha}\|f_2\|^2_{L^\infty(I,V^*)} + \frac{1+\|A\|}{2}\|u_{n0}\|^2_V + \frac{1}{2}\|f_1\|^2_{L^2(I,H)} \tag{B.1.9}$$

and thus, by weak lower semicontinuity of norms and because we have weak convergence of the time derivative, and V-strong convergence of the initial data (see again [34] for this):

$$\int_0^T \|u'\|^2_H \leq \|f_2'\|^2_{L^2(I,V^*)} + (1+\alpha^{-1})\|f_2\|^2_{L^\infty(I,V^*)} + (1+\|A\|)\|u_0\|^2_V + \|f_1\|^2_{L^2(I,H)} + \text{limsup}_n\left(\frac{\lambda}{2}\|u_n\|^2_{C([0,T],H)} + \frac{1}{2}\|u_n\|^2_{L^2(I,V)}\right)$$

For the last term, employing the exact arguments in [34], page 21:

$$\text{limsup}_n\left(\frac{\lambda}{2}\|u_n\|^2_{C([0,T],H)} + \frac{1}{2}\|u_n\|^2_{L^2(I,V)}\right) \leq C_0\|u_0\|^2_H + \alpha^{-1}\|f_1\|^2_{L^2(I,V^*)} + \alpha^{-1}\|f_2\|^2_{L^2(I,V^*)} \tag{B.1.10}$$

where $C_0 = 2^{-1}\max(1,\lambda)\max(1,\alpha^{-1})\exp(2\lambda T)$.
Therefore, and by using that the embedding $H^1(I,V^*) \hookrightarrow C([0,T],V^*)$ has norm that can be bounded by $1+T$:

$$\int_0^T \|u'\|^2_H \leq (1+(1+C_0)\alpha^{-1})\|f_2\|^2_{H^1(I,V^*)} + (1+\|A\|)\|u_0\|^2_V + C_0\|u_0\|^2_H + \|f_1\|^2_{L^2(I,H)} + C_0\alpha^{-1}\|f_1\|^2_{L^2(I,V^*)}$$

□

Proving higher time regularity under additional compatibility assumptions and smoothness of the data can be done as follows.

Proposition B.1.11 (Higher time regularity)
Let $k \geq 1$. Suppose $f \in H^k(I,V^*)$, together with:

- $g_j := f^{(j-1)}(0) - Ag_{j-1} \in H$, for $j = k$
- $g_{j-1} \in V$ for $1 \leq j \leq k$

where $g_0 = u_0$. Then, there holds $u \in H^k(I,V)$, $u^{(k+1)} \in L^2(I,V^*)$ and, for $1 \leq j \leq k$:

$$\begin{cases} u^{(j+1)} + Au^{(j)} = f^{(j)} \\ u^{(j)}(0) = f^{(j-1)}(0) - Ag_{j-1} \end{cases}$$

Proof.
See [65], theorem 27.2, page 406. □

B.2. Inhomogeneous heat equations

Here we apply the results of the last section to tackle a general inhomogeneous heat equation, which comprises e.g. the PDEs of problem 2.1.1. We make the following assumption.

Assumption B.2.1 (Basic assumption for the well-posedness of problem B.2.2)

1. $u_0 \in H^1(U)$
2. $\Omega \subset\subset D$ are bounded Lipschitz domains (in the sense of [35], definition 1.2.1.1.), call $U := D \setminus \overline{\Omega}$, another bounded Lipschitz domain
3. $g_D \in H^1(I, H^{1/2}(\Gamma_D))$. Here $\Gamma_D \neq \emptyset$ is either $\partial U, \partial D$ or $\partial\Omega$, with $g_D(0) = u_0$ on Γ_D
4. $g_N \in H^1(I, L^2(\Gamma_N))$, where $\Gamma_N = \partial U \setminus \Gamma_D$
5. $f \in L^2(I, L^2(U))$

Call $H = L^2(U)$, $V = \{v \in H^1(U), \mathrm{tr} u = 0 \text{ on } \Gamma_D\} =: H^1_{0,D}$. V is a closed subspace of H^1, which is Hilbert separable, hence also Hilbert separable. We norm it with the full H^1 norm. Because $H^1_0(U)$ is dense in H, so is V and we obtain a Gelfand triple.

We define A by $(Au)v := \int_u \nabla u \nabla v$. The general heat equation is then:

Problem B.2.2 (Inhomogeneous heat equation, general case)

$$\begin{aligned} u_t - \Delta u &= f \text{ in } (0,T) \times U \\ \partial_\nu u(\Sigma_N) &= g_N \\ u(\Sigma_D) &= g_D \\ u(0) &= u_0 \end{aligned}$$

By this we mean:

$$\begin{aligned} u &\in W(I, H^1) \\ u_t + Au &= f + G \text{ in the sense of } V^* \text{ and for a.e. } t \in (0,T) \\ \mathrm{tr} u &= g_D \text{ on } \Sigma_D \\ u(0) &= u_0 \end{aligned}$$

where $\langle G(t), v\rangle_{V^*,V} := \displaystyle\int_{\Gamma_N} g(t) \mathrm{tr} v d\sigma$, σ is the 1-codimensional Hausdorff measure.

It is known that global-in-time regularity of solutions to parabolic equations depends on the satisfaction of certain compatibility conditions between the boundary data, the source term and the initil condition, see [45], chapter 2, for instance. Taking these into account, in a situation of minimal regularity on the problem data, is beyond the scope of this work: we will see that by assuming slightly more regularity on the data, it is possible to obtain higher regularity of the solution in a fairly easy way.

Assumption B.2.3 (Time regularity assumption for problem B.2.2)
Let $k \geq 1$, consider any splitting $u = \bar{u} + \delta$, where, similarly to eq. (B.2.7), $\bar{u}$ extends the Dirichlet data.
We ask, aside from assumption B.2.1:

1. $g_D \in H^{k+1}(I, H^{1/2}(\Gamma_D))$
2. $g_N \in H^k(I, L^2(\Gamma_N))$
3. $f \in H^k(I, H)$
4. $g_j(\delta) \in V$, for $j = 0, ..., k-1$, where $g_j(\delta)$ are the terms g_j of proposition B.1.11, for the equation satisfied by δ
5. $g_k(\delta) \in H$

Assumption B.2.4 (Additional time regularity assumptions)
Apart from assumption B.2.1 and assumption B.2.3, suppose that, for $k \geq 1$, there holds:

- $g_N \in H^{k+1}(I, L^2(\Gamma_N))$
- $g_k(\delta) \in V$

Assumption B.2.5 (Spatial regularity assumptions)
Let assumption B.2.1 hold for $k = 0$, and also assumption B.2.3 and assumption B.2.4 for $k \geq 1$. Further assume:

- $\partial U \in C^{1,1}$
- $g_D \in H^k(I, H^{3/2}(\Gamma_D))$
- $g_N \in H^k(I, H^{1/2}(\Gamma_N))$

Theorem B.2.6 (Some results for problem B.2.2)
Under assumption B.2.1, for $k \geq 0$ and for $\bar{u}$ extending g_D to $I \times U$:

- there exists a unique $u \in W(I, H^1(U))$ solution to problem B.2.2

- for such u there holds $u' \in L^2(I, L^2(U))$ with:

$$\|u\|^2_{C([0,T];H)} + \|u\|^2_{L^2(I,H)} + \|\nabla u\|^2_{L^2(I,H)} + \|u'\|^2_{L^2(I,H)} \leq$$
$$C(T)\left(\|f\|^2_{L^2(I,H)} + \|g_N\|^2_{H^1(I,L^2(\Gamma_N))} + \|\bar{u}\|^2_{H^1(I,H^1(U))} + \|u_0\|^2_{H^1(U)}\right)$$
$$C(T)\left(\|f\|^2_{L^2(I,H)} + \|g_N\|^2_{H^1(I,L^2(\Gamma_N))} + C(U)\,\|g_D\|^2_{H^1(I,H^{1/2}(\Gamma_D))} + \|u_0\|^2_{H^1(U)}\right)$$

  with $C > 1$, only dependent on T, smoothly, exploding for large T.

Under assumption B.2.4, $u^{k+1} \in H^1(I, H)$, i.e. $u \in H^{(k+1)}(I, H)$, and, for $1 \leq j \leq k$:

$$\begin{cases} (u^{(j+1)}, v)_H + (\nabla u^{(j)}, \nabla v)_H = (f^{(j)}, v)_H + (g_N^{(j)}, v)_{L^2(\Gamma_N)} \\ u^{(j)}(0) \in H^1(U) \\ \mathrm{tr} u^{(j)}(\Sigma_D) = g_D^{(j)} \end{cases}$$

Finally, if assumption B.2.5 holds, then $u \in H^k(I, H^2(U)) \cap H^{k+1}(I, H)$.

Proof.

Well-posedness, stability

We conjecture the splitting $u = \bar{u} + \delta$, $\delta = \delta(\bar{u})$. Here $\bar{u}$ is a space-time extension of g_D, which we can find because $U := D \setminus \overline{\Omega}$ is bounded Lipschitz and by proposition A.2.5. Using the results of trace theory and proposition A.2.1 we also know, in particular, that $\bar{u} \in H^1(U)$ with $\|\bar{u}\|_{H^1} \leq C(U)\,\|g_D\|_{H^{1/2}(U)}$, for almost every $t \in I$.

On the other hand, $\delta \in W(I, V) \cap H^1(I, H)$ is the unique solution (see theorem B.1.5) to:

$$\begin{cases} (\delta_t, v)_H + (\nabla \delta, \nabla v)_H = (f - \partial_t \bar{u}, v)_H + (g_N, v)_{L^2(\Gamma_N)} \text{ for all } v \in V \\ \delta(0) = u_0 - \bar{u}(0) \in V \end{cases} \tag{B.2.7}$$

Note that $\bar{u}(0)$ makes sense, being $g_D \in C([0,T], H^{1/2}(\Gamma_D))$, and that $u := \bar{u} + \delta$ solves problem B.2.2. By making use of the stability estimates of theorem B.1.5 we can also conclude that problem B.2.2 is uniquely solvable, because the difference of two solutions satisfies a problem with zero boundary data, source and initial conditions.

It is also easy to see that eq. (B.2.7) and problem B.2.2 are in fact equivalent: if u, then $\delta(\bar{u}) := u - \bar{u}$ solves eq. (B.2.7), and if $\delta(\bar{u})$ solves eq. (B.2.7), then $\bar{u} + \delta(\bar{u})$ solves problem B.2.2.

By the splitting $u = \bar{u} + \delta$ and using proposition B.1.8 and the triangle inequality:

$$\|u\|^2_{C([0,T],H)} + \|u\|^2_{L^2(I,H)} + \|\nabla u\|^2_{L^2(I,H)} + \|u'\|^2_{L^2(I,H)} \leq$$
$$C(T)\left(\|f\|^2_{L^2(I,H)} + \|g_N\|^2_{H^1(I,L^2(\Gamma_N))} + \|\bar{u}\|^2_{H^1(I,H^1(U))}\right) \leq$$
$$C(T)\left(\|f\|^2_{L^2(I,H)} + \|g_N\|^2_{H^1(I,L^2(\Gamma_N))} + C(U)\,\|g_D\|^2_{H^1(I,H^{1/2}(\Gamma_D))} + \|u_0\|^2_{H^1(U)}\right)$$

with $C > 1$, only dependent on T, smoothly, exploding for large T.

Regularity: time smoothness

So, proposition B.1.11 ensures then that $\delta \in H^k(I, V)$, $\delta^{(k+1)} \in L^2(I, V^*)$. Because $\bar{u} \in H^{k+1}(I, H^1(U))$ by our assumptions and by proposition A.2.1, we obtain that $u = \bar{u} + \delta$ is in $H^{k+1}(I, H^1(U)) + H^{k+1}(I, V^*)$ and in $H^k(I, H^1(U))$.

Regularity: time smoothness again

By proposition B.1.11 we also have:

$$\begin{cases} \langle \partial_t \delta^{(k)}, v \rangle_{V^*,V} + (\nabla \delta^{(k)}, \nabla v)_H = \langle F^{(k)}, v \rangle_{V^*,V} \\ \delta^{(k)}(0) = g_k \in H \end{cases}$$

The right hand side $F^{(k)} = (f^{(k)} - G_D^{(k+1)}, \cdot)_H + (g_N^{(k)}, \mathrm{tr}(\cdot))_{L^2(\Gamma_N)}$ is now an element of $L^2(I, H) + H^1(I, V^*)$, meaning that we can apply proposition B.1.8 to obtain $\delta \in H^{k+1}(I, H)$, provided that we ask for $g_k \in V$. We conclude that $u \in H^{(k+1)}(I, H)$, and, for $1 \leq j \leq k$:

$$\begin{cases} (u^{(j+1)}, v)_H + (\nabla u^{(j)}, \nabla v)_H = (f^{(j)}, v)_H + (g_N^{(j)}, v)_{L^2(\Gamma_N)} \\ u^{(j)}(0) = g_k + \bar{u}^{(j)}(0) \in V \\ \mathrm{tr} u^{(j)}(\Sigma_D) = g_D^{(j)} \end{cases}$$

Spatial regularity

This last equation reads also:

$$\begin{cases} -\Delta u^{(j)} = f^{(j)} - u^{(j+1)} \\ u^{(k)}(\Gamma_D) = g_D^{(k)} \\ \partial_\nu u^{(j)}(\Gamma_N) = g_N^{(j)} \end{cases}$$

This holds for $0 \le j \le k$, and for a.e. $t \in I$. Elliptic H^2 regularity results that can be found in chapter 2 of [35] let us conclude the proof. □

B.3. Alternative reformulations

The two parabolic equations of interest contained in problem 2.1.1 can be recasted into problem B.2.2 and in particular, into finding $u \in W(I,V)$, $u(0) = 0$, $u_t + Au = F$ for a.e. t in V^*, a proper right hand side $F \in L^2(I,V^*)$ and $V := H^1_{0,m}$, the space of H^1 functions vanishing on the moving boundary Γ_m, or $V = H^1_0$. If inhomogeneous Dirichlet data are present, we always refer to the equivalent form B.2.7.

Here, $Au \in L^2(I,V^*)$ too (because $A \in L(V,V^*)$, and by proposition A.2.1). Call then $\mathcal{E}(u) := u_t + Au - F \in L^2(I,V^*)$ and $W_0(I,V)$ the set of $W(I,V)$ functions with zero initial value. Then, the differential equation reads $\langle \mathcal{E}(u)(t), v\rangle_{V^*,V} = 0$ for all $v \in V$, for a.a. t, equivalently, $\mathcal{E}(u) = 0$ for a.a. t. Thus, we are interested in the abstract problem:

Problem B.3.1 (Even more abstract parabolic equation)
Given a function $\mathcal{E} : W(I,V) \to L^2(I,V^*)$, find $u \in W_0(I,V)$, such that $\mathcal{E}(u) = 0$ for a.a. t.

We can view $L^2(I,V^*) \cong L^2(I,V)^*$. Hence $\langle \mathcal{E}(u), v\rangle_{L^2(I,V)^*,L^2(I,V)} = \int_I \langle \mathcal{E}(u)(t), v(t)\rangle_{V^*,V} dt$ (see [38], theorem 1.31 at page 39). We are now ready to restrict both state and adjoint space, in view of the proof of proposition 2.2.10.

Definition B.3.2 ($Q(I,V)$)
We define $Q(I,V) = H^{1,1} = L^2(I,V) \cap H^1(I,H)$, with the norm $\|v\|_Q^2 = \|v\|^2_{L^2(I,V)} + \|v_t\|^2_{L^2(I,H)}$.

Proposition B.3.3 (Properties of Q)
There holds:

- $Q = Q(I,V)$ is Hilbert with $(v,w)_{L^2(I,V)} + (v_t,w_t)_{L^2(I,H)}$
- $Q(I,V)$ is dense in $L^2(I,V)$
- $Q(I,V) \hookrightarrow C([0,T],H)$
- $Q_0(I,V)$ is dense in $L^2(I,V)$, $Q_0(I,V)$ being the space of $Q(I,V)$ function with zero initial value
- $Q(I,V) = W(I,V) \cap H^1(I,H)$, $Q_0(I,V) = W_0(I,V) \cap H^1(I,H)$ as sets
- integration by parts in time holds: $\displaystyle\int_I (v_t,w)_H = -\int_I (w_t,v)_H + (v(T),w(T))_H - (v(0),w(0))_H$
- if q_n is bounded in $Q(I,V)$, then there exists a weakly convergent subsequence q_k such that $q_k \rightharpoonup q$ in $L^2(I,H)$, $\nabla q_k \rightharpoonup \nabla q$ in $L^2(I,H)$ and $q'_k \rightharpoonup q'$ in $L^2(I,H)$

Proof.
Continuity

Follows from the embedding $H^1(I,H) \hookrightarrow C([0,T],H)$, as seen in [28], theorem 2 of page 286.

Density

We have $C_c^\infty(I,V) \subseteq Q(I,V) \subseteq L^2(I,V)$. The first inclusion holds because of proposition A.2.3, so that $C_c^\infty(I,V) \subseteq H^1(I,V)$, and because $H^1(I,V) \subseteq Q(I,V)$. $C_c^\infty(I,V)$ is dense in $L^2(I,V)$ by [38], page 39, lemma 1.9. In particular, $C_c^\infty(I,V) \subseteq Q_0(I,V) \subseteq L^2(I,V)$, and as before, the density result follows.

Integration by parts

We note that $v, w \in Q(I,V) \subseteq W(I,V)$: we can now apply theorem 3.11 at page 148 of [61].

Weak convergence

At first we note that ∂_k (the spatial weak derivatives, $k = 1,...,n$), ∂_t are linear bounded operators from $Q(I,V)$ to $L^2(I,H)$. Remember that in any case, V is a closed subspace of H^1. Then, $\partial_k : V \to H$ is linear and bounded, because we chose V to be normed by the full H^1 norm. By proposition A.2.1, ∂_i extends to a linear bounded map from $L^2(I,V)$ to $L^2(I,H)$, therefore, to a linear bounded map on $Q(I,V)$, in the sense of:

$$Q(I,V) \xhookrightarrow{i} L^2(I,V) \xrightarrow{\partial_i} L^2(I,H)$$

Here, i is the natural injection. Because q_n is bounded in the Hilbert space $Q(I,V)$, it has a weakly convergent subsequence $q_m \rightharpoonup q \in Q(I,V)$. Therefore, $\partial_k(i(q_k)) \rightharpoonup \partial_k(i(q))$ in $L^2(I,H)$. By the Hilbert space property of $L^2(I,H)$ we conclude that $(\partial_k q_m, p)_{L^2(I,H)} \to_m (\partial_k q, p)_{L^2(I,H)}$ for all $p \in L^2(I,H)$.

For the time derivative, and the convergence $(q_m, p)_{L^2(I,H)} \to (q,p)_{L^2(I,H)}$ for all $p \in L^2(I,H)$, we can reason analogously. □

We can now restrict the testing space.

Proposition B.3.4 (Equivalent testing)
Let $\mathcal{E} : W(I,V) \to L^2(I,V^*)$, and $u \in W_0(I,V)$. Then:

$$\mathcal{E}(u) = 0 \iff \langle \mathcal{E}(u), v\rangle_{L^2(I,V)^*,L^2(I,V)} = 0 \quad \forall v \in L^2(I,V) \text{ or } \forall v \in W^0(I,V) \text{ or } \forall v \in Q^0(I,V)$$

We have also seen that with smoothness assumption on data (assumption B.2.1) we obtain that the solution problem B.2.2 has $Q_0(I,V)$ smoothness.

We can therefore formulate the two partial differential equations of problem 2.1.1 in equivalent form directly on $Q_0(I,V)$ as follows:

$$\begin{aligned} w \in W_0(I,H^1_{0,m}), \bar{u} + v_0 \in W_0(I,H^1_{0,m}), v_0 \in W_0(I,H^1_0) \\ w' + Aw = (g,\cdot)_{L^2(\Gamma_f)} \text{ in } H^{1*}_{0,m} \text{ and for a.e. } t \in (0,T) \\ v_0' + Av_0 = -((\bar{u}',\cdot)_H + A\bar{u}) \text{ in } H^{-1} \text{ and for a.e. } t \in (0,T) \end{aligned}$$

with $\bar{u}$ any given $\bar{u} \in H^1(I,H^1_{0,m})$ such that $\mathrm{tr}\bar{u} = f$ on Σ_f, and with $\bar{u}(0) = 0$. We are working under assumption B.2.1. Thanks to proposition B.3.4, by the regularity ensured by assumption B.2.1 and thanks to proposition B.3.3, we get:

$$\begin{aligned} w \in Q_0(I,H^1_{0,m}), \bar{u} + v_0 \in Q_0(I,H^1_{0,m}), v_0 \in Q_0(I,H^1_0) \\ \int_I (w',q)_H + (\nabla w, \nabla q)_H = \int_I (g, \mathrm{tr}q)_{L^2(\Gamma_f)}, \quad \forall q \in Q^0(I,H^1_{0,m}) \\ \int_I (v_0',p)_H + (\nabla v_0, \nabla p)_H = -\int_I (\bar{u}',p)_H + (\nabla \bar{u}, \nabla p)_H, \quad \forall p \in Q^0(I,H^1_0) \end{aligned}$$

where now the derivatives are in the $H^1(I,H)$ sense.

Conversely, a solution $w \in Q_0(I,H^1_{0,m}), \bar{u} + v_0 \in Q_0(I,H^1_{0,m}), v_0 \in Q_0(I,H^1_0)$ to the above problem satisfies $w \in W_0(I,H^1_{0,m}), \bar{u} + v_0 \in W_0(I,H^1_{0,m}), v_0 \in W_0(I,H^1_0)$, see proposition B.3.3, and the proof of theorem B.2.6. And by proposition B.3.3 at first, and then by proposition B.3.4 we obtain back:

$$\begin{aligned} w \in W_0(I,H^1_{0,m}), \bar{u} + v_0 \in W_0(I,H^1_{0,m}), v_0 \in W_0(I,H^1_0) \\ w' + Aw = (g,\cdot)_{L^2(\Gamma_f)} \text{ in } H^{1*}_{0,m} \text{ and for a.e. } t \in (0,T) \\ v_0' + Av_0 = -((\bar{u}',\cdot)_H + A\bar{u}) \text{ in } H^{-1} \text{ and for a.e. } t \in (0,T) \end{aligned}$$

Therefore:

Proposition B.3.5 (Equivalent formulation)
Under assumption B.2.1, the PDEs of problem 2.1.1 can be equivalently formulated as:

$$\begin{aligned} w \in Q_0(I,H^1_{0,m}), \bar{u} + v_0 \in Q_0(I,H^1_{0,m}), v_0 \in Q_0(I,H^1_0) \\ \int_I (w',q)_H + (\nabla w, \nabla q)_H = \int_I (g, \mathrm{tr}q)_{L^2(\Gamma_f)}, \quad \forall q \in Q^0(I,H^1_{0,m}) \\ \int_I (v_0',p)_H + (\nabla v_0, \nabla p)_H = -\int_I (\bar{u}',p)_H + (\nabla \bar{u}, \nabla p)_H, \quad \forall p \in Q^0(I,H^1_0) \end{aligned}$$

Existence, uniqueness and stability proved already in theorem B.2.6, carry over to this new formulation.

Appendix C. Deformations

C.1. Deforming domains

Throughout, D is a bounded Lipschitz domain. We define as in [56] the following spaces of transformations:

Definition C.1.1 (Spaces of transformations)
We define:

- $\mathcal{V}^k = \{\tau : \mathbb{R}^n \to \mathbb{R}^n, \tau - \mathrm{Id} \in W^{k,\infty}(\mathbb{R}^n, \mathbb{R}^n)\}$, $k \geq 1$
- $\mathcal{T}^k = \{\tau \in \mathcal{V}^k$ with an $\eta \in \mathcal{V}^k, \tau \circ \eta = \eta \circ \tau = \mathrm{Id}\}$.

Proposition C.1.2 (Chain rule for $k = 1$)
Let $f \in W^{1,\infty}(\mathbb{R}^n, \mathbb{R}^n)$ or $f \in \mathcal{V}^1$, together with $\psi \in \mathcal{T}^1$. Then:

- $f \circ \psi$ has essentially bounded weak derivatives, and $D(f \circ \psi) = Df \circ \psi D\psi$.
- $D(\psi^{-1}) = (D\psi)^{-1} \circ \psi^{-1}$
- $|\det(D\psi)|$ is an essentially bounded measurable function with $|\det(D\psi)| \geq \delta > 0$ a.e..

Proof.
See [56], lemme and corollaire 2.1 at page II-6, and (4.16), pag. IV-8. □

We go on to define the space of admissible transformations.

Definition C.1.3 (Admissible transformations)
We define $\Theta := \{\theta \in W^{1,\infty}(\mathbb{R}^n, \mathbb{R}^n)$ with $\theta = 0$ on $\mathbb{R}^n \setminus D\}$, a Banach subspace of $W^{1,\infty}(\mathbb{R}^n, \mathbb{R}^n)$.
We also define $\mathcal{T} := \{\tau \in \mathcal{T}^1, \tau^{\pm 1}|_{\mathbb{R}^n \setminus D} = \mathrm{Id}\}$.

Proposition C.1.4 (Some group properties of $\mathcal{T}$)
Let $\eta, \tau \in \mathcal{T}, \delta\theta \in \Theta$. Then:

- $\eta \circ \tau \in \mathcal{T}$
- $\delta\theta \circ \tau \in \Theta$
- Id is the neutral element
- $\tau^{-1} \in \mathcal{T}$

Proposition C.1.5 (Some boundedness and continuity results)
Let $\delta\theta \in W^{1,\infty}(\mathbb{R}^n; \mathbb{R}^n)$, $\tau \in \mathcal{T}$. Then:

- $\|\delta\theta \circ \tau\|_{W^{1,\infty}(\mathbb{R}^n;\mathbb{R}^n)} \leq C \|\delta\theta\|_{W^{1,\infty}(\mathbb{R}^n;\mathbb{R}^n)} (1 + \|\tau - \mathrm{Id}\|_{W^{1,\infty}(\mathbb{R}^n;\mathbb{R}^n)})$
- the map $\eta \mapsto \eta \circ \tau$ is affine and continuous $\mathcal{V}^1 \to \mathcal{V}^1$
- the maps $\tau \mapsto \|\det(D\tau)\|_{L^\infty(\mathbb{R}^n;\mathbb{R})}, \tau \mapsto \left\|\det((D\tau)^{-1})\right\|_{L^\infty(\mathbb{R}^n;\mathbb{R})}, \tau \mapsto \|D\tau\|_{L^\infty(\mathbb{R}^n;\mathbb{R}^{n\times n})}, \tau \mapsto \left\|(D\tau)^{-1}\right\|_{L^\infty(\mathbb{R}^n;\mathbb{R}^{n\times n})}$ are continuous at every $\tau \in \mathcal{T}$, with respect to the $\mathcal{V}^1$ topology (given by the affine structure $\tau = \mathrm{Id} + \theta$)

Proof.
These are exacly lemme 2.2 at page II .8 and (4.12) of remarque 4.1, page IV.6 of [56]. □

Proposition C.1.6 (Small perturbations of $\mathcal{T}$)
Let $\delta\theta \in \Theta$ with small enough $\|\delta\theta\|_{W^{1,\infty}(\mathbb{R}^n;\mathbb{R}^n)}$, and $\tau \in \mathcal{T}$. Then, $\tau + \delta\theta \in \mathcal{T}$.

Proof.

We solve the equation $\tau + \delta\theta = \eta \circ \tau$, i.e., we define $\eta := \mathrm{Id} + \delta\theta \circ \tau^{-1}$. Because $\tau^{-1} \in \mathcal{T}$ and $\delta\theta \in \Theta$ we observe that $\delta\theta \circ \tau^{-1} \in \Theta$, thanks to proposition C.1.4.

But $\delta\theta \circ \tau^{-1}$ is small by proposition C.1.5, so that we can apply lemme 2.4 of [56] to conclude that $\eta \in \mathcal{T}^1$. We easily see $\eta \in \mathcal{T}$ and $\tau + \delta\theta = \eta \circ \tau \in \mathcal{T}$ by proposition C.1.2. □

Theorem C.1.7 (Small perturbations of identity, Lipschitz property)
Let $U \subset\subset D$ be bounded Lipschitz (in the sense of [35], definition 1.2.1.1.). There exists $0 < C(U) < 1$ such that, for $\tau \in W^{1,\infty}(\mathbb{R}^n;\mathbb{R}^n)$ and $\|\tau - \mathrm{Id}\|_{W^{1,\infty}(\mathbb{R}^n;\mathbb{R}^n)} \leq C(U)$, then $T(U)$ is also bounded Lipschitz, where T is the unique Lipschitz continuous representative of τ (see proposition A.1.2).

Proof.

It is done in [3], lemma 3, page 629. □

C.2. Deforming function spaces

Theorem C.2.1 (Change of variables)
Let U be open, $\tau \in \mathcal{T}^1$, and let $p \in [1, \infty]$. Then:

1. $f \in L^p(T(U)) \iff f \circ \tau \in L^p(U)$ and there holds, for $f \in L^p(\tau(U))$:
$$\|f\|_{L^p(\tau(U))} \leq \left(\|\det D\tau\|_{L^\infty(\mathbb{R}^n)}\right)^{1/p} \|f \circ \tau\|_{L^p(U)}$$
2. $f \in W^{1,p}(\tau(U)) \iff f \circ \tau \in W^{1,p}(U)$ and there holds, for $f \in W^{1,p}(\tau(U))$:
$$Df \circ \tau = (Df)^{-t} D(f \circ \tau)$$
$$\|Df\|_{L^p(\tau(U);\mathbb{R}^n)} \leq \left(\|\det D\tau\|_{L^\infty(\mathbb{R}^n)}\right)^{1/p} \left\|(D\tau)^{-1}\right\|_{L^\infty(\mathbb{R}^n;\mathbb{R}^{n\times n})} \|D(f \circ \tau)\|_{L^p(U;\mathbb{R}^n)}$$
3. if $p \in (1, \infty)$, $f \in W_0^{1,p}(\tau(U)) \iff f \circ \tau \in W_0^{1,p}(U)$
4. therefore, composition by τ is a linear isomorphism between $W^{k,p}(\tau(U)) \to W^{k,p}(U)$ for $k = 0, 1$, and between $W_0^{1,p}(\tau(U)) \to W_0^{1,p}(U)$, $p \in (1, \infty)$
5. for D a bounded Lipschitz domain, we get, for $f \in H^1(D)$, that $\mathrm{tr}_D f = \mathrm{tr}_D(f \circ \tau)$
6. if moreover, $\Omega, \tau(\Omega) \subset\subset D$ are also bounded Lipschitz domains, letting $U := D \setminus \overline{\Omega}$, another bounded Lipschitz domain, for $f \in H^1(\tau(U))$ and $\mathrm{tr}_{\tau(U)} f = 0$ on $\partial\tau(\Omega)$, then $\mathrm{tr}_U f \circ \tau = 0$ on $\partial\Omega$ and $\mathrm{tr}_{\tau(U)} f = \mathrm{tr}_U f \circ \tau$ on ∂D
7. so, $\circ\tau$ is a linear isomorphism of $H^1_{0,m}(U)$ and $H^1_{0,m}(\tau(U))$ ($H^1_{0,m}$ is defined in appendix B.2 as $\{u \in H^1, u(\Gamma_m) = 0\}$)

Proof.

We need to prove only the points 5 and 6, for the other ones are proved in [56], pages IV.4, IV.5, IV.6, 4 follows from $1, 2, 3$ and proposition A.2.1 and 7 follows analogously from $5, 6$.

5: static strace

Let $f_n \in C^\infty(\overline{D}) \cap H^1(D)$ converging in $H^1(D)$ to f (see theorem 3.18 of [1], page 54). By point 4, we have $f_n \circ \tau \to f \circ \tau$ in $H^1(D)$. Therefore, also by $\tau|_{D^c} = \mathrm{Id}$, we have:

$$\mathrm{tr}_D f \leftarrow_{L^2(\partial D)} \mathrm{tr}(f_n) = f_n|_{\partial D} = (f_n \circ \tau)|_{\partial D} = \mathrm{tr}(f_n \circ \tau) \rightarrow_{L^2(\partial D)} \mathrm{tr}_D(f \circ \tau)$$

6: moving trace

First of all, as τ is a homeomorphism of $\mathbb{R}^n$, we have that $\tau(U) = D \setminus \overline{\tau(\Omega)}$, $\tau(\partial U) = \partial D \sqcup \partial\Omega$, $\tau(\partial\Omega) = \partial\tau(\Omega)$. Now, an application of theorem A.1.1 yields that the zero extension to $\tau(\Omega)$ of f, call it $\bar{f}$, is $H^1(D)$, with $\partial_i \bar{f} = \partial_i f$ in $\tau(U)$, 0 in $\tau(\Omega)$.

We have moreover $\mathrm{tr}_D \bar{f} = \mathrm{tr}_{\tau(U)} f|_{\partial D}$ (using approximation arguments based on theorem 3.18 of [1], page 54).

Using this: $\mathrm{tr}_{\tau(U)} f|_{\partial D} = \mathrm{tr}_D \bar{f} = \{\text{ point 5 }\} = \mathrm{tr}_D(\bar{f} \circ \tau) = \mathrm{tr}_D(\overline{f \circ \tau}) = \mathrm{tr}_U(f \circ \tau)|_{\partial D}$, where we used that $\bar{f} \circ \tau$ is zero in $\tau^{-1}(\tau(\Omega)) = \Omega$ (because τ maps Lebesgue null sets into null sets, being bi-Lipschitz), so it is the zero extension $\overline{f \circ \tau}$ of $f \circ \tau$, and applied the same reasoning as above to conclude $\mathrm{tr}_D(\overline{f \circ \tau}) = \mathrm{tr}_U(f \circ \tau)|_{\partial D}$. Both $\bar{f} \circ \tau$ and $f \circ \tau$ are H^1 functions by point 2.

Now that we know that $\mathrm{tr}_{\tau(U)} f|_{\partial D} = \mathrm{tr}_U(f \circ \tau)|_{\partial D}$, it is left to show $\mathrm{tr}_U f \circ \tau = 0$ on $\partial\Omega$, via some additional steps.

Multiplication by a $W^{1,\infty}$ function

For $\psi \in W^{1,\infty}(\mathbb{R}^n; \mathbb{R})$ and $f \in H^1(U)$, $f\psi$ has the same trace as f as long as $\psi = 1$ in a neighbourhood of ∂U. This follows again by an approximation argument on f by smooth functions and by proposition A.1.2.

A function of 0 trace

Let η be a smooth cut-off function which is 1 close to ∂D and 0 close to $\partial\tau(\Omega)$, $\beta = 0$ close to ∂D and 1 close to $\partial\tau(\Omega)$. They can be found by e.g. building a suitable partition of unity of the compact sets $\partial\Omega$ and ∂D. $f\beta$ has zero trace, as can be verified by approximating f by suitable smooth functions f_n: $\operatorname{tr}_{\tau(U)} f\beta \leftarrow_{L^2(\partial\tau(U))} \operatorname{tr}_{\tau(U)} f_n\beta$, where the latter quantity is $\operatorname{tr}_{\tau(U)} f_n$ on $\partial\tau(\Omega)$ and 0 on ∂D.

Domain transformation

We have that $\beta\circ\tau+\eta\circ\tau$ is $W^{1,\infty}$ and 1 near ∂U. So, $\operatorname{tr}_U f\circ\tau = \operatorname{tr}_U((f\circ\tau)(\beta\circ\tau+\eta\circ\tau)) = \operatorname{tr}_U((f\circ\tau)(\beta\circ\tau)) + \operatorname{tr}_U((f\circ\tau)(\eta\circ\tau))$.

Approximate $f\circ\tau$ by g_n smooth as seen above. Then, $\operatorname{tr}_U(g_n(\eta\circ\tau))$ is 0 on $\partial\Omega$, and selecting an almost everywhere convergent subsequence, we conclude $\operatorname{tr}_U((f\circ\tau)(\eta\circ\tau)) = 0$ on $\partial\Omega$.

Finally, $\operatorname{tr}_U f\circ\tau|_{\partial\Omega} = tr_U(f\circ\tau)(\beta\circ\tau)|_{\partial\Omega} = tr_U((f\beta)\circ\tau)|_{\partial\Omega} = 0$, where for the last step we used point 3 (zero trace functions in $H^1(\tau(U))$, since $\tau(U)$ is assumed to be bounded Lipschitz, are exactly the functions $H^1_0(\tau(U))$, by theorem 18.7 at page 595 of [43]). □

Proposition C.2.2 (Isomorphism between Q spaces)
Let $\tau\in\mathcal{T}$ be small enough for point 7 for C.2.1 to hold. Then:

$$\circ\tau : Q(I,V_\tau)\to Q(I,V), Q_0(I,V_\tau)\to Q_0(I,V)$$

are linear isomorphisms. In particular, $(u\circ\tau)' = u'\circ\tau$.

Proof.

From theorem C.2.1, with the help of proposition A.2.1 and thanks to the properties of Q listed in proposition B.3.3, we obtain that $\circ\tau : Q(I,V_\tau)\to Q(I,V)$ is linear bounded, and by the inverse function theorem, an isomorphism. Reasoning by continuous representatives (in time), we get $(\circ\tau)(Q_0(I,V_\tau))\subseteq Q_0(I,V)$, and the same goes for $\circ\tau^{-1}$. □

C.3. Deforming PDEs

We consider again the two parabolic equations of interest from proposition B.3.5. We stress that we need the following.

Assumption C.3.1
We have $\tau\in\mathcal{T}$, $U\subset\subset D$ bounded Lipschitz domains and we also assume that $\tau(U)$ is bounded Lipschitz.

Suppose the problem is formulated on $\tau(U)$. To ease the notation, call $H^1_{0,m}(\tau(U)) = \mathtt{W}_\tau$, $H^1_{0,m}(U) = \mathtt{W}$, $H^1_0(U) = \mathtt{V}$ and analogously for the other spaces. We continue from proposition B.3.5. Applying a change of variables (e.g. (4.8) at page IV-4 of [56]), and noticing that:

- $\operatorname{tr}_{\tau(U)} q = \operatorname{tr}_U(q\circ\tau)$ on Σ_f by theorem C.2.1
- $w^\tau_t\circ\tau = (w^\tau\circ\tau)_t$ by proposition C.2.2 and analogously for v_0
- by proposition C.2.2, $\circ\tau$ is a bijection between $Q^0(I,\mathtt{W}_\tau)$ and $Q^0(I,\mathtt{W})$ and analogously for $\mathtt{V}$ (and also for the zero initial values in place of zero final values)
- $\bar u\in H^1(I,\mathtt{W}_\tau)$, and by proposition A.2.1, $\bar u\circ\tau\in H^1(I,\mathtt{W})$ with $(\bar u\circ\tau)' = \bar u'\circ\tau$

we get, equivalently:

$$\begin{aligned} &w^\tau\in Q_0(I,\mathtt{W}_\tau), v^\tau_0\in Q_0(I,\mathtt{V}_\tau)\\ &\int_I ((w^\tau\circ\tau)_t, q|\det(D\tau)|)_H + (A_\tau\nabla(w^\tau\circ\tau),\nabla q)_H = \int_I (g,\operatorname{tr}_U q)_{L^2(\Gamma_f)}, \quad \forall q\in Q^0(I,\mathtt{W})\\ &\int_I ((v^\tau_0\circ\tau)_t, p|\det(D\tau)|)_H + (A_\tau\nabla(v^\tau_0\circ\tau),\nabla p)_H = -\int_I ((\bar u\circ\tau)', p|\det(D\tau)|)_H + (A_\tau\nabla(\bar u\circ\tau),\nabla p)_H, \quad \forall p\in Q^0(I,\mathtt{V})\end{aligned}$$

and by proposition C.2.2, we also get $w^\tau\circ\tau\in Q_0(I,\mathtt{W}), v^\tau_0\circ\tau\in Q_0(I,\mathtt{V})$. Here $A_\tau = |\det(D\tau)|D\tau^{-1}(D\tau)^{-t}$.

On the other hand, consider:

$$\begin{aligned} &w\in Q_0(I,\mathtt{W}), v_0\in Q_0(I,\mathtt{V})\\ &\int_I (w_t, q|\det(D\tau)|)_H + (A_\tau\nabla w,\nabla q)_H = \int_I (g,\operatorname{tr}_U q)_{L^2(\Gamma_f)}, \quad \forall q\in Q^0(I,\mathtt{W})\\ &\int_I (v_{0t}, p|\det(D\tau)|)_H + (A_\tau\nabla v_0,\nabla p)_H = -\int_I ((\bar u\circ\tau)', p|\det(D\tau)|)_H + (A_\tau\nabla(\bar u\circ\tau),\nabla p)_H, \quad \forall p\in Q^0(I,\mathtt{V})\end{aligned}$$

Then, we note the following:

- by proposition C.2.2, $w\circ\tau^{-1}\in Q_0(I,\mathtt{W}_\tau), v_0\circ\tau^{-1}\in Q_0(I,\mathtt{V}_\tau)$, and as seen above, $((w\circ\tau^{-1})\circ\tau)_t = (w\circ\tau^{-1})_t\circ\tau$ and the same goes for $v_0\circ\tau^{-1}$

Therefore we obtain, equivalently:

$$
\begin{aligned}
w \circ \tau^{-1} \in Q_0(I, \mathtt{W}_\tau), v_0 \circ \tau^{-1} &\in Q_0(I, \mathtt{V}_\tau) \\
\int_I ((w \circ \tau^{-1})_t, q^\tau)_{H_\tau} + (\nabla(w \circ \tau^{-1}), \nabla q^\tau)_{H_\tau} = \int_I (g, \operatorname{tr}_{\tau(U)} q^\tau)_{L^2(\Gamma_f)}, &\quad \forall q^\tau \in Q^0(I, \mathtt{W}_\tau) \\
\int_I ((v_0 \circ \tau^{-1})_t, p^\tau)_{H_\tau} + (\nabla(v_0 \circ \tau^{-1}), \nabla p^\tau)_{H_\tau} = -\int_I (\bar{u}', p^\tau)_{H_\tau} + (\nabla \bar{u}, \nabla p^\tau)_{H_\tau}, &\quad \forall p^\tau \in Q^0(I, \mathtt{V}_\tau)
\end{aligned}
$$

and $w \circ \tau^{-1} \in Q_0(I, \mathtt{W}_\tau), v_0 \circ \tau^{-1} \in Q_0(I, \mathtt{V}_\tau)$.
These findings can be summarized as follows.

Theorem C.3.2 (Equivalent formulations with transported domain)
Let assumption B.2.1, assumption C.3.1 hold.
Consider the following problems, where $\tau \in \mathcal{T}$.

Problem C.3.3 (Joint parabolic problem, moving domain)

$$
\begin{aligned}
w^\tau \in Q_0(I, \mathtt{W}_\tau), v_0^\tau &\in Q_0(I, \mathtt{V}_\tau) \\
\int_I (w_t^\tau, q^\tau)_{H_\tau} + (\nabla w^\tau, \nabla q^\tau)_{H_\tau} = \int_I (g, \operatorname{tr}_{\tau(U)} q^\tau)_{L^2(\Gamma_f)}, &\quad \forall q^\tau \in Q^0(I, \mathtt{W}_\tau) \\
\int_I (v_{0t}^\tau, p^\tau)_{H_\tau} + (\nabla v_0^\tau, \nabla p^\tau)_{H_\tau} = -\int_I (\bar{u}', p^\tau)_{H_\tau} + (\nabla \bar{u}, \nabla p^\tau)_{H_\tau}, &\quad \forall p^\tau \in Q^0(I, \mathtt{V}_\tau)
\end{aligned}
$$

Problem C.3.4 (Joint parabolic problem, reference domain)

$$
\begin{aligned}
w \in Q_0(I, \mathtt{W}), v_0 &\in Q_0(I, \mathtt{V}) \\
\int_I (w_t, q |\det(D\tau)|)_H + (A_\tau \nabla w, \nabla q)_H = \int_I (g, \operatorname{tr}_U q)_{L^2(\Gamma_f)}, &\quad \forall q \in Q^0(I, \mathtt{W}) \\
\int_I (v_{0t}, p |\det(D\tau)|)_H + (A_\tau \nabla v_0, \nabla p)_H = -\int_I ((\bar{u} \circ \tau)', p |\det(D\tau)|)_H + (A_\tau \nabla(\bar{u} \circ \tau), \nabla p)_H, &\quad \forall p \in Q^0(I, \mathtt{V})
\end{aligned}
$$

We have the following:

- consider $w^\tau \in Q_0(I, \mathtt{W}_\tau), v_0^\tau \in Q_0(I, \mathtt{V}_\tau)$. They solve problem C.3.3 $\iff$ $w^\tau \circ \tau, v_0^\tau \circ \tau$ solve problem C.3.4
- consider $w \in Q_0(I, \mathtt{W}), v_0^\tau \in Q_0(I, \mathtt{V})$. They solve problem C.3.4 $\iff$ $w \circ \tau^{-1}, v_0 \circ \tau^{-1}$ solve problem C.3.3

Here, $A_\tau := (D\tau)^{-1}(D\tau)^{-t} |\det(D\tau)|$.

Appendix D. FEM and smooth domains

Handling smooth geometries in finite element analysis is not a trivial task. On one hand, finite element discretizations are naturally set up on polygonal/polyhedral domains, whereas the smoothness of the analytical solutions required to obtain optimal order error estimates, can only be achieved with a smooth boundary (or more generally, when U is convex, which it isn't, in our case). An apparent contradiction therefore arises, and many authors simply conduct theoretical analysis on the polyhedral domains, but assuming enough smoothness of the solutions (this is the contradiction of "polygonal smooth" domains, mentioned in [60]): an example of this in a setting close to ours, is contained in [39].

There are few different ways to go about this dilemma, many of them are only a partially satisfactory answer to the problem. For instance, finite elements formulated directly on arbitrarily curved simplices have been studied in [66]. This requires complete knowledge of the (curved) boundary of the computational domain. Optimal order estimates are also observed in [10]. Their techniques work with smooth and rough data, but also require complete knowledge of a parametrization of the boundary, and are not easily extendable to a dimension higher than 2. Interestingly, shape optimization techniques can be applied to analyze the discrepancy between discrete and smooth geometry in the solution process, see [60]: the techniques therein presented only yield optimal order estimates in the H^1 norm.

The presence of Dirichlet boundary conditions further complicates the analysis. The Dirichlet values might be imposed strongly, i.e. enforced at the boundary nodes, or weakly (see e.g. [18] for the elliptic case, or, more generally, the discussion in [19], and that in [8] for the parabolic case). The latter solution is viable only if one can extend the boundary data to the whole volume, or to a strip around it.

We chose an approach that was as little intrusive as possible with regards to the exact geometry and data: it only requires the knowledge of the smooth domain and boundary data at some points of the smooth boundary. It is straightforward to implement, both from a meshing point of view and from a finite element code point of view. Standard meshing tools can be used without modification, GMSH being our choice ([32]), and powerful finite element libraries (e.g. Fenics ([47])) can be directly used to simulate the partial differential equations.

In short, the discrete solution is computed on a polygonal/polyhedral approximation U_h of the smooth domain U, where the nodes of ∂U_h lie on ∂U, and the Dirichlet conditions are imposed strongly at every time step. The boundary data is substituted by its Langrange interpolant, thus requiring its knowledge only on the boundary nodes of ∂U_h.

We have to ask "unnatural" smoothness to the boundary data, because we evaluate it pointwise ("unnatural" is compared to he hypothesis necessary to obtain H^2 regularity in the elliptic case, i.e. $H^{1/2}$ smoothness for Neumann data and $H^{3/2}$ smoothness for Dirichlet data: we will require both to be H^2 on the boundary). A surplus of smoothness is however present in the majority of the other works that analyze the change in geometry in detail. Strong imposition of Dirichlet boundary conditions, on the other hand, may not me the best solution for all PDEs, see e.g. [7].

The approach we took is based on the work of [26], [25], [9] and [24]. We remark that all the estimates we are about to obtain will be U dependent, and this dependence will not be tracked, for simplicity.

D.1. Preliminaries

Assumption D.1.1 (Geometric assumptions)
Consider a domain $U \subseteq \mathbb{R}^n$, $n = 2, 3$, with C^2 boundary.
We define a polygonal/polyhedral meshing U_h of U made of triangles/tetrahedra, which has boundary nodes lying on ∂U. The family of meshes for U_h must be regular and quasi-uniform in the sense of [12].
Denoting by $\Gamma_D, \Gamma_N \subseteq \partial U$ subsets of ∂U where Dirichlet and Neumann boundary conditions will be imposed, we call their discretizations $\Gamma_{D,h}, \Gamma_{N,h}$.
We assume $\Gamma_D \neq \emptyset$ for simplicity (but many of the following arguments work with suitable adaptations otherwise), and $\overline{\Gamma_D} \cap \overline{\Gamma_N} = \emptyset$.

Call $S^1_{0,D,h}$ the space of piecewise linear lagrangian FEM S^1_h which are zero on $\Gamma_{D,h}$.

We collect some useful tools to relate U and U_h, and indicate $\lesssim$ instead of $\leq C$, $C > 0$ and independent on h.

Proposition D.1.2 (Deformation into smooth domain)
Assume we have a shape regular and quasi-uniform mesh (see [12] for a definition). There exists, for h small enough, $G_h : \overline{U_h} \to \overline{U}$ satisfying:

- $G_h|_T = \mathrm{Id}$ on interior simplices T (those with at most one node on ∂U)
- $G_h(\partial U_h) = \partial U$, $G_h|_e = p$, where e is an edge/face of ∂U_h and p is the closest point operator to ∂U (so that $G_h|_{\partial U_h}$ coincides with the boundary lift in definition 4.12 of [26])
- G_h is bi-Lipschitz, with $\|\mathrm{Id} - G_h\|_{W^{1,\infty}(U_h)} \leq Ch$, and $\||\det(DG_h)| - 1\|_{L^\infty(U_h)} \lesssim h$ (and $C > 0$ doesn't depend on h)
- given $G_h(K)$, all of its facets are at least C^1 smooth

- $G_h|_T$ is of class $C^1(T)$ for all closed simplices T composing U_h

Proof.

See section 4.1 of [26] for the first two points, which follow from the definition of G_h. See also lemma 8.16 of [25].

The last point is contained in lemma 8.12, [25]. We give more detail for the third and fourth point, which are not addressed in [25], [26].

<u>G_h is a bi-Lipschitz homeomorphism</u>

We first note that $G_h|_K$ agrees with $G_h|_{K'}$ for $K \cap K' \neq \emptyset$. Therefore G_h is continuous on $\overline{U_h}$.

Then, we also note that G_h has $DG_h \in L^\infty(U_h)$ as weak derivative, where the gradient is defined element-wise. To see this, pick $\phi \in C_c^\infty(U_h)$. Then, applying theorem A.1.1:

$$\int_{U_h} G_h \partial_i \phi = \sum_K \int_{\partial K} G_h|_K \phi \nu_{K,i} - \int_{U_h} \partial_i G_h \phi$$

The first integral on the right is zero, because G_h is continuous, the normal on an interior facet only differs in the sign, when referred to the two parent simplices it belongs to, and because $\phi = 0$ on exterior facets.

Thus, $G_h \in W^{1,\infty}(U_h)$, and lemma 8.12 of [25] shows that $\|\mathrm{Id} - G_h\|_{W^{1,\infty}(U_h)} \lesssim h$. Thanks to proposition A.1.2, we obtain that G_h has a bounded Lipschitz representative, i.e., G_h is bounded and Lipschitz on U_h. Then G_h is Lipschitz on all of $\overline{U_h}$, and $\mathrm{Lip}(\mathrm{Id} - G_h) \lesssim \|\mathrm{Id} - G_h\|_{W^{1,\infty}(U_h)}$.

So, G_h is a Lipschitz perturbation of identity, on $\overline{U_h}$. An application of the reverse triangle inequality also shows that $|G_h(x) - G_h(y)| \geq (1 - \mathrm{Lip}(G_h))|x - y|$, which yields that G_h is bijective (for small h), with a Lipschitz inverse.

<u>Smooth facets of curved simplex</u>

From the last point we know that G_h is of class C^1 when restricted to K, a closed simplex. By Whitney's extension theorem on simplices (see [63]) we can conclude that $G_h|_K$ extends to a C^1 function on a neighbourhood of K. This extension is injective on K as we saw before, and by lemma 8.16 of [25] (the determinant of G_h is small), it has invertible jacobian on K. An application of a global version of the inverse function theorem (see e.g. [36], chapter 1) yields that G_h extends to a C^1 diffeomorphism around K, so that the smoothness of ∂K follows. □

Given G_h, we can define pullbacks and pushforwards of functions defined on U or U_h.

Proposition D.1.3 (Lift)
We define, for $u : U \to \mathbb{R}$, $u^{-l} := u \circ G_h : U_h \to \mathbb{R}$, and analogously for $u_h : U_h \to \mathbb{R}$ we define $u_h^l := u_h \circ G_h^{-1}$. We stress again that we need the mesh to be quasi-uniform (see proposition 4.7 of [26]).
There holds:

- $v \in H^m(Q)$ if and only if $v^{-l} \in H^m(G_h^{-1}(Q))$, for $m = 0, 1$, and $Q \subseteq U$ open
- for $v_h \in S^1_{0,D,h}$, we have $v_h^l \in H^1(U)$, with zero trace on Γ_D
- for $v_h \in S^1_h$, one has the following norm equivalences, which don't depend on h:
  1. $\|v_h\|_{L^2(\partial U_h)} \sim \|v_h^l\|_{L^2(\partial U)}$
  2. $\|v_h\|_{L^2(U_h)} \sim \|v_h^l\|_{L^2(U)}$
  3. $\|\nabla v_h\|_{L^2(U_h)} \sim \|\nabla v_h^l\|_{L^2(U)}$
- consequently, the lifting operator $S^1_{0,D,h} \subseteq L^2(U_h) \to L^2(U)$ or $S^1_{0,D,h} \subseteq H^1_{0,D,h} \to H^1_{0,D}$ is linear bounded

Proof.

The first point follows by the fact that G_h is bi-Lipschitz, see proposition D.1.2, and theorem 11.53 of [43].

The second point follows by applying the arguments about conformity outlined in section 5 of [9]. Following example 2 therein, we discover that we can apply proposition and corollary 5.1. Alternatively, we can use the Lipschitz continuity of G_h and arrive and arrive at the same conclusion.

The last point can be found in [26], see e.g proposition 4.9 and 4.13. □

Proposition D.1.4 (Interpolation on curved domains)
Let $u \in H^2(U)$, let $g \in H^2(\partial U)$ and define $\Pi_c u = (\Pi_h u)^l$, where Π_h is the usual pointwise Lagrange interpolator on S^1_h. We can also define $\Pi_c g$ for $g \in H^2(\partial U)$ in the same fashion.
It follows that:

- $\|u - \Pi_c u\|_{L^2(U)} + h \|u - \Pi_c u\|_{H^1(U)} \lesssim h^2 \|u\|_{H^2(U)}$
- $\|g - \Pi_c g\|_{L^2(\partial U)} + h \|g - \Pi_c g\|_{H^1(\partial U)} \lesssim h^2 \|g\|_{H^2(\partial U)}$

Both of these interpolators are stable, uniformly with respect to h, in both the L^2 and H^1 norms.

Proof.
See proposition 5.4 of [26]. $\square$

Proposition D.1.5 (Approximation of linear and bilinear forms)
Let $v_h, w_h \in S_h^1$, $v, w \in H^2(U)$, $\delta\theta_h \in (S_h^1)^n$ (n is the dimension of U), $\delta\theta \in W^{1,\infty}(U;\mathbb{R}^n)$, $\delta\theta_h \in W^{1,\infty}(U_h;\mathbb{R}^n)$. Then:

1. $\left|\int_U v_h^l w_h^l - \int_{U_h} v_h w_h\right| \lesssim h^{k+1} \|v_h\|_{H^k(U_h)} \|w_h\|_{H^k(U_h)}$, $k = 0, 1$
2. $\left|\int_{\partial U} v_h^l w_h^l - \int_{\partial U_h} v_h w_h\right| \lesssim h^2 \|v_h\|_{L^2(\partial U_h)} \|w_h\|_{L^2(\partial U_h)}$
3. $\left|\int_U \nabla v_h^l \nabla w_h^l - \int_{U_h} \nabla v_h \nabla w_h\right| \lesssim h \|v_h\|_{H^1(U_h)} \|w_h\|_{H^1(U_h)}$
4. $\left|\int_U \nabla v \nabla w - \int_{U_h} \nabla v^{-l} \nabla w^{-l}\right| \lesssim h^2 \|v\|_{H^2(U)} \|w\|_{H^2(U)}$
5. $\left|\int_U v_h^l w_h^l \mathrm{div}(\delta\theta_h^l) - \int_{U_h} v_h w_h \mathrm{div}(\delta\theta_h)\right| \lesssim h^{k+1} \|v_h\|_{H^k(U_h)} \|w_h\|_{H^k(U_h)} \|\mathrm{div}(\delta\theta_h)\|_{L^\infty(U_h)}$, $k = 0, 1$
6. $\left|\int_U (A'(\delta\theta_h^l)\nabla v_h^l)\nabla w_h^l - \int_{U_h} (A'(\delta\theta_h)\nabla v_h)\nabla w_h\right| \lesssim h \|v_h\|_{H^1(U_h)} \|w_h\|_{H^1(U_h)} \|D\delta\theta_h\|_{L^\infty(U_h)}$
7. $\left|\int_U (A'(\delta\theta)\nabla v)\nabla w - \int_{U_h} (A'(\delta\theta^{-l})\nabla v^{-l})\nabla w^{-l}\right| \lesssim h^2 \|v\|_{H^2(U)} \|w\|_{H^2(U)} \|D\delta\theta\|_{L^\infty(U)}$

Proof.
See [24]. Only the last three points are not already present in the literature, but they follow with very similar arguments as the others. See for instance, section 6 of [26]: one needs to apply a change of variables to the integrals on U_h, and then use the approximation properties in proposition D.1.2. To obtain $O(h^2)$ estimates, the "narrow band" inequality lemma 6.3, [26], as suggested in lemma 6.4 of [26], has to be used.

$\square$

Proposition D.1.6 (Uniform coercivity)
For h small enough, $a_h(v_h, w_h) := \int_{U_h} \nabla v_h \nabla w_h$ is coercive, uniformly with respect to h.

Proof.
For C not depending on h:

$$a_h(v_h, v_h) \geq C \left\|v_h^l\right\|_{H^1(U)}^2 - |a_h(v_h, v_h) - a(v_h^l, v_h^l)| \geq C \|v_h\|_{H^1(U_h)}^2 - Ch \left\|v_h^l\right\|_{H^1(U)}^2 \geq C(1-h) \|v_h\|_{H^1(U_h)}^2$$

We used the $h-$uniform coercivity of a (descending from the Poincaré inequality in which functions vanish only on part of the boundary, Γ_D, see e.g. lemma 1 of [23]), proposition D.1.3 on $\left\|v_h^l\right\|_{H^1(U)}^2$ and proposition D.1.5. $\square$

D.2. Semidiscrete estimates

We partly build upon the previous section, to deal with problems of the following form.

Problem D.2.1 (Inhomogeneous parabolic problem)
With reference to problem B.2.2, we define:

$$\begin{cases} \partial_t u - \Delta u = f & \text{on } U \times I \\ u = g_D & \text{on } \Gamma_D \times I \\ \partial_\nu u = g_N & \text{on } \Gamma_N \times I \\ u(0) = u_0 \end{cases}$$

We ask assumption B.2.1.

We provide a spatially semidiscrete estimate, to start with. To do so we follow a classical argument involving the use of Ritz projections, see [59] in e.g. theorem 1.2. To deal with the polygonal/polyhedral domain approximation we adapt and extend some arguments contained in [25]. Throughout this section, $\lesssim$ means $\leq C$, for C independent of both the discretization parameter h, and time. We start indeed to examine the Ritz projection, by keeping the same notation as in the last section for the lift.

Definition D.2.2 (Inhomogeneous Ritz projection)
Consider $z \in H^2(U)$. We define $R_h z \in S_h^1$ by:

$$a_h(R_h z, v_h) = a(z, v_h^l), v_h \in S_{0,D,h}^1$$
$$R_h z = \Pi_h z \text{ on } \partial U_h$$

We denote $R_c z := (R_h z)^l$.

Here are some useful properties of such projection.

Proposition D.2.3 (Properties of the Ritz projection)
The following facts hold true about R_h, where we assume that h is small enough:

1. R_h is well defined
2. R_h is continuous, uniformly in h, from $H^2(U)$ to S_h^1, i.e., $\|R_h z\|_{H^1(U_h)} \lesssim \|z\|_{H^2(U)}$
3. $\|R_c z - z\|_{H^1(U)} \lesssim h \|z\|_{H^2(U)}$
4. $\|R_c z - z\|_{L^2(U)} \lesssim h^2 \|z\|_{H^2(U)} + \|z - \Pi_c z\|_{L^2(\Gamma_D)}$
5. for $z \in H^1(I, H^2(U))$, $R_c \frac{d}{dt} = \frac{d}{dt} R_c$ and we can therefore use the above properties also for z_t

Proof.
Existence, uniqueness and stability

The splitting $\delta_h := R_h z - \Pi_h z$, the fact that a_h is (h-uniformly) coercive on $S_{0,D,h}^1$ by proposition D.1.6 and the Lax-Milgram lemma yield existence, uniqueness follows as in theorem B.2.6

Now, for the stability: by uniform coercivity and the definition of R_h: $\|R_h z\|_{H^1(U_h)}^2 \lesssim a_h(R_h z, R_h z) = a_h(\delta_h, R_h z) + a_h(\Pi_h z, R_h z)$, so that $\|R_h z\|_{H^1(U_h)} \lesssim \|\delta_h\|_{H^1(U_h)} + \|\Pi_h z\|_{H^1(U_h)}$. We only need now to apply proposition D.1.3, proposition D.1.4, proposition D.1.5.

Error bounds

For the H^1 error bound, we refer to [25], in particular to the proof of lemma 3.8 at page 1720. Note that H^2 stability of R_h is sufficient, instead of the stronger H^1 stability the authors employ.

For the L^2 error bound, we apply a variant of the Aubin-Nitsche trick. Call $e := z - R_c z \in H^1(U)$ (this holds by proposition D.1.3), and define w by:

$$\begin{cases} -\Delta w = e & \text{on } U \\ w = 0 & \text{on } \Gamma_D \\ \partial_\nu w = 0 & \text{on } \Gamma_N \end{cases}$$

Now, by H^2 regularity:

$$\|e\|_{L^2(U)}^2 = a(w, e) - \int_{\partial U} e \partial_\nu w$$

and:

$$\|e\|_{L^2(U)}^2 \leq a(w, e) + C \|e\|_{L^2(\Gamma_D)} \|e\|_{L^2(U)}$$

For the first term we emply the last part of the proof of lemma 3.8 of [25], so that we are able to conclude:

$$\|z - R_c z\|_{L^2(U)} \lesssim h^2 \|z\|_{H^2(U)} + \|z - \Pi_c z\|_{L^2(\Gamma_D)}$$

Commutation with time derivative

Follows from proposition A.2.1, and the fact that R_c is linear and bounded. The latter is true as lifting a finite element function is a linear bounded map, see proposition D.1.3. □

Assumption D.2.4 (Smoothness requirement on continuous solution)
We assume that $u \in H^1(I, H^2(U))$.

Note, for the parabolic problems arising from shape optimization (problem 2.1.1), theorem B.2.6 can ensure such smoothness, this is made precise in section 3.1. We can now derive an error estimate for problem D.2.1, for the following spatially semidiscrete formulation.

Problem D.2.5 (Spatially semidiscrete approximation of problem D.2.1)
We look for $u_h \in H^1(I, S_h^1)$ satisfying:

$$(\partial t u_h, v_h)_{L^2(U_h)} + a_h(u_h, v_h) = (f_h, v_h)_{L^2(U_h)} + (g_{N,h}, v_h)_{L^2(\Gamma_{N,h})}, v_h \in S^1_{0,D,h}, \text{ for a.e. } t \in I$$

$$u_h = g_{D,h} \text{ for a.e. } t, \text{ on } \Gamma_{D,h}$$

$$u_h(0) = u_{0h}$$

We are making the following assumptions:

Assumption D.2.6 (Assumptions for the spatial semidiscretization)

- assumption D.1.1
- $g_N \in L^2(I, H^2(U))$, so that $g_{N,h} := \Pi_h g_N \in L^2(I, S_h^1(\Gamma_{N,h}))$
- $g_D \in H^1(I, H^2(\Gamma_D))$, so that, with reference to proposition A.2.5, we have $G_D := Eg_D \in H^1(I, H^2(U))$ and therefore (see proposition A.2.1), there holds $G_{D,h} := \Pi_h G_D \in H^1(I, S_h^1)$ and $g_{D,h} := G_{D,h}|_{\Gamma_{D,h}} \in H^1(I, S_h^1(\Gamma_{D,h}))$ (note, $g_{D,h} = \Pi_h g_D$)
- $f \in L^2(I, L^2(U))$ and $f_h \in L^2(I, S_h^1)$, with error bound $\|f - f_h^l\|_{L^2(U_h)} \lesssim C_f h^2$, for a.e. t, C_f independent of h and belonging to $L^2(I)$.
- $u_0 \in H^2(U)$, with the compatibility condition $u_0 = g_D(0)$ on Γ_D, and $u_{0h} := \Pi_h u_0$

(note that these assumptions can be relaxed for proving the well-posedness of the scheme, but are needed as they are for error estimates, and that other choices of the discrete data might be possible. In particular, one could choose $f_h = \Pi_h f$, for $f \in L^2(I, H^2(U))$ and obtain the same results).

Proposition D.2.7 (Well posedness of problem D.2.5)
There exists a unique solution to problem D.2.5, and this satisfies the stability estimate, holding for small enough h:

$$\|u_h\|_{C([0,T],L^2(U_h))} + \|u_h\|_{L^2(I,H^1(U_h))} \lesssim \\ \|f_h\|_{L^2(I,(S^1_{0,D,h})^*)} + \|g_N\|_{L^2(I,H^2(\Gamma_N))} + \|g_D\|_{H^1(I,H^{3/2}(\Gamma_D)))} + \|u_0\|_{H^2(U)}$$

We remember that $\lesssim$ stands for $\leq C$, $C \geq 0$ independent of h and t.

Proof.
Existence and uniqueness
A function $\delta_h \in H^1(I, S^1_{0,D,h})$ can be written as $\delta_h = \sum_j d_{hj}(t) v_{hj}$, for the usual finite element basis $\{v_{hj}\}_j$ of $S^1_{0,D,h}$. We employ the splitting technique $\delta_h = u_h - G_{D,h}$. By testing with the equation of problem D.2.5 with the basis functions v_{hj} we obtain the problem:

$$M_h d_h'(t) + A_h d_h(t) = F_h(t), \text{ a.e. } t \tag{D.2.8}$$

$$d_h(0) = d_{h,0} \tag{D.2.9}$$

Here, $M_{h,ij} = (v_{hi}, v_{hj})_{L^2(U_h)}, A_{h,ij} = a(v_{hi}, v_{hj})$ are the so-called mass and stiffness matrices, both invertible, with respect to the nodal basis of $S^1_{0,D,h}$. We also have $F_{h,j}(t) := -(\partial_t G_{D,h}, v_{hj})_{L^2(U_h)} - a_h(G_{D,h}, v_{hj}) + (f_h, v_{hj})_{L^2(U_h)} + (g_{N,h}, v_{hj})_{L^2(\Gamma_{N,h})}$, together with $d_{h,0} := u_{0h} - G_{D,h}$, in the sense of the non-Dirichlet nodal values (we are able to come to this problem thanks to the assumed compatibility between $u_{0h}, g_{D,h}$).

Thanks to the smoothness assumptions on the data, we have that F has $L^2(I)$ entries.

Hence, by basic theory of ordinary differential equations (theorem 3.4 of [52], for instance), we conclude the existence (and uniqueness) of $d \in H^1(I)$ solving the problem above. The function $u_h := \sum_j d_j(t) v_{hj} + G_{D,h}$ is therefore a solution to the original problem.

Uniqueness (and hence, independence on the particular extension $G_{D,h}$) follows by usual stability estimates.

Stability
Following [34], page 20, 21, we can prove stability estimates for δ_h and then, by triangle inequality:

$$\|u_h\|_{C([0,T],L^2(U_h))} + \|u_h\|_{L^2(I,H^1(U_h))} \lesssim \|f_h\|_{L^2(I,(S^1_{0,D,h})^*)} + \|g_{N,h}\|_{L^2(I,L^2(\Gamma_{N,h}))} + \|G_{D,h}\|_{H^1(I,H^1(U_h)))} + \|u_{0h}\|_{L^2(U_h)}$$

Now, thanks to assumption D.2.6:

- $\|g_{N,h}\|_{L^2(I,L^2(\Gamma_{N,h}))} \lesssim \|g_N\|_{L^2(I,H^2(\Gamma_N))}$ (here is suffices to use proposition D.1.4))
- because the Lagrange interpolator is linear bounded $H^2(U) \to S_h^1$ there holds, by proposition D.1.4: $\partial_t G_{D,h} = \Pi_h \partial_t G_D$, so that $\|\partial_t G_{D,h}\|_{H^1(U_h)} = \|\Pi_h \partial_t G_D\|_{H^1(U_h)} \lesssim \|\partial_t G_D\|_{H^2(U))}$, where we used proposition D.1.4 and proposition D.1.3, but

also proposition A.2.1 to move the time derivative operator. Similarly, there holds $\|\partial_t G_{D,h}\|_{H^1(U_h)} \lesssim \|\partial_t g_D\|_{H^{3/2}(\Gamma_D)}$. With analogous reasonings we can conclude that $\|G_{D,h}\|_{H^1(I,H^1(U_h)))} \lesssim \|g_D\|_{H^1(I,H^{3/2}(\Gamma_D))}$

- $\|u_{0h}\|_{L^2(U_h)} \lesssim \|u_0\|_{H^2(U)}$

All in all:

$$\|u_h\|_{C([0,T],L^2(U_h))} + \|u_h\|_{L^2(I,H^1(U_h))} \lesssim \|f_h\|_{L^2(I,(S^1_{0,D,h})^*)} + \|g_N\|_{L^2(I,H^2(\Gamma_N))} + \|g_D\|_{H^1(I,H^{3/2}(\Gamma_D)))} + \|u_0\|_{H^2(U)}$$

□

Theorem D.2.10 (Semidiscrete error bound)
Under assumption D.2.4, assumption D.2.6 and assumption B.2.1, there holds:

$$\left\|u(t) - u_h^l(t)\right\|^2_{L^2(U)} + h^2 \int_0^T \left\|u - u_h^l\right\|^2_{H^1(U)} \lesssim h^4 A^2$$

where $A^2 := \|u\|^2_{H^1(I,H^2(U))} + \|g_D\|^2_{H^1(I,H^2(\Gamma_D))} + \|u_0\|^2_{H^2(U)} + \int_0^T C_f^2 + \|f_h\|^2_{L^2(I,H^1(U_h))} + \|g_N\|^2_{L^2(I,H^2(\Gamma_N))}$.

Proof.

For this proof we adapt the argument from [25], in particular, those of pages 1727, 1728, 1729, which are modifications of standard techniques that can be traced in e.g. [59], theorem 1.2.

Error split

We want to bound $e := u - u_h = u - R_c u + R_c u - u_h^l =: \rho + \theta_h^l$.

An equation for θ_h

Consider then $\theta_h := R_h u - u_h$. It is an element of $H^1(I, S^1_{0,D,h})$ (i.e. it is 0 on the Dirichlet boundary), making it a suitable test function: this is the primary reason to impose boundary conditions on R_h. So, we have, for $v_h \in S^1_{0,D,h}$:

$$\begin{aligned}(\partial_t R_h u, v_h)_{L^2(U_h)} + a_h(R_h u, v_h) = \{ \text{ definition of Ritz projection } \} =\\ (\partial_t R_h u, v_h)_{L^2(U_h)} + a(u, v_h^l) =\\ (\partial_t R_h u, v_h)_{L^2(U_h)} - (\partial_t u, v_h^l)_{L^2(U)} + (f, v_h^l)_{L^2(U)} + (g_N, v_h^l)_{L^2(\Gamma_N)}\end{aligned}$$

Adding the equation for u_h, and then adding and subtracting $(\partial_t R_c u, v_h^l)_{L^2(U)}$:

$$(\partial_t \theta_h, v_h)_{L^2(U_h)} + a_h(\theta_h, v_h) = (\partial_t R_h u, v_h)_{L^2(U_h)} - (\partial_t R_c u, v_h^l)_{L^2(U)} \tag{D.2.11}$$
$$-(\partial_t \rho, v_h^l)_{L^2(U)} \tag{D.2.12}$$
$$+(f, v_h^l)_{L^2(U)} - (f_h, v_h)_{L^2(U_h)} \tag{D.2.13}$$
$$+(g_N, v_h^l)_{L^2(\Gamma_N)} - (g_{N,h}, v_h)_{L^2(\Gamma_{N,h})} \tag{D.2.14}$$

This means that we can estimate the right hand sides of the above equation to quantify the size of θ_h.

Estimating the size of θ_h: right hand sides

By proposition A.2.1 we can write $\partial_t R_h u = R_h \partial_t u, \partial_t R_c u = (R_h \partial_t u)^l$.
Hence, $|(\partial_t R_h u, v_h)_{L^2(U_h)} - (\partial_t R_c u, v_h^l)_{L^2(U)}| \lesssim h^2 \|\partial_t u\|_{H^2(U)} \|v_h\|_{H^1(U_h)}$, where we used proposition D.1.5, and proposition D.2.3.
Similarly, we have $\partial_t \rho = \partial_t u - R_c \partial_t u$. Thus $|(\partial_t \rho, v_h^l)_{L^2(U)}| \lesssim h^2 \|\partial_t u\|_{H^2(U)} \|v_h\|_{H^1(U_h)} + \|\partial_t (g_D - g_{D,h})\|_{L^2(\Gamma_D)} \|v_h\|_{H^1(U_h)}$ by proposition D.2.3. By the choice of $g_{D,h}$ and by proposition D.1.4, $|(\partial_t \rho, v_h^l)_{L^2(U)}| \lesssim h^2(\|\partial_t u\|_{H^2(U)} + \|\partial_t g_D\|_{H^2(\Gamma_D)}) \|v_h\|_{H^1(U_h)}$.
Moreover:

$$|(g_N, v_h^l)_{L^2(\Gamma_N)} - (g_{N,h}, v_h)_{L^2(\Gamma_{N,h})}| \leq |(g_N - g_{N,h}^l, v_h^l)_{L^2(\Gamma_N)}| + |(g_{N,h}^l, v_h^l)_{L^2(\Gamma_N)} - (g_{N,h}, v_h)_{L^2(\Gamma_{N,h})}|$$

By proposition D.1.5 and trace theorems there holds:

$$|(g_N, v_h^l)_{L^2(\Gamma_N)} - (g_{N,h}, v_h)_{L^2(\Gamma_{N,h})}| \lesssim \left\|g_N - g_{N,h}^l\right\|_{L^2(\Gamma_N)} \left\|v_h^l\right\|_{H^1(U)} + h^2 \|g_{N,h}\|_{L^2(\Gamma_{N,h})} \|v_h\|_{H^1(U_h)}$$

Using the choice of $g_{N,h}$ and also proposition D.1.4, proposition D.1.3, we obtain:

$$|(g_N, v_h^l)_{L^2(\Gamma_N)} - (g_{N,h}, v_h)_{L^2(\Gamma_{N,h})}| \lesssim h^2 \|g_N\|_{H^2(\Gamma_N)} \|v_h\|_{H^1(U_h)}$$

Analogously:

$$|(f, v_h^l)_{L^2(U)} - (f_h, v_h)_{L^2(U_h)}| \lesssim \left\| f - f_h^l \right\|_{L^2(U)} \|v_h\|_{H^1(U_h)} + h^2 \|f_h\|_{H^1(U_h)} \|v_h\|_{H^1(U_h)} \lesssim (C_f + \|f_h\|_{H^1(U_h)}) h^2 \|v_h\|_{H^1(U_h)}$$

We used throughout assumption D.2.6. Calling $E_h(v_h) := (\partial_t \theta_h, v_h)_{L^2(U_h)} + a_h(\theta_h, v_h)$, we discovered that:

$$|E_h(v_h)| \lesssim h^2 \|v_h\|_{H^1(U_h)} (C_f + \|f_h\|_{H^1(U_h)} + \|g_N\|_{H^2(\Gamma_N)} + \|\partial_t u\|_{H^2(U)} + \|\partial_t g_D\|_{H^2(\Gamma_D)}) \tag{D.2.15}$$

<u>Estimating the size of θ_h: stability estimate</u>

By the equation of θ_h, and by the possibility of testing with $v_h = \theta_h$ itself, we obtain:

$$\frac{1}{2} \frac{d}{dt} \|\theta_h\|_{L^2(U_h)}^2 + \|\theta_h\|_{H^1(U_h)}^2 - \|\theta_h\|_{L^2(U_h)}^2 = E_h(\theta_h)$$

Hence, calling $Q := C_f + \|f_h\|_{H^1(U_h)} + \|g_N\|_{H^2(\Gamma_N)} + \|\partial_t u\|_{H^2(U)} + \|\partial_t g_D\|_{H^2(\Gamma_D)}$, by Young's inequality, some algebraic manipulations and by using Gronwall's inequality (25, page 19 of [34]), for all $t \in [0, T]$ we have:

$$\|\theta_h(t)\|_{L^2(U_h)}^2 + \int_0^T \|\theta_h\|_{H^1(U_h)}^2 \lesssim 8h^4 \int_0^T Q^2 + 2 \|\theta_h(0)\|_{L^2(U_h)}^2 \tag{D.2.16}$$

We can also apply proposition D.1.3 to obtain an estimate in spaces that don't depend on h:

$$\left\|\theta_h^l(t)\right\|_{L^2(U)}^2 + \int_0^T \left\|\theta_h^l\right\|_{H^1(U)}^2 \lesssim h^4 \int_0^T Q^2 + \left\|\theta_h^l(0)\right\|_{L^2(U)}^2$$

<u>Conclusion</u>

We have, for $e = u - u_h^l = \rho + \theta_h^l$, and h small, by combining eq. (D.2.16) and proposition D.2.3:

$$\|e(t)\|_{L^2(U)}^2 + h^2 \int_0^T \|e\|_{H^1(U)}^2 \lesssim h^4 \|u(t)\|_{H^2(U)}^2 + h^4 \|g_D(t)\|_{L^2(\Gamma_D)}^2 + h^2 h^2 \int_0^T \|u\|_{H^2(U)}^2 + h^4 \int_0^T Q^2 + \left\|\theta_h^l(0)\right\|_{L^2(U)}^2$$

A triangle inequality applied to $\left\|\theta_h^l(0)\right\|_{L^2(U)}^2$, an application of proposition D.2.3 and the definition of Q allow us to conclude. □

We can also prove convergence of the derivatives in a rather strong norm.

Corollary D.2.17 (Refined error estimate)
Apart from assumption D.2.4, assumption D.2.6 and assumption B.2.1, further assume that $g_N \in H^1(I, H^{3/2}(\Gamma_N))$. Then, for all $t \in (0, T)$:

$$\int_0^T \left\| \partial_t u - (\partial_t u_h)^l \right\|_{L^2(U)}^2 + \left\| u(t) - u_h^l(t) \right\|_{H^1(U)}^2 \lesssim h^2 B^2$$

where $B := \|u\|_{H^1(I, H^2(U))}^2 + \|g_D\|_{H^1(I, H^2(\Gamma_D))}^2 + \int_0^T C_f^2 + \|f_h\|_{L^2(I, L^2(U_h))}^2 + \|g_N\|_{L^2(H^2(\Gamma_N))}^2 + \|\partial_t g_N\|_{L^2(H^{3/2}(\Gamma_N))}^2 + \|u_0\|_{H^2(U)}^2$.

Proof.
We employ again the error decomposition $e = \rho + \theta_h^l$.

<u>Another estimate for θ_h</u>

Consider again eq. (D.2.11). We intend to test by $\partial_t \theta_h \in L^2(I, S_{0,D,h}^1)$. This is possible also by the reasonings in [38], (1.61), page 42. Integrate from 0 to t to obtain:

$$\begin{aligned} \int_0^t \|\partial_t \theta_h\|_{L^2(U_h)}^2 + \frac{1}{2} (a_h(\theta_h(t), \theta_h(t)) - a_h(\theta_h(0), \theta_h(0))) = \int_0^t (\partial_t R_h u, \partial_t \theta_h)_{L^2(U_h)} - \int_0^t (\partial_t R_c u, \partial_t \theta_h^l)_{L^2(U)} \\ - \int_0^t (\partial_t \rho, \partial_t \theta_h^l)_{L^2(U)} \\ + \int_0^t (f, \partial_t \theta_h^l)_{L^2(U)} - \int_0^t (f_h, \partial_t \theta_h)_{L^2(U_h)} \\ + \int_0^t (g_N, \partial_t \theta_h^l)_{L^2(\Gamma_N)} - \int_0^t (g_{N,h}, \partial_t \theta_h)_{L^2(\Gamma_{N,h})} \end{aligned}$$

By suitable estimations of the left hand side (involving proposition D.1.6), using integration by parts for the terms with $g_N, g_{N,h}$ and proposition D.1.5 on the right hand side, plus the Young inequality, we get:

$$
\begin{aligned}
\int_0^t \|\partial_t\theta_h\|^2_{L^2(U_h)} + \frac{1}{2}\|\theta_h(t)\|^2_{H^1(U_h)} \leq \frac{1}{2}\|\theta_h(t)\|^2_{L^2(U_h)} + \frac{1}{2}\|\theta_h(0)\|^2_{H^1(U_h)} \\
+Ch^2\int_0^t \|\partial_t u\|^2_{H^2(U)} + \frac{1}{6}\int_0^t \|\partial_t\theta_h\|^2_{L^2(U_h)} \\
+Ch^2\int_0^t (\|\partial_t u\|_{H^2(U)} + \|\partial_t g_D\|_{H^2(\Gamma_D)})^2 + \frac{1}{6}\int_0^t \|\partial_t\theta_h\|^2_{L^2(U_h)} \\
+Ch^2\int_0^t C_f^2 + Ch^2\int_0^t \|f_h\|^2_{L^2(U_h)} + \frac{1}{6}\int_0^t \|\partial_t\theta_h\|^2_{L^2(U_h)} \\
+Ch^2\int_0^t \|\partial_t g_N\|^2_{H^2(\Gamma_N)} + \int_0^t \|\theta_h\|^2_{H^1(U_h)} \\
+Ch^2\|g_N(t)\|^2_{H^{3/2}(\Gamma_N)} + \frac{1}{4}\|\theta_h(t)\|^2_{H^1(U_h)} \\
+Ch^2\|g_N(0)\|^2_{H^2(\Gamma_N)} + \frac{1}{2}\|\theta_h(0)\|^2_{H^1(U_h)}
\end{aligned}
$$

where C is independent of h and t. We rearrange, and apply eq. (D.2.16) to the term $\|\theta_h(t)\|^2_{L^2(U_h)} + \int_0^t \|\theta_h\|^2_{H^1(U_h)}$.

Calling $q = \int_0^T \left[\|\partial_t u\|^2_{H^2(U)} + \|\partial_t g_D\|^2_{H^2(\Gamma_D)} + C_f^2 + \|f_h\|^2_{L^2(U_h)} + Q^2 + \|g_N\|^2_{H^2(\Gamma_N)} + \|\partial_t g_N\|^2_{H^{3/2}(\Gamma_N)}\right]$, and upon using proposition D.1.3, proposition D.2.3 and proposition D.1.4:

$$
\int_0^T \left\|\partial_t\theta_h^l\right\|^2_{L^2(U)} + \left\|\theta_h(t)^l\right\|^2_{H^1(U)} \lesssim \|\theta_h(0)\|^2_{H^1(U_h)} + h^4 q \lesssim h^2\|u_0\|^2_{H^2(U)} + h^4 q
$$

<u>Conclusion</u>

There holds:

$$
\begin{aligned}
\|e(t)\|^2_{H^1(U)} + \int_0^T \|\partial_t e\|^2_{L^2(U)} \leq \\
\int_0^T \|\partial_t\rho\|^2_{L^2(U)} + h^2\|\rho(t)\|^2_{H^1(U)} + \int_0^T \left\|\partial_t\theta_h^l\right\|^2_{L^2(U)} + \left\|\theta_h^l(t)\right\|^2_{H^1(U)} \leq \{\text{ above, and proposition D.2.3 }\} \leq \\
h^2\int_0^T (\|\partial_t u\|^2_{H^2(U)} + \|\partial_t g_D\|^2_{H^2(\Gamma_D)}) + h^2\|u(t)\|^2_{H^2(U)} + h^2\|u_0\|^2_{H^2(U)} + h^4 q
\end{aligned}
$$

□

In a weaker dual norm and with slightly less restrictive smoothness assumptions on g_N, we can actually obtain $O(h^2)$ convergence for the error in the derivatives. To do so, it is crucial to establish the H^1 stability of a suitable L^2 projection, following [6] and making use of the interpolation theory of [9]. However, since we can do away with this type of result in section 3.2, we refrain from stating it here, and writing the proof.

D.3. Fully discrete estimates

Here, we derive fully discrete estimates given the semidiscrete results just above.

Assumption D.3.1 (Assumptions for full discretization)

We discuss the implicit Euler method ($\theta = 1$) and the Crank-Nicolson method ($\theta = 1/2$).
We ask assumption D.2.6. We further assume:

- $g_N \in H^{1/\theta+1}(I, H^{3/2}(\Gamma_N))$
- $g_D \in H^{1/\theta+1}(I, H^{3/2}(\Gamma_D))$
- $f_h \in H^{1/\theta}(I, S_h^1)$

We consider f_h^k to be a suitable approximation of $f_h(t^k)$, i.e. $f_h^k \simeq f_h(t^k)$ (suitable in a way that will be further specified later on).

Problem D.3.2 (Numerical scheme)
Under assumption D.3.1, we look for $u_h^k \in S_h^1$, $k = 0, ..., K$, with:

$$\left(\frac{u_h^{k+1}-u_h^k}{\delta t}, v_h\right)_{L^2(U_h)} + a_h(\theta u_h^{k+1} + (1-\theta)u_h^k, v_h) = (\theta f_h^{k+1} + (1-\theta) f_h^k, v_h)_{L^2(U_h)} + (\theta g_{N,h}^{k+1} + (1-\theta) g_{N,h}^k, v_h)_{L^2(\Gamma_{N,h})},$$

$$v_h \in S^1_{0,D,h}, 1 \le k \le K$$

$$u_h^{k+1} = g_{D,h}^{k+1}, \quad 1 \le k \le K, \text{ on } \Gamma_{D,h}$$

$$u_h^0 = u_{0h}$$

This problem is well posed by usual argument: one can for instance see it as a sequence of elliptic problems, for $k = 1, ..., K$, and use standard tools as the theorem of Lax-Milgram.

Proposition D.3.3 (Discrete versus semidiscrete)
We are working under assumption D.3.1. Call $e_h^k := u_h^k - u_h(t^k)$ and $\delta f_h^k := f_h^k - f_h(t^k)$. Then, for $\theta = 1, 1/2$, we have $u_h \in H^{1/\theta+1}(I, S_h^1)$ and, for $1 \le n \le K$:

$$\|e_h^n\|^2_{L^2(U_h)} + \delta t \sum_{k=0}^{K-1} \left\|\theta e_h^{k+1} + (1-\theta) e_h^k\right\|^2_{H^1(U_h)} \lesssim D^2 + (\delta t)^{2/\theta} C^2$$

where (see the proof of proposition D.2.7 for the definition and properties of δ_h):

$$C^2 := \int_I \left\|f_h^{(1/\theta)}\right\|^2_{-1,h} + \int_I \left\|g_N^{(1/\theta)}\right\|^2_{H^{3/2}(\Gamma_N)} + \int_I \left\|g_D^{(1/\theta+1)}\right\|^2_{H^{3/2}(\Gamma_D)} + \left\|\delta_h(0)^{(1/\theta)}\right\|^2_{L^2(U_h)}$$

$$D^2 := \delta t \sum_{k=0}^{K-1} \left\|\theta \delta f_h^{k+1} + (1-\theta) \delta f_h^k\right\|^2_{L^2(U_h)}$$

Proof.
Recall the semidiscrete problem, problem D.2.5, for $u_h \in H^1(I, S_h^1)$. For the L^2, H^1 estimate we refer to [53], page 385 and following, specifically to theorem 11.3.1 and 11.3.2. In particular, calling $e_h^k := u_h^k - u_h(t^k)$, and $\delta f_h^k := f_h^k - f_h(t^k)$:

$$\left(\frac{e_h^{k+1}-e_h^k}{\delta t}, v_h\right)_{L^2(U_h)} + a_h(\theta e_h^{k+1} + (1-\theta) e_h^k, v_h) = (\theta \delta f_h^{k+1} + (1-\theta)\delta f_h^k + Q_h^k, v_h)_{L^2(U_h)} \tag{D.3.4}$$

$$e_h^{k+1} = 0, \text{ on } \Gamma_{D,h} \tag{D.3.5}$$

$$e_h^0 = 0 \tag{D.3.6}$$

where we defined $Q_h^k := \dfrac{u_h(t^{k+1}) - u_h(t^k)}{\delta t} - \theta \partial_t u_h(t^{k+1}) - (1-\theta)\partial_t u_h(t^k)$. The proof now consists in deriving discrete stability estimates for eq. (D.3.4), exactly how it is done in [53]. We only remark a few facts that will be referenced in other proofs.

Estimating Q_h^k

We provide estimates of Q_h^k in a suitable norm. In the case $\theta = 1/2$, from the smoothness assumptions on the data we obtain $u_h \in H^3(I, S_h^1)$ and, exactly as in [53]:

$$\delta t \sum_{k=0}^{n-1} \left\|Q_h^k\right\|^2_{-1,h} \lesssim \delta t^4 \int_I \|u_h'''\|^2_{-1,h}$$

Differentiating problem D.2.5 twice we obtain:

$$\|u_h'''(t)\|_{-1,h} \le \|f_h''\|_{-1,h} + \|g_{N,h}''\|_{L^2(\Gamma_{N,h})} + \|u_h''\|_{H^1(U_h)}$$

By stability estimates, as in proposition D.2.7, through the splitting $u_h = \delta_h + G_{D,h}$ (see assumption D.2.6):

$$\|u_h''\|_{L^2(I,H^1(U_h))} \lesssim \|f_h''\|_{L^2(I,(S^1_{0,D,h})^*)} + \|g_{N,h}''\|_{L^2(I,L^2(\Gamma_{N,h}))} + \|G_{D,h}'''\|_{L^2(I,H^1(U_h)))} + \|\delta_h(0)''\|_{L^2(U_h)} \tag{D.3.7}$$

Under our hypothesis assumption D.3.1, we have that $\|\delta_h''(0)\|^2_{L^2(U_h)} \lesssim 1$. This, and assumption D.2.6, yield a bound, uniform on h, on $\int_I \|u_h'''\|^2_{-1,h}$. This bound is:

$$\int_I \|u_h'''(t)\|^2_{-1,h} \lesssim \int_I \|f_h''\|^2_{-1,h} + \int_I \|g_{N,h}''\|^2_{L^2(\Gamma_{N,h})} + \int_I \|G_{D,h}'''\|^2_{H^1(U_h)} + \|\delta_h(0)''\|^2_{L^2(U_h)}$$

But $\|g''_{N,h}\|_{L^2(\Gamma_{N,h})} = \|\Pi_h g''_N\|_{L^2(\Gamma_{N,h})}$, where Π_h is the nodal interpolator (see assumption D.2.6). By proposition D.1.5, $\|g''_{N,h}\|_{L^2(\Gamma_{N,h})} \lesssim \|\Pi_c g''_N\|_{L^2(\Gamma_N)} \leq (1+h)\, \|g''_N\|_{H^{3/2}(\Gamma_N)}$, where we also used proposition D.1.4.
Moreover $\|G'''_{D,h}\|_{H^1(U_h)} = \|\Pi_h G'''_D\|_{H^1(U_h)} \lesssim \|\Pi_c G'''_D\|_{H^1(U)} \lesssim (1+h)\, \|G''_D\|_{H^2(U)} \lesssim \|g'''_D\|_{H^{3/2}(\Gamma_D)}$. Therefore:

$$\int_I \|u'''_h(t)\|^2_{-1,h} \lesssim \int_I \|f''_h\|^2_{-1,h} + \int_I \|g''_N\|^2_{H^{3/2}(\Gamma_N)} + \int_I \|g'''_D\|^2_{H^{3/2}(\Gamma_D)} + \|\delta_h(0)''\|^2_{L^2(U_h)}$$

The proof for $\theta = 1$ is very similar.
and we can conlude by the above estimates on Q_h^k and the H^1 estimate. □

Proposition D.3.8 (Estimate for difference quotient)
With the hypothesis and notation of proposition D.3.3, there holds:

$$\sqrt{\delta t \sum_{k=0}^{K-1} \left\| \frac{u_h(t^{k+1}) - u_h(t^k)}{\delta t} - \frac{u_h^{k+1} - u_h^k}{\delta t} \right\|^2_{L^2(U_h)}} \lesssim \delta t^{1/\theta} E + \sqrt{\delta t \sum_{k=0}^{K-1} \|\theta \delta f_h^{k+1} + (1-\theta)\delta f_h^k\|^2_{L^2(U_h)}}$$

where $E^2 := \left\|g_D^{(1+1/\theta)}\right\|^2_{L^2(I,H^{3/2}(U))} + \left\|g_N^{(1+1/\theta)}\right\|^2_{L^2(I,H^{3/2}(\Gamma_N))} + \left\|\delta_h^{(1/\theta)}(0)\right\|^2_{H^1(U_h)} + \left\|f_h^{(1/\theta)}\right\|^2_{L^2(I,L^2(U_h))}$.

Proof.
We again perform a separation into semidiscretization in space, and then full discretization, and adopt the notation u to represent either one of the two state variables.
Estimating Q_h^k in the L^2 norm
With reference to the proof of proposition D.3.3, let us bound Q_h^k in the stronger L^2 norm. From the definitions of Q_h^k (also see [53], pages 388, 389), there holds $\delta t \sum_{k=0}^{K-1} \|Q_h^k\|^2_{L^2(U_h)} \leq \delta t^{2/\theta} \left\|u_h^{(1+1/\theta)}\right\|^2_{L^2(I,L^2(U_h))}$, also by an application of the Cauchy-Schwarz inequality. The latter norm can be bounded uniformly on h. This is achieved by the same reasonings as in the proof of proposition B.1.8:

$$\begin{aligned}\left\|u_h^{(1+1/\theta)}\right\|^2_{L^2(I,L^2(U_h))} &\lesssim \left\|G_{D,h}^{(1+1/\theta)}\right\|^2_{L^2(I,H^1(U_h))} + \left\|g_{N,h}^{(1+1/\theta)}\right\|^2_{L^2(I,L^2(\Gamma_{N,h}))} + \left\|\delta_h^{(1/\theta)}(0)\right\|^2_{H^1(U_h)} + \left\|f_h^{(1/\theta)}\right\|^2_{L^2(I,L^2(U_h))} \\ &\lesssim \left\|g_D^{(1+1/\theta)}\right\|^2_{L^2(I,H^{3/2}(U))} + \left\|g_N^{(1+1/\theta)}\right\|^2_{L^2(I,H^{3/2}(\Gamma_N))} + \left\|\delta_h^{(1/\theta)}(0)\right\|^2_{H^1(U_h)} + \left\|f_h^{(1/\theta)}\right\|^2_{L^2(I,L^2(U_h))} =: E^2\end{aligned}$$

We see that we need the stronger compatibility condition that $\delta'_h(0)$ is bounded in H^1.
Semidiscrete bound
Consider eq. (D.3.4), where we remind that $e_h^k = u_h^k - u_h(t^k)$. We can test it by $\dfrac{e_h^{k+1} - e_h^k}{\delta t}$, and employing Young and Cauchy-Schwarz inequalities we obtain:

$$\left\|\frac{e_h^{k+1} - e_h^k}{\delta t}\right\|^2_{L^2(U_h)} + \frac{1}{2\delta t}\left(\left\|\nabla e_h^{k+1}\right\|^2_{L^2(U_h)} - \left\|\nabla e_h^k\right\|^2_{L^2(U_h)}\right) \leq \left(\left\|Q_h^k\right\|_{L^2(U_h)} + \left\|\theta\delta f_h^{k+1} + (1-\theta)\delta f_h^k\right\|_{L^2(U_h)}\right) \left\|\frac{e_h^{k+1} - e_h^k}{\delta t}\right\|_{L^2(U_h)}$$

Passing to summations, because $e_h^0 = 0$ and by the Cauchy-Schwarz inequality:

$$\sqrt{\delta t \sum_{k=0}^{K-1} \left\|\frac{e_h^{k+1} - e_h^k}{\delta t}\right\|^2_{L^2(U_h)}} \lesssim \delta t^{1/\theta} E + \sqrt{\delta t \sum_{k=0}^{K-1} \|\theta\delta f_h^{k+1} + (1-\theta)\delta f_h^k\|^2_{L^2(U_h)}}$$

where we used the first part of the proof. □

Suitably combining the last estimates one can obtain estimates of the error between continuous and fully discrete solutions. We refrain from doing this, since we will not need such estimates to be spelled in detail, in section 3.2.

Bibliography

[1] R.A. Adams. *Sobolev Spaces. Adams.* Pure and applied mathematics. Academic Press, 1975. URL: https://books.google.it/books?id=JxzpSAAACAAJ.

[2] G. Allaire, C. Dapogny, and F. Jouve. "Shape and topology optimization". In: *Geometric partial differential equations, part II.* Ed. by Andrea Bonito and Ricardo H. Nochetto. Vol. 22. Handbook of Numerical Analysis. Jan. 2021. DOI: 10.1016/bs.hna.2020.10.004. URL: https://hal.archives-ouvertes.fr/hal-02496063.

[3] J. F. Almagro Bello et al. "The Differentiability of the Drag with Respect to the Variations of a Lipschitz Domain in a Navier–Stokes Flow". In: *Siam Journal on Control and Optimization* 35 (1997), pp. 626–640.

[4] T. Aubin. *Some Nonlinear Problems in Riemannian Geometry.* Springer Monographs in Mathematics. Springer Berlin Heidelberg, 1998. ISBN: 9783540607526. URL: https://books.google.it/books?id=l2nEoSxpHfoC.

[5] D. Azagra, E. Le Gruyer, and C. Mudarra. "Kirszbraun's Theorem via an Explicit Formula". In: *Canadian Mathematical Bulletin* 64.1 (2021), 142–153. DOI: 10.4153/S0008439520000314.

[6] R. E. Bank and T. Dupont. "An Optimal Order Process for Solving Finite Element Equations". In: *Mathematics of Computation* 36.153 (1981), pp. 35–51. ISSN: 00255718, 10886842. URL: http://www.jstor.org/stable/2007724 (visited on 09/09/2022).

[7] Y. Bazilevs and T.J.R. Hughes. "Weak imposition of Dirichlet boundary conditions in fluid mechanics". In: *Computers and Fluids* 36.1 (2007). Challenges and Advances in Flow Simulation and Modeling, pp. 12–26. ISSN: 0045-7930. DOI: https://doi.org/10.1016/j.compfluid.2005.07.012. URL: https://www.sciencedirect.com/science/article/pii/S0045793005001258.

[8] P. Benner and J. Heiland. "Time-dependent Dirichlet Conditions in Finite Element Discretizations". In: *ScienceOpen Research* (Oct. 2015). DOI: 10.14293/S2199-1006.1.SOR-MATH.AV2JW3.v1.

[9] C. Bernardi. "Optimal Finite-Element Interpolation on Curved Domains". In: *SIAM Journal on Numerical Analysis* 26.5 (1989), pp. 1212–1240. DOI: 10.1137/0726068. eprint: https://doi.org/10.1137/0726068. URL: https://doi.org/10.1137/0726068.

[10] J. H. Bramble and J. T. King. "A Robust Finite Element Method for Nonhomogeneous Dirichlet Problems in Domains with Curved Boundaries". In: *Mathematics of Computation* 63.207 (1994), pp. 1–17. ISSN: 00255718, 10886842. URL: http://www.jstor.org/stable/2153559 (visited on 10/06/2022).

[11] C. Brandenburg et al. "A Continuous Adjoint Approach to Shape Optimization for Navier Stokes Flow". In: *Optimal Control of Coupled Systems of Partial Differential Equations.* Basel: Birkhäuser Basel, 2009, pp. 35–56.

[12] S. Brenner and L.R. Scott. *The Mathematical Theory of Finite Element Methods.* Texts in Applied Mathematics. Springer New York, 2002. ISBN: 9780387954516. URL: https://books.google.it/books?id=YhPJf_4pu8kC.

[13] R. Brügger, H. Harbrecht, and J. Tausch. "On the Numerical Solution of a Time-Dependent Shape Optimization Problem for the Heat Equation". In: *SIAM Journal on Control and Optimization* 59.2 (2021), pp. 931–953. DOI: 10.1137/19M1268628. eprint: https://doi.org/10.1137/19M1268628. URL: https://doi.org/10.1137/19M1268628.

[14] V.I. Burenkov. *Sobolev Spaces on Domains.* Rechtswissenschaftliche Veroffentlichungen. Vieweg+Teubner Verlag, 1998. ISBN: 9783815420683. URL: https://books.google.it/books?id=vr0ie4uxh3YC.

[15] J. Cea. "Conception optimale ou identification de formes, calcul rapide de la dérivée directionnelle de la fonction coût". fr. In: *ESAIM: Mathematical Modelling and Numerical Analysis - Modélisation Mathématique et Analyse Numérique* 20.3 (1986), pp. 371–402. URL: http://www.numdam.org/item/M2AN_1986__20_3_371_0/.

[16] R. Chapko, R. Kress, and J.-R. Yoon. "An inverse boundary value problem for the heat equation: the Neumann condition". In: *Inverse Problems* 15.4 (1999), pp. 1033–1046. DOI: 10.1088/0266-5611/15/4/313. URL: https://doi.org/10.1088/0266-5611/15/4/313.

[17] R. Chapko, R. Kress, and J.-R. Yoon. "On the numerical solution of an inverse boundary value problem for the heat equation". In: *Inverse Problems* 14.4 (1998), pp. 853–867. DOI: 10.1088/0266-5611/14/4/006. URL: https://doi.org/10.1088/0266-5611/14/4/006.

[18] Y. Chiba and N. Saito. *Nitsche's method for a Robin boundary value problem in a smooth domain.* 2019. DOI: 10.48550/ARXIV.1905.01605. URL: https://arxiv.org/abs/1905.01605.

[19] F. Chouly. "A review on some discrete variational techniques for the approximation of essential boundary conditions". In: (Aug. 2022).

[20] Cruz-Uribe D. and Neugebauer C. J. "An Elementary Proof of Error Estimates for the Trapezoidal Rule". In: *Mathematics Magazine* 76.4 (2003), pp. 303–306. URL: http://www.jstor.org/stable/3219088.

[21] K. Deckelnick, P. J. Herbert, and M. Hinze. "A novel W 1,infty approach to shape optimisation with Lipschitz domains". In: *ESAIM: Control, Optimisation and Calculus of Variations* 28 (2022), p. 2. DOI: 10.1051/cocv/2021108. URL: https://doi.org/10.1051%2Fcocv%2F2021108.

[22] J. S. Dokken, S. Mitusch, and S. Funke. "Automatic shape derivatives for transient PDEs in FEniCS and Firedrake". In: (Jan. 2020).

[23] W. Dörfler and M. Rumpf. "An Adaptive Strategy for Elliptic Problems Including a Posteriori Controlled Boundary Approximation". In: *Mathematics of Computation* 67.224 (1998), pp. 1361–1382. ISSN: 00255718, 10886842. URL: http://www.jstor.org/stable/2584853 (visited on 08/23/2022).

[24] D. Edelmann. “Isoparametric finite element analysis of a generalized Robin boundary value problem on curved domains”. en. In: *The SMAI journal of computational mathematics* 7 (2021), pp. 57–73. DOI: 10.5802/smai-jcm.71. URL: https://smai-jcm.centre-mersenne.org/articles/10.5802/smai-jcm.71/.

[25] C. M. Elliott and T. Ranner. “A unified theory for continuous-in-time evolving finite element space approximations to partial differential equations in evolving domains”. In: *IMA Journal of Numerical Analysis* 41.3 (Nov. 2020), pp. 1696–1845. ISSN: 0272-4979. DOI: 10.1093/imanum/draa062. eprint: https://academic.oup.com/imajna/article-pdf/41/3/1696/38983520/draa062.pdf. URL: https://doi.org/10.1093/imanum/draa062.

[26] Charles M. Elliott and Thomas Ranner. “Finite element analysis for a coupled bulk–surface partial differential equation”. In: *IMA Journal of Numerical Analysis* 33.2 (2013), pp. 377–402. DOI: 10.1093/imanum/drs022.

[27] K. Eppler and H. Harbrecht. “A regularized Newton method in electrical impedance tomography using shape Hessian information”. eng. In: *Control and Cybernetics* 34.1 (2005), pp. 203–225. URL: http://eudml.org/doc/209343.

[28] L.C. Evans. *Partial Differential Equations*. Graduate studies in mathematics. American Mathematical Society, 2010. ISBN: 9780821849743. URL: https://books.google.it/books?id=Xnu0o_EJrCQC.

[29] T. Flaig. *Discretization strategies for optimal control problems with parabolic partial differential equations*. Jan. 2013. ISBN: 9783843911023.

[30] T. M. Flett. “Mean value theorems for vector-valued functions”. In: *Tohoku Mathematical Journal, Second Series* 24.2 (1972), pp. 141–151.

[31] S. Funke and P. Farrell. “A framework for automated PDE-constrained optimisation”. In: (Feb. 2013).

[32] C. Geuzaine and J.-F. Remacle. “Gmsh: A 3-D finite element mesh generator with built-in pre- and post-processing facilities”. In: *International Journal for Numerical Methods in Engineering* 79.11 (2009), pp. 1309–1331. DOI: https://doi.org/10.1002/nme.2579. eprint: https://onlinelibrary.wiley.com/doi/pdf/10.1002/nme.2579. URL: https://onlinelibrary.wiley.com/doi/abs/10.1002/nme.2579.

[33] G. Gilardi. *Analisi matematica di base*. Collana di istruzione scientifica. McGraw-Hill Companies, 2011. ISBN: 9788838666599. URL: https://books.google.it/books?id=H-0nuQAACAAJ.

[34] G. Gilardi. “Equazioni paraboliche astratte: impostazione variazionale”.

[35] P. Grisvard. *Elliptic Problems in Nonsmooth Domains*. Classics in Applied Mathematics. Society for Industrial and Applied Mathematics, 2011. ISBN: 9781611972023. URL: https://books.google.it/books?id=lJTtujsZSgkC.

[36] V. Guillemin and A. Pollack. *Differential Topology*. AMS Chelsea Publishing. AMS Chelsea Pub., 2010. ISBN: 9780821851937. URL: https://books.google.it/books?id=FdRhAQAAQBAJ.

[37] H. Harbrecht and J. Tausch. “On the Numerical Solution of a Shape Optimization Problem for the Heat Equation”. In: *SIAM Journal on Scientific Computing* 35.1 (2013), A104–A121. DOI: 10.1137/110855703. eprint: https://doi.org/10.1137/110855703. URL: https://doi.org/10.1137/110855703.

[38] M. Hinze et al. *Optimization with PDE Constraints*. Mathematical Modelling: Theory and Applications. Springer Netherlands, 2008. ISBN: 9781402088391. URL: https://books.google.it/books?id=PFbqxa2uDS8C.

[39] R. Hiptmair, A. Paganini, and S. Sargheini. “Comparison of approximate shape gradients”. In: *BIT Numerical Mathematics* 55.2 (2015), pp. 459–485. ISSN: 1572-9125. DOI: 10.1007/s10543-014-0515-z. URL: https://doi.org/10.1007/s10543-014-0515-z.

[40] L. S. Hou and W. Zhu. “Error Estimates Under Minimal Regularity for Single Step Finite Element Approximations of Parabolic Partial Differential Equations”. In: *International Journal of Numerical Analysis and Modeling* 3.4 (2006), pp. 504–524. ISSN: 2617-8710. DOI: https://doi.org/. URL: http://global-sci.org/intro/article_detail/ijnam/915.html.

[41] A. Kirsch. *An Introduction to the Mathematical Theory of Inverse Problems*. Applied Mathematical Sciences. Springer New York, 2013. ISBN: 9781461428510. URL: https://books.google.it/books?id=IWhSmwEACAAJ.

[42] M. Kreuter. “Sobolev Spaces of Vector-Valued Functions”. MA thesis. Ulm University, 2015.

[43] G. Leoni. *A First Course in Sobolev Spaces*. Graduate studies in mathematics. American Mathematical Society, 2017. ISBN: 9781470429218. URL: https://books.google.it/books?id=qoA8DwAAQBAJ.

[44] F. Lindemann. “Theoretical and Numerical Aspects of Shape Optimization with Navier-Stokes Flows”. PhD thesis. 2012.

[45] J.L. Lions, P. Kenneth, and E. Magenes. *Non-Homogeneous Boundary Value Problems and Applications: Volume II*. Grundlehren der mathematischen Wissenschaften. Springer Berlin Heidelberg, 2012. ISBN: 9783642652172. URL: https://books.google.it/books?id=xD71CAAAQBAJ.

[46] J. Liu and Z. Wang. “Non-commutative discretize-then-optimize algorithms for elliptic PDE-constrained optimal control problems”. In: *Journal of Computational and Applied Mathematics* 362 (2019), pp. 596–613. ISSN: 0377-0427. DOI: https://doi.org/10.1016/j.cam.2018.07.028. URL: https://www.sciencedirect.com/science/article/pii/S0377042718304485.

[47] J. Hake A. Johansson B. Kehlet A. Logg C. Richardson J. Ring M. E. Rognes M. S. Alnaes J. Blechta and G. N. Wells. “The FEniCS Project Version 1.5”. In: *Archive of Numerical Software* 3 (2015). DOI: 10.11588/ans.2015.100.20553.

[48] W. McLean and W.C.H. McLean. *Strongly Elliptic Systems and Boundary Integral Equations*. Cambridge University Press, 2000. ISBN: 9780521663755. URL: https://books.google.it/books?id=RILqjEeMfK0C.

[49] D. Meidner and B. Vexler. “A Priori Error Estimates for Space-Time Finite Element Discretization of Parabolic Optimal Control Problems Part I: Problems Without Control Constraints”. In: *SIAM Journal on Control and Optimization* 47.3 (2008), pp. 1150–1177. DOI: 10.1137/070694016. URL: https://doi.org/10.1137/070694016.

[50] S. Mitusch, S. Funke, and J. S. Dokken. “dolfin-adjoint 2018.1: automated adjoints for FEniCS and Firedrake”. In: *Journal of Open Source Software* 4 (June 2019), p. 1292. DOI: 10.21105/joss.01292.

[51] J.R. Munkres and Karreman Mathematics Research Collection. *Topology; a First Course*. Prentice-Hall, 1974. ISBN: 9780139254956. URL: https://books.google.it/books?id=LtEPAQAAMAAJ.

[52] D. O'Regan. *Existence Theory for Nonlinear Ordinary Differential Equations*. Mathematics and Its Applications. Springer Netherlands, 2013. ISBN: 9789401715171. URL: https://books.google.it/books?id=ijjpCAAAQBAJ.

[53] A. Quarteroni and A. Valli. *Numerical Approximation of Partial Differential Equations*. Springer Series in Computational Mathematics. Springer Berlin Heidelberg, 2009. ISBN: 9783540852681. URL: https://books.google.it/books?id=nfdDAAAAQBAJ.

[54] F. Rathgeber et al. "Firedrake". In: *ACM Transactions on Mathematical Software* 43.3 (2017), pp. 1–27. DOI: 10.1145/2998441. URL: https://doi.org/10.1145%2F2998441.

[55] T. Schwedes et al. "Mesh dependence in PDE-constrained optimisation". In: July 2017, pp. 53–78. ISBN: 978-3-319-59482-8. DOI: 10.1007/978-3-319-59483-5_2.

[56] J. Simon. *Sur le contrôle par un domaine géométrique*. Jan. 1976.

[57] G. Strang and G.J. Fix. *An Analysis of the Finite Element Method*. Prentice-Hall Series in Electronic Technology. Prentice-Hall, 1973. ISBN: 9780130329462. URL: https://books.google.it/books?id=VZRRAAAAMAAJ.

[58] K. Sturm and A. Laurain. "Distributed shape derivative via averaged adjoint method and applications". In: *ESAIM Mathematical Modelling and Numerical Analysis* 50 (Sept. 2015). DOI: 10.1051/m2an/2015075.

[59] V. Thomee. *Galerkin Finite Element Methods for Parabolic Problems*. Springer Series in Computational Mathematics. Springer Berlin Heidelberg, 2013. ISBN: 9783662033593. URL: https://books.google.it/books?id=nfHrCAAAQBAJ.

[60] T. Tiihonen. "Shape Calculus And Finite Element Method In Smooth Domains". In: *Mathematics of Computation* 70 (Dec. 1997). DOI: 10.1090/S0025-5718-00-01323-5.

[61] F. Tröltzsch and J. Sprekels. *Optimal Control of Partial Differential Equations: Theory, Methods, and Applications*. Graduate studies in mathematics. American Mathematical Society, 2010. ISBN: 9780821849040. URL: https://books.google.it/books?id=04yDAwAAQBAJ.

[62] N. Weaver. *Lipschitz Algebras*. World Scientific, 1999. ISBN: 9789810238735. URL: https://books.google.it/books?id=45rnwyVjg_QC.

[63] H. Whitney. "Functions Differentiable on the Boundaries of Regions". In: *Annals of Mathematics* 35.3 (1934), pp. 482–485. ISSN: 0003486X. URL: http://www.jstor.org/stable/1968745 (visited on 09/12/2022).

[64] A. Wirgin. "The inverse crime". In: *arXiv: Mathematical Physics* (2004).

[65] J. Wloka, C.B. Thomas, and M.J. Thomas. *Partial Differential Equations*. Cambridge University Press, 1987. ISBN: 9780521277594. URL: https://books.google.it/books?id=Eix7JA9VVy0C.

[66] M. Zlamal. "Curved Elements in the Finite Element Method. I". In: *SIAM Journal on Numerical Analysis* 10.1 (1973), pp. 229–240. ISSN: 00361429. URL: http://www.jstor.org/stable/2156389 (visited on 10/06/2022).